



Programme Area: Carbon Capture and Storage

Project: Aquifer Brine

Title: The impact of brine production on aquifer storage of captured CO₂.

Abstract:

This project aims to assess the potential for brine production through dedicated wells in target CO₂ storage formations to increase CO₂ storage capacity and reduce the overall cost of storage - as well as any other potential benefits for CO₂ store operators associated with brine production.

Context:

This £200,000 nine-month long project, studied the impact of removing brine from undersea stores that could, in future, be used to store captured carbon dioxide. It was carried out by Heriot-Watt University, a founder member of the Scottish Carbon Capture & Storage (SCCS) research partnership, and Element Energy. T2 Petroleum Technology and Durham University also participated in the project. It built on earlier CCS research work and helped develop understanding of potential CO₂ stores, such as depleted oil and gas reservoirs or saline aquifers, located beneath UK waters. It also helped to build confidence among future operators and investors for their operation. Reducing costs and minimising risks is crucial if CCS is to play a long-term role in decarbonising the UK's future energy system.



The impact of brine production on aquifer storage of captured CO₂

Final Report – 24/10/17

Deliverable 4.0

Min Jin, Peter Olden, Saeed Ghanbari, Gillian Pickup and Eric Mackay (Heriot-Watt University) and Davey Fitch (Scottish Carbon Capture and Storage)

ETI Project Code	CC2010
Project Title	Impact of Brine Production on Aquifer Storage
Deliverable Reference	D4.0
Version	v2

Executive Summary

This project aimed to assess the potential for brine production through dedicated wells in target Carbon Dioxide (CO₂) storage formations to increase CO₂ storage capacity and reduce overall cost of storage - as well as any other potential benefits for CO₂ store operators associated with brine production.

Brine production is proposed as a method to manage pressure in storage sites, as a corollary to water injection during hydrocarbon extraction. In the case of CO₂ storage, the concept is that the production of water creates voidage to increase storage capacity and reduce the extent of pressure increase due to CO₂ injection. This in turn reduces the risk of caprock failure, fault reactivation and induced seismicity. Additionally, brine production reduces the energy available to drive fluids through legacy well paths and other potential seep features. Spatial reduction in the extent of the pressure plume cuts down the area of potential drilling interference, the number of impacted legacy wells, and the area of investigation for monitoring where brine movement is a concern.

This report presents findings from the entire project, and references other project reports where appropriate.

The Benefits of Brine Production

The project demonstrates that, for certain CO₂ stores, the benefits of brine production for CO₂ storage can be summarised as listed below. For such stores, at least one of the following benefits may occur:

- (a) an increase in storage capacity;
- (b) a reduction in the £/t (Pounds per tonne) unit cost of storage;
- (c) the opportunity to convert some 'smaller' CO₂ aquifers into economically viable options
- (d) therefore, the development of a smaller number of CO₂ stores, at lower cost, for a given amount of captured CO₂;
- (e) the opportunity to consider increasing CO₂ injection rate at a store at a later date, as new CO₂ sources come on stream;
- (f) the opportunity to extend the life of a CO₂ store beyond that previously envisaged, at a later date
- (g) a viable engineering option for a CO₂ store operator to mitigate store performance risks;
- (h) the option to reduce CO₂ store pressure past the end of CO₂ injection, with the potential to reduce Measurement, Monitoring and Verification (MMV) and/or liability for store operators.

This report identifies cases in which such benefits do arise – primarily those where pressure increase is the factor that limits storage capacity, and cases in which they do not – primarily where CO₂ plume migration beyond the boundary of the store is the factor that limits storage capacity.

Methodology

The primary methodology used in this project was to perform numerical fluid flow simulations of CO₂ injection into various selected CO₂ storage systems, comparing scenarios where brine production does not occur with scenarios where it does. The results of these numerical fluid flow simulations include cumulative CO₂ storage as a function of injection rate, and duration of CO₂ injection before a criterion for stopping injection is reached. The primary criteria are maximum allowable pressure increase, or migration of CO₂ out of a predetermined storage area. For the saline aquifer systems considered, flow model parameters such as locations of wells and clusters, and output parameters such as well flow rates, pressures, and duration of injection are then used as inputs for a purpose-built Cost Benefit Analysis (CBA) tool, which enables an economic comparison of scenarios with and without brine production to be made.

The project also gives consideration to injection of CO₂ into depleted hydrocarbon reservoirs for the purpose of CO₂ storage, but where previous or current hydrocarbon production may impact the timing or the rate of brine production necessary to achieve the desired control on overall pressure. This addresses the potential of synergistic opportunities where a CCS project would benefit from the pressure management achieved by brine production, but where additionally the CCS project may occur subsequent to, or simultaneously with, a hydrocarbon recovery project.

Stores Considered and Summary of Results

The project considered a number of stores, chosen in conjunction with the ETI as exemplars of the various UK offshore CO₂ storage sites, and with respect to the availability of suitable geological models. These included models from the 2016 Pale Blue Dot (PBD) led Strategic UK Storage Appraisal project for the ETI, models licensed from the British Geological Survey (BGS) and Heriot-Watt University (HW), and those used in the 2012 CO₂ Aquifer Storage Site Evaluation and Monitoring (CASSEM) project.

A two-stage process assessed these stores, first for the potential benefits of brine production under a range of CO₂ injection rates and durations, before a second stage delivered detailed assessment of a chosen subset of these under a number of scenarios, as summarised:

Stage 1 (stores selected with the ETI)

Store	Type	Notes on Model Used	Stage 1 Results	Progress to Stage 2?
Synthetic tilted	Fully confined 'closed box'	Proof of Concept case based on a real geological formation with features expected to suit brine production – but simple enough that multiple sensitivities can be tested	Significant increase to CO ₂ storage capacity (up to 42x) with brine production	YES – with scope to consider permeability, dip angle and inter well distance sensitivities
Forties 5 system	Aquifer; open with identified structural/stratigraphic confinement	Part of Forties Aquifer but different location to PBD model, at lower permeability and not including hydrocarbon trap	Increase to CO ₂ storage capacity with brine production. Decrease in £/t storage costs with brine production, especially for injection rates at or above 15 Mega tonnes per year (Mt/y)	YES – increasing permeability to match PBD model
Bunter 36 Zone 4	Aquifer; structural/stratigraphic trap	Part of Bunter Aquifer including 4 domes; larger than PBD Bunter 36 model and assuming connectivity between domes	No increase in CO ₂ capacity with brine production, and slight increase in £/t storage costs	YES – but assuming no connectivity with other domes to test brine production as mitigation strategy
Tay	Aquifer; open with no identified structural/stratigraphic trap	Large dipping structure in Central North Sea. Model licensed from BGS and HW	Significant increase in CO ₂ storage with brine production, and slight decrease in £/t storage costs	NO
Firth of Forth	Aquifer; structural/stratigraphic trap – low permeability	Smaller anticlinal structure close to shore. Model licensed from BGS and HW; model used in CASSEM project	Significant increase in CO ₂ storage with brine production, and significant decrease in £/t storage costs	YES – consider capacity to accommodate increase or extension of CO ₂ supply
Hamilton gas field	Depleted gas field and connected aquifer; structural/stratigraphic trap	History matched gas production and CO ₂ injection model supplied by PBD via ETI	Complicated by initial CO ₂ injection being gas phase, but benefit from delayed brine production once system re-pressurised	NO
North Sea oil field	Active oil field and connected aquifer; structural/stratigraphic trap	History matched oil production model supplied by current operator and used under condition of confidentiality; not assessed with CBA tool	CO ₂ injection into aquifer provides storage and pressure support for oilfield production, which in turn enhances CO ₂ storage capacity	NO

Stage 2 (stores for further consideration agreed following project Stage Gate meeting)

Store	Stage 2 results
Synthetic tilted	Inter-well distance critical for efficiency of brine production; optimum location readily determined to maximise pressure benefit and minimise CO ₂ breakthrough, but affected by uncertainties in reservoir characterisation
Forties 5 system	An increase of average permeability from 1 to 36 millidarcies (mD) improved pressure communication more significantly than it increased risk of CO ₂ breakthrough; brine production thus more effective
Bunter 36	Brine production can mitigate risk of rapid pressure build-up in compartmentalised formation
Firth of Forth	Brine production creates opportunity to increase storage capacity and/or extend life of store after initial period of CO ₂ injection

Stage 1 Review of Various Aquifer Types and Hydrocarbon Fields

The initial analysis of the various aquifer types present in CO₂Stored identified that the primary benefit of brine production occurs where the main limitation on storage capacity arises from a pressure restriction as opposed to a migration restriction. Brine production is most useful where further increase in pore pressure creates a risk of caprock failure, and has more limited usefulness where there is a risk of CO₂ migrating outside of the storage complex due to displacement beyond a spill point, say. The benefit of brine production is principally due to pressure management. The biggest limitation in this benefit is identified as CO₂ breakthrough at the brine producer. The work presented in this report treats this issue using a conservative assumption that brine production from that well would cease at that point. (Options exist to separate CO₂ from the produced brine stream, compress it and feed it into the injection stream; however, the economics of undertaking this process were not considered here.)

A system with a geological configuration that is pressure confined and that can produce large volumes of brine before injected CO₂ reaches the production wells is the one that will benefit the most from brine production, potentially increasing CO₂ storage capacity by a factor of 40 times, or more. In very large systems with moderate initial injection rates, additional capacity can be delivered by drilling additional CO₂ injection wells away from the existing injectors without using brine production. However, in systems that are near capacity, or where the cost of injection away from existing CO₂ injectors may be high due to additional appraisal, infrastructure (say platform) and/or monitoring costs, then brine production will yield benefits in terms of extending the life of the injection project,

and hence increasing the overall capacity (eg Forties 5 aquifer) and/or reducing unit injection costs (eg Tay aquifer).

Study of CO₂ injection in the pressure depleted Hamilton gas field showed that initially brine production would yield little benefit as the field was re-pressurised, but that once the system pressure exceeded the critical point for CO₂, at which point the compressibility of CO₂ decreases significantly, brine production would increase the storage capacity.

Injection of CO₂ into an aquifer adjacent to a currently producing oil field, Field X, was shown to be advantageous in terms of storing CO₂ *and* increasing oil production compared to the existing water injection strategy. Instead of drilling dedicated brine production wells, the pressure management for the CO₂ injection process could be achieved by the existing oil and predominantly water production using existing wells in the field, and by reducing the seawater injection rates since the CO₂ injection provides the requisite pressure support for the oil field. While economic calculations related to oil production were outside of the scope of this study, there would be clear synergistic benefits arising from storing CO₂, increasing oil production rates and reducing seawater injection requirements – in a system that is already being developed and therefore is data rich and well characterised.

The analysis results from the review of various aquifer types and hydrocarbon fields are summarised below:

System	Analysis
Forties	<p>Brine production not required for 2 Mt/yr of CO₂ injection.</p> <p>Maximum practical storage capacity increases from ~400 Mt to 450 Mt with brine production.</p> <p>Minimum lifetime T&S unit cost (for > 2Mt/yr) reduces from £19.1/tCO₂ to £16.2/tCO₂ with brine production.</p> <p>More injection scenarios with higher storage capacities become feasible with brine production (eg 15 Mt/yr for 20 and 30 years, and 20 Mt/yr for up to 20 years)</p>
Bunter	<p>Maximum practical storage capacity of ~200Mt not enhanced by brine production</p> <p>Minimum lifetime T&S unit cost of £6.8/tCO₂ not improved by brine production.</p> <p>Consideration should be given to potential to mitigate risk of confinement (see case study below)</p>

Tay	<p>Brine production is not required for 2Mt/yr of CO₂ injection.</p> <p>Maximum practical storage capacity increases from ~150Mt to 450Mt with brine production.</p> <p>Minimum lifetime T&S unit cost (5 Mt/yr for 30 years) reduces from £7.9/tCO₂ to £4.8/tCO₂ with brine production.</p> <p>More injection scenarios with higher storage capacities become feasible with brine production (eg for an injection rate of 5Mt/yr, brine production can increase CO₂ injection duration from 30 years to 40 years as well as reducing lifetime unit T&S costs from £7.9 to £7.2/tCO₂).</p>
Firth of Forth	<p>Brine production is not required for 2Mt/yr of CO₂ injection.</p> <p>Maximum practical storage capacity increases from ~100Mt to 300Mt with brine production.</p> <p>More injection scenarios with higher storage capacities become feasible with brine production (see case studies below).</p>
Hamilton gas field	Brine production can increase capacity storage capacity once CO ₂ injection has repressurised field above CO ₂ critical point pressure
Field X oil field	<p>Brine and oil production from existing oil field producers can achieve same pressure benefit for CO₂ storage in adjacent aquifer as dedicated brine production wells in aquifer.</p> <p>Oil recovery increases by 8% during CO₂ injection into aquifer relative to base case extended waterflood scenario</p>

Stage 2 Case Studies

In addition to the optimisation carried out on the exemplar stores in Stage 2, Element Energy carried out analysis of specific case studies designed to explore the benefits of brine production, as outlined previously.

Four case studies were considered, which confirm and illustrate the specific additional benefits of brine production, over and above the simple £/t economics.

In the first three case studies, the scenarios compared relate to using brine production at the Firth of Forth site to increase CO₂ capacity under specific conditions, compared with the prospect of concurrently developing a 'Cheap Central North Sea aquifer', with associated additional transport development costs of pipeline transport from Central Scotland overland to St Fergus, and offshore from there.

The Firth of Forth site is chosen as both a strong exemplar store with greatly improved prospects for CO₂ storage by using brine production, and as a geographically convenient storage site from the Grangemouth industrial cluster CO₂ emissions. However, it must be made clear that no assessment of any planning or environmental issues are made for this site within this study.

The fourth case study considers using brine production at the Bunter 36 site, compared with the need to develop another nearby aquifer concurrently. The Bunter site was chosen as an exemplar site of great significance for storage of CO₂ emissions from eastern England.

Case study 1 - Increasing storage duration of an attractive storage site, to avoid making additional investment in a secondary storage unit (Firth of Forth)

This case study attempted to illustrate the principle that using brine production to increase CO₂ storage in one site can be cheaper than having to develop a further site for the same amount of total CO₂ stored. In one scenario, the storage capacity of Firth of Forth is increased from 100Mt (5Mt/yr for 20 years) to 200Mt (5Mt/yr for 40 years) with brine production. This scenario is compared with an alternative scenario, in which another cheap aquifer is developed after 20 years.

Benefits illustrated:

- (a) an increase in storage capacity;
- (b) a reduction in the £/t unit cost of storage;
- (c) the opportunity to convert some 'smaller' CO₂ aquifers into economically feasible options;
- (d) therefore, the development of a smaller number of CO₂ stores, at lower cost, for a given amount of captured CO₂

Although the UK has sufficient storage capacity for potential CO₂ emitters, brine production could be vital to enable cost saving by use of existing infrastructure, or for other regions/countries that have limited storage capacity.

Case study 2 – Increasing injection rate for new emitters (Firth of Forth)

This case study investigated a scenario where a store operator agrees to a CO₂ storage contract for a specified duration. Then, after a number of years, another CO₂ source comes on stream, in search of a suitable store. The options are either to use brine production to increase the storage capacity of the Firth of Forth site, or develop a new site for the increased emissions.

Benefits illustrated:

- (a) an increase in storage capacity;
- (b) a reduction in the £/t unit cost of storage;
- (c) the chance to consider increasing CO₂ injection rate at a store at a later date, as new CO₂ sources come on stream

Case study 3 – Increasing storage duration after 10 years of injection without brine production (Firth of Forth)

This case study explored a scenario where a store operator agrees to a CO₂ storage contract for a specified duration. Then, after 10 years of successful operation, there is a request to increase this duration. The options are either to use brine production to allow this increased duration, or develop a new site.

Benefits illustrated:

- (a) an increase in storage capacity;
- (b) a reduction in the £/t unit cost of storage;
- (c) the opportunity to extend the life of a CO₂ store beyond that previously envisaged, at a later date

Case study 4 - Improving performance of an aquifer that does not perform as expected (Bunter)

This case study examined the option for a store operator to use brine production as an engineering intervention to improve storage performance, in a scenario where the store does not perform as expected. A store operator at Bunter agrees a CO₂ storage contract of 5Mt for 30 years, but realises that this will only be possible for 10 years, due to excessive pressure build up arising from unexpected compartmentalisation. The options are either to drill brine production wells at additional cost to continue using the Bunter 36 store, or develop a new site nearby to fulfil the storage contract.

Benefits illustrated:

- (a) a viable engineering option for a CO₂ store operator to mitigate store performance risks

The Cost Benefit Analysis results from these case studies are summarised below:

Case study		Total cost saving (Discounted, 10%)	Reduction in levelised cost of Transport & Storage (T&S)
1	Increasing storage capacity of an attractive storage unit (Firth of Forth)	~£1 billion	~£5/tCO ₂
2	Increasing injection rate for new emitters (Firth of Forth)	~£0.5 billion	~£2/ tCO ₂
3	Increasing storage duration after 10 years of injection without brine production (Firth of Forth)	~£1 billion	~£6/ tCO ₂
4	Improving performance of an aquifer, which does not perform as expected (Bunter 36)	~£0.1 billion	~£1/ tCO ₂

The detail calculations, assumptions and findings are presented in the remainder of this report and in report “D3.3 Brine production cost-benefit analysis tool documentation and results” and the CBA tool itself is included as an MS Excel document “D3.2 Brine production CBA tool - Element Energy.xlsm”. Details of the numerical simulations are presented in “D2.0 Initial Technical Analysis of Exemplar Stores” and “D3.0 Appendix Final Technical Analysis and Case Studies”.

Additional Work

Assessments were also made of the impact of grid resolution on the accuracy of the fluid flow calculations, of the impact of high permeability ‘thief’ zones, of potential risks and potential opportunities associated with brine production, and of whether or not there is opportunity to consider use of the type of data in CO₂ Stored to develop analytical models that could at least in part provide the types of inputs for the CBA tool that were derived from the numerical models. The rationale for this latter assessment was that numerical simulations require extensive input data, specialist commercial software, specialist operator knowledge and they are computationally intensive to carry out, whereas analytical calculations are more readily performed. While seven subsurface systems have been studied using the numerical simulations, only an analytical approach would enable the 400+ systems in CO₂ Stored to be considered.

Grid resolution is an important constraint on the accuracy of numerical simulations of CO₂ injection and brine production. Increasing resolution (within current hardware limitations) generally further improves accuracy (depending on the accuracy of the reservoir characterisation), but at highest resolutions the changes are moderate. The key issue is the prediction of risk of CO₂ breakthrough at producers, and thus monitoring and contingency planning are required.

Risks and Opportunities

The physical risks associated with brine production are presented in “*D3.0 Appendix Potential Risks from Brine Production*” and include:

- Breakthrough of CO₂ at the production wells. The impact can be mitigated by monitoring of plume migration and of produced brine compositions, and either shut in of the production well or separation of produced gas stream, compression, and introduction to the injection stream.
- Oil in water content exceeding 30 ppm, should there be any hydrocarbon accumulation in the vicinity of the producers. This can be mitigated by analysis of produced water and conventional “polishing” of produced water using hydrocyclones.
- Scale precipitation in the production system (eg CaCO₃ in Forties and NaCl in Bunter). These scales are routinely managed in oilfield operations by chemical application, either continuous chemical injection if the scale first forms in the tubing above the packer or anywhere downstream of that point.

There are opportunities associated with brine production, presented in “*D3.0 Appendix Potential Opportunities from Brine Production*”, and which include:

- Extraction of minerals. While the value of certain minerals present in aquifer brines is increasing, this is not currently viable for brines produced by the oil industry.
- Pressurised water for desalination. One of the largest operating costs associated with desalination is the requirement to boost the feed brine pressure to ca. 7,000 kPa. An increase in reservoir pressure above hydrostatic due to CO₂ injection will result in the brine produced at surface being above standard pressure, thus reducing the cost for a coupled desalination system.
- Sulphate free water for oilfield waterflooding. Sulphate scaling of oil wells occurs in oilfields where seawater is injected. Aquifer brine re-injection provides an opportunity to reduce this risk and associated cost of well cleanup.

Recommendations for Future Work

This work, presented in “*D3.0 Appendix Brine production model – Approximate methods*”, has identified that the risk of CO₂ breakthrough at brine production wells is dependent on inter well distances, the geometry of aquifer system, the density difference between brine and CO₂, and the distribution of permeabilities within the formation. CO₂ density and mobility are very sensitive to pressure and temperature near the CO₂ critical point. Thus a specific study of the impact of system temperature, pressure and permeability distribution (fining up vs. coarsening up permeabilities, say) on optimum inter well distances should be conducted.

Large volumes of permeable rock may be separated by relatively thin zones of impermeable rock. Thus, there may be potential storage volume in the vicinity of an identified aquifer. In some cases, lateral shale layers may be extensive but incomplete. Brine production from a lower sandstone interval may be very effective where an intervening but incomplete shale layer separates it from the upper interval into which CO₂ is injected, as the shale may act as a barrier to CO₂ migration to the production well, but the pressure depletion at the brine producer may nonetheless have a beneficial impact at the CO₂ injector. In such a scenario, the degree to which pressure transmission can take place across the barrier would be critical. Furthermore, there may be opportunities to deliberately engineer pressure communication between adjacent sandstone intervals, or between adjacent fault

blocks, such that pressure propagation through the brine phase occurs, but the CO₂ remains in the vicinity of the injection well.

All injection calculations presented have been performed using numerical models. Analysis of the type of data contained in CO₂Stored identifies that it is possible to perform analytical calculations to predict the impact of brine production on storage capacities using only the data in CO₂Stored. The initial methodology to do that has been formulated, but requires further validation. These methods depend on identifying the volume of incremental CO₂ that can be injected before breakthrough occurs (the pressure constraint) or before the CO₂ advances beyond a spill point or other limit of the system (the migration constraint). These methods, which show promise, should be refined and tested against the numerical predictions, and if applicable, coupled with CO₂Stored.

Documents Associated with this Report

- *D3.3 Brine production cost-benefit analysis tool documentation and results*
- *D3.2 Brine production CBA tool - Element Energy.xlsm*
- *D3.0 Appendix Final Technical Analysis and Case Studies*
- *D3.0 Appendix Potential Risks from Brine Production*
- *D3.0 Appendix Potential Opportunities from Brine Production*
- *D3.0 Appendix Brine production model – Approximate methods*

Contents

Executive Summary	2
The Benefits of Brine Production.....	2
Methodology	3
Stores Considered and Summary of Results.....	3
Stage 1 Review of Various Aquifer Types and Hydrocarbon Fields	5
Stage 2 Case Studies	7
Additional Work.....	11
Risks and Opportunities	11
Recommendations for Future Work.....	12
Documents Associated with this Report.....	13
1 Introduction	16
1.1 Approach.....	21
2 Forties Model.....	25
2.1 Development of Model-36mD.....	27
2.2 Results from Development Plan Three (Model-36mD).....	28
2.3 Summary.....	35
3 Bunter Model.....	36
3.1 Modified Bunter Models with a Partially or a Fully Sealing Boundary.....	38
3.2 Post Injection Brine Production (PIBP)	45
3.3 Delayed Water Production	47
3.4 Impact of Compartmentalisation on CO ₂ Storage Characteristics in the Bunter Formation	49
3.5 Limited Vertical Transmissibility	57
3.6 The Benefit of an Aquifer	62
4 Firth of Forth Model with Brine Production.....	65
4.1 Geology of Firth of Forth Aquifer.....	65
4.2 ECLIPSE Model and Injection Plan.....	69
4.3 Simulation Results and Analysis	71
4.4 Value of Brine Production Later in the Life of the Project	76
5 Tay Formation with Brine Production.....	80
5.1 Geology Data	80
5.1.1 Pressure and Temperature.....	81
5.1.2 Porosity and Permeability	81
5.1.3 Formation Compressibility.....	81
5.2 Multiple Layers between Top and Base Surfaces	82

5.3	Reservoir Simulation Model (ECLIPSE)	83
5.4	Methodology.....	84
5.5	Static Storage Capacity.....	86
5.6	Maximum Injection Pressure and Minimum Production Pressure	86
5.7	Simulation Results and Analysis.....	87
5.8	Conclusion.....	93
6	Impact of Grid Resolution.....	94
6.1	Grid Resolution Sensitivity in a Flat Homogenous Model	94
6.1.1	Lateral and Vertical Grid Resolution Sensitivity.....	94
6.1.2	The Impact of Grid Resolution on Pressure.....	98
6.1.3	The Impact of Grid Resolution on CO ₂ Migration	100
6.1.4	Impact of Grid Resolution on Trapping.....	106
6.1.5	CPU Saving.....	108
6.2	Study of Sensitivity of CO ₂ Migration to Grid Resolution in Tilted Model	110
7	Conclusions.....	115
8	Future Work.....	120
9	References.....	121

1 Introduction

The Energy Technologies Institute (ETI) *United Kingdom Storage Appraisal Project* (UKSAP) was undertaken to assess the CO₂ storage potential in the rock formations underlying the offshore UK Continental Shelf (UKCS). The project led to the initial development of the CO₂Stored database and website. UKSAP, completed in 2011, was delivered by a consortium of project partners, including Senergy Alternative Energy Ltd, BGS, the Scottish Centre for Carbon Storage (University of Edinburgh, Heriot-Watt University), Durham University, GeoPressure Technology Ltd, Geospatial Research Ltd, Imperial College London, RPS Energy and Element Energy Ltd., (Gammer et al., 2011). Data were gathered about formations which met certain criteria (such as porosity and permeability constraints, the presence of impermeable caprocks, etc) that meant they could potentially act as storage sites. Aquifers and producing hydrocarbon fields were considered. The limiting factor for storage capacity was generally pressure increase and the risk of fracturing the caprock, although migration of CO₂ beyond a predetermined spill point was also considered. However, the impact of deliberate pressure relief to increase CO₂ storage capacity was outside the scope of UKSAP.

UKSAP was followed by further development of the CO₂Stored database and website, and improved access to external users. This activity involved The Crown Estate and the British Geological Survey. UKSAP was also succeeded by a project led by Pale Blue Dot on behalf of the ETI that was completed in 2015, and which provided data for this current project.

The current ETI funded project, *Impact of Brine Production on Aquifer Storage*, addresses whether or not there is potential to significantly increase storage capacity, and thereby reduce overall cost of storage, by producing brine through dedicated production wells, as demonstrated in the final report of the Scottish Carbon Capture, Transport and Storage Development Study (Akhurst et al., 2011). This is proposed as a method to manage pressure in storage sites, as a corollary to water injection during hydrocarbon extraction. In the case of CO₂ storage, the production of water creates voidage to increase storage capacity and reduce the extent of pressure increase due to CO₂ injection, and hence reduce the risk of caprock failure. Thus it would be possible to inject CO₂ at a higher rate into a given store, or inject for longer, rather than developing another storage site to meet the required storage volume. In addition to the potential increase in CO₂ storage capacity, the production of water reduces the areal extent of pressure increase due to CO₂ injection, and hence, as well as reducing the risk of caprock failure, fault reactivation and induced seismicity, it reduces the energy available to drive fluids through legacy well paths and other potential seep features. Spatially the reduction in the extent of the pressure plume reduces the affected area which can reduce the area of potential drilling

interference, the number of impacted legacy wells, and the area of investigation for monitoring where brine movement is a concern.

In the published development plan for the Chevron operated Gorgon project at Barrow Island, Western Australia (Chevron Australia, 2016), 220 MMscf/d of CO₂ injection into the Dupuy Formation through nine injectors is “supported” by some 60,000-80,000 stb/d brine production through four producers located approximately 4-6 kms distant (Chevron Australia, 2016). The brine production is facilitated by Electrical Submersible Pumps (ESPs), with the brine being displaced into the overlying Barrow Group by means of pressure management wells. The CO₂ injection uses CO₂ that is co-produced with hydrocarbon gas from Gorgon and Jansz-Lo gas fields, reducing emissions by 40%. This is the first reported occasion that brine production is being used to support an industrial scale CCS project.

This report, which details an initial technical analysis of exemplar stores in the UKCS, shows that increased CO₂ storage capacity can be achieved, and provides data that is used for an economic evaluation of the impact of brine production on the overall cost of CO₂ storage projects. The exemplar sites are chosen from both aquifers and hydrocarbon producing fields. In the case of the aquifers, the UKSAP methodology of calculating number of CO₂ injection wells as a function of required injection rate and of injection duration is followed. In the case of the hydrocarbon fields, the impact of historical hydrocarbon production is taken into account – something not done in UKSAP.

The following is the structure of the project:

Phase 1	Development and application of numerical reservoir simulations	Development and application of CBA tool
Structures considered	1) Synthetic tilted structure	
	2) Forties 5 Aquifer	CBA tool applied
	3) Bunter Zone 4 Aquifer	CBA tool applied
	4) Tay Aquifer	CBA tool applied
	5) Firth of Forth Aquifer	CBA tool applied
	6) Hamilton gas field	
	7) Field X oil field	

Phase 2		
Sensitivity Calculations	Grid resolution analysis	
	Heterogeneity analysis	
Case Studies	Forties permeability	CBA tool applied
	Bunter compartmentalisation	CBA tool applied
	Firth of Forth and step out	CBA tool applied
Risks	Risk associated with brine extraction, such as wellbore scaling	
Opportunities	Opportunities arising from brine production, such as mineral extraction	
Future work	Development of analytical methodology to apply to CO ₂ Stored	

In all seven aquifers and the hydrocarbon field scenarios considered, the objective of this work is to evaluate the number and timing of brine production wells that are additionally considered, and the impact this has on CO₂ injection capacity and formation pressure. These data are then supplied to project partners (Element Energy) to evaluate whether or not any additional injection capacity (within the pressure constraints) warrants the cost of incremental infrastructure required for the brine production. The evaluation of the facilities required to process and displace produced brine is considered in this project by project partners Element Energy and T2 Production Technology.

The following are the seven systems studied:

- 1) A **synthetic tilted structure**, selected specifically to demonstrate the potential increase in storage capacity that brine production may deliver. This system is used for proof of concept and to study the reservoir engineering conditions that are most favourable for the brine production concept, and economic calculations are not performed. However, it should clearly identify whether or not brine production can make storage sites that are nearby to existing infrastructure, which might otherwise have been excluded from consideration, viable options by increasing their storage capacity.

Having demonstrated the concept of brine production using a synthetic system, the next four systems to be modelled are based on actual offshore or near shore aquifer structures found in the UK Continental Shelf, and they represent exemplars of the four principal types of system identified in

CO₂Stored. In each of these four cases, results of the numerical simulations would be used as inputs for the CBA tool, and the impacts on storage capacity and on the undiscounted lifetime cost of transport and storage (T&S) (calculated in £/tCO₂) would be evaluated.

- 2) The **Forties 5 system** is a large open aquifer with identified structural/stratigraphic confinement. Storage efficiencies of only up to 0.33% are identified, and so it may be considered that there is good opportunity for brine production to enhance these, but it should be borne in mind that the system is very large and thus for modest CO₂ injection rates increased capacity will be readily achieved by drilling another CO₂ injection well into another part of the formation.
- 3) The **Bunter Zone 4 system** is a structural/stratigraphic trap connected to a large aquifer. Storage efficiency without brine production of 11.7% is achievable in an incumbent dome, but this depends on pressure propagation outside of the dome to adjacent sectors of the aquifer. The primary constraint on injection capacity in this system is not pressure, but CO₂ migration outside of the designated storage dome, and so, if good communication with the rest of the aquifer is assumed, it is to be expected that pressure relief will have less of a positive impact than in more confined systems.
- 4) The **Tay aquifer system**, is an open aquifer with no identified structural/stratigraphic trap. A storage efficiency of 1.09% is possible without brine production. What distinguishes this system is that while it is large, it is nonetheless bounded on some sides, and so, especially at higher injection rates, without brine production the local pressure increase is such that injection has to be curtailed.
- 5) The **Firth of Forth system** is a near shore aquifer not included in CO₂Stored. It is a structural/stratigraphic trap with relatively low permeability, but with a steeply dipping anticline. In the absence of brine production storage efficiency of 0.4% is calculated, but the permeability and geometry of the system mean that it may be possible to delay CO₂ breakthrough. Since the aquifer is relatively close to potential CO₂ capture sites in Central Scotland, if the volume of CO₂ that can be stored in this system can be enhanced, and, if due to proximity to shore it is the first store to be developed, there may be significant cost savings relative to transporting the CO₂ a much greater distance to reach the next closest storage sites in the Central North Sea.

In addition to the reduction in unit costs that brine production may enable by extending injection in the same site rather than commencing injection in a new site, there is also a more difficult to quantify benefit of reduced risk associated with operating a site for which historical observed data have been collected compared to the development of a greenfield site. For example, a flow simulation model that has been history matched against historical injection (and production) data will provide a much more accurate forecast of performance than will a model that has not been history matched, and therefore the continued management of an existing system will generally pose lower risk than the development of a new system. This principle also means that development of a system that is already associated with hydrocarbon production may result in a lower risk, since there will be much more data available for such a system. In addition the previous (and current) production of fluids for the sake of hydrocarbon recovery may be used to support the benefits derived from brine production. Thus two further systems are considered, one in which hydrocarbon production predates use of the site for CO₂ injection, while the other considers simultaneous production of oil and brine from a field that is in pressure communication with an aquifer into which CO₂ is injected. In neither case are economics calculated, since the CBA tool was not developed to consider hydrocarbon systems.

- 6) The depleted **Hamilton gas field** is also of interest due to its geographical location in Morecambe Bay.

- 7) A model of a **North Sea oil field** is available to this study, and the model contains CO₂ as a component in the Equation of State (EoS). The model itself, however, is confidential, and thus limited results may be reported.

In addition to the above, four specific circumstances were studied:

- (i) Where before a decision is made to inject CO₂ there is a desire to identify an increased storage capacity for an already attractive store, such as the Firth of Forth, to improve the value of the investment proposition.

- (ii) Where after a period of CO₂ injection, say 10 years, new CO₂ emitters are identified, and so there is an opportunity to increase the injection rate.

- (iii) Where after a period of CO₂ injection, say 10 years again, an existing CO₂ emitter identifies that the period of CO₂ generation may be extended, and so there is an opportunity to prolong the period of injection.

- (iv) Where an injection well is drilled into what is anticipated to be a large high permeability store, such as the Bunter Store 4 system, but after drilling the well it is discovered that the rock around the injection well is compartmentalised, and so the volume of rock into which CO₂ may be injected is much smaller.

1.1 Approach

This report details calculations that are used to demonstrate the methodology and considers scenarios that may yield benefit, but does not provide an optimised solution for each case. Indeed, it is to be expected that some scenarios will not prove cost effective. However, it is important that a robust methodology is developed.

In addition to providing data similar, or in extension to, the type of data generated during UKSAP, this project also considers possible innovations, such as:

- altering the timing of brine production to best suit the need to manage pressure;
- the opportunity to use brine production to increase the injection capacity in depleted gas reservoirs; and
- the opportunity not to produce brine, but to decrease brine injection in waterflooded oil reservoirs to achieve the same net effect of increased voidage to maximise CO₂ storage.

The difference with the latter scenario is that the voidage is achieved by oilfield production, with the injected CO₂ replacing (or partially replacing) seawater injection wells as the pressure support mechanism, albeit the CO₂ injection wells are set deep within the adjoining aquifer.

In each exemplar store case considered, calculations are performed using a reservoir simulation model - a single geological realisation of the system - since the purpose of the study is to identify the potential for improvement in storage capacity, not the impact of geological uncertainty. Geological uncertainty is an important issue, and is considered in this report only for the case of compartmentalisation in the Bunter Zone 4 system; it would need to be considered in full for any detailed assessment of a potential store. In particular, as with waterflooding of oilfields, breakthrough of the injectant at production wells can detrimentally affect the efficiency of the process, and this in turn can be strongly affected by heterogeneity in the system geology, and the balance between viscous, gravitational and capillary

forces. This means that optimisation of a specific storage site would have to take account of the uncertainty in the geological description, and would have to consider the ideal inter-well distances that would maximise pressure relief whilst minimising CO₂ breakthrough, which would be dependent on the geological description. While this optimisation is beyond the scope of this current study, analysis of synthetic systems has considered the impact of geological heterogeneity on the process. This activity has identified what are the key geological uncertainties that need to be taken into consideration.

Following a site screening process, the Forties and Bunter aquifers, the Hamilton Gas Field and a North Sea oil field were chosen as initial study cases in this project. The process involved Heriot-Watt University and ETI assessing the different types of structure identified during UKSAP (Gammer, 2011), and ensuring that these structures were represented in the selected list of sites. Availability of datasets that were already developed to perform CO₂ injection calculations was another factor, since the setup and verification of such models can be time consuming. The two aquifers were chosen as two exemplars from ETI UKSAP because of their generic storage unit types, i.e. open with structural/stratigraphic confinement (Forties) and structural/stratigraphic trap (Bunter). There are two models, a Pale Blue Dot (PBD) model and a Heriot-Watt University (HW) model, available for each aquifer, although the location of the two Forties models are not exactly in the same area. The Hamilton Gas Field model was supplied by PBD, and the North Sea Oil Field model has been supplied by an operating company on the condition of anonymity.

Both of the aquifers are large in terms of potential storage capacity (100s Mt), but with different geological features and properties which may cause different CO₂ migration and pressure propagation effects. The Hamilton Gas Field is relatively much smaller, and the North Sea Oil Field, while larger than the Hamilton Gas Field, is small relative to the aquifers.

Additionally, a case study of a synthetic, steeply dipping system uses the geological description of an existing subsurface formation and considers CO₂ injection near the top of the structure with brine production at various distances downdip.

Several pre-simulation studies were carried out before running the reported simulations. One of the activities was a study on well spacing. Two well (quarter 5-spot pattern) models were used with the properties of Forties and Bunter formations. By fixing the size of a cell (400m x 400m areally) and changing the distance between one injector and one producer, it was possible to identify the relation between injection rate and the CO₂ breakthrough time. Another sensitivity study was performed to compare vertical injectors/producers and horizontal injectors/producers under the conditions of offshore CCS in order to reduce the total number of platforms. To assess the differences that may

arise due to the use of different types of simulator (i.e. black oil E100 simulator or compositional E300 simulator), the E100 Forties model from PBD was converted into an E300 model. The results from the two simulations were compared, particularly attention being paid to the calculated properties of CO₂ and the amount of brine containing dissolved CO₂. The major differences arose not from differences in fluid property input parameters or calculations, but from the fact that the PBD model included hydrocarbon extraction prior to CO₂ injection, whereas the HW scenario did not include this.

In the main simulation stage, two groups of calculations were performed. One group provides the base reference case in which no water production was used, and uses the same ranges of injection rates and periods as were used in UKSAP. The field injection rates were set to 2, 5, 10, 15, 20, and 40 Mt/year. The injection periods were 10, 20, 30, and 40 years. (It is recognised that CO₂ injection at a rate of, for example, 40 Mt/year for 40 years is an unlikely scenario, but these calculations were included for completeness and to maintain consistency with CO₂Stored.) The minimum number of wells required for each case was entered into a table, using the same format as those in the CO₂Stored website. The second group of simulations is a comparison group including water production. Three different injector-producer patterns were used for each case, and then the minimum numbers of injectors and producers were entered into a second table. At the same time, other data such as the maximum water production rate, the water injection period and starting time were also calculated and entered into the corresponding tables. To keep the study generic the well locations were chosen without detailed optimisation, even though the injection capacity of some layers would be low. The models do have significant vertical resolution, however, to capture the impact of heterogeneity in the permeability layering and to capture gravity segregation and the propagation of the so called Dietz tongue underneath vertical flow barriers and the cap rock.

In Phase I of the study brine production was used in simulations of the Forties Formation, the Bunter Formation, the Hamilton gas field, and an oil field in the North Sea. The economic analysis from the comparison of development plans with or without brine production has shown the potential economic and technological advantages of the method. In Phase I brine production during CCS was shown to (a) provide system wide pressure relief and therefore increase CO₂ storage capacity; (b) improve injectivity by local pressure relief to extend the life of injectors; and (c) under certain conditions alter the CO₂ migration path to improve the sweep efficiency and to delay CO₂ propagation to a spill point in a structural trap.

The Phase I study also showed that a key to maximising the effect of brine production is to delay the CO₂ breakthrough time and/or to extend the lifetime of the brine producers (Buscheck et al., 2011, 2012). The effect of pressure relief is inversely proportional to the well spacing (between a CO₂ injector

and a brine producer). However, the CO₂ breakthrough time is proportional to the well spacing. During Phase I various approaches to optimise these contradictory effects were considered for the Forties field, including use of horizontal wells, comparing different well patterns, and converting abandoned brine producers into CO₂ injectors. In Phase II, the study continued to address the impact of parameters such as permeability, permeability ratio, location of well perforations, well spacing and dip angle; these impact the effectiveness of brine production by influencing the trade-off between pressure relief and delayed CO₂ breakthrough. The sensitivity studies were carried out on a homogenous box model and a heterogeneous synthetic model, and were analysed and optimized by using the CMOST software (CMG, 2016a), a Computer Modelling Group Ltd (CMG) optimisation suite coupled to the GEM reservoir simulator (CMG, 2016b).

This report also covers brine production simulations performed in Phase II for some exemplars, including platform centred horizontal well CO₂ injection and vertical well brine production in Forties, impact of connectivity uncertainty in Bunter D36, post-injection pressure management for security of storage, potential for multiple stores in Bunter and Tay formations, and brine production in the Firth of Forth site. It should be noted that in all reservoir simulations calculations for both Phase I and Phase II which have not been constructed *ab initio* for this study, the numerical models have been used as supplied and properties such as permeability, porosity and net-to-gross have not been altered – except where permeability has explicitly been identified as a sensitivity parameter.

2 Forties Model

During an earlier phase of the current project a model of the Forties system that had originally been developed by HW and BGS was used by HW to study the potential impact of brine production. As shown in Table 2-1 the average permeability in this previously reported HW model (10 mD) is lower than that in the PBD model (36 mD). Because the HW and PBD models were not taken from the same area of Forties, some oil fields included in the PBD model are not present in the HW model, and average permeabilities in and around these oil fields are higher than the average aquifer permeability. Low permeability is an advantage for an open storage site with high dip angle in terms of reducing the velocity of migration, but it is a disadvantage in terms of reducing injectivity. In an open dipping aquifer with identified structural trapping, as is the case for Forties, besides the limited structural trapping the main trapping mechanism is residual trapping, and this depends on permeability and dip angle (Goater, 2013). However, in a formation with low permeability the local pressure build-up is the main constraint which limits the well injection rate. The simulations in Phase I show that as a result more injectors would be required, and to enable adequate pressure relief the water producers would have to be located close to the injectors.

In Phase II the following modifications have been made to the Forties model:

- Increasing the field average permeability from 10 mD to 36 mD without changing the seed number in the Petrel model to create a similar permeability distribution as in Phase I but an average permeability comparable with that of the PBD model. The porosity distribution was not changed.
- Changing the completions in all injection and production wells to be horizontal, and locating the wells specifically in areas where permeability is relatively higher (and not distributing the wells uniformly throughout the system).

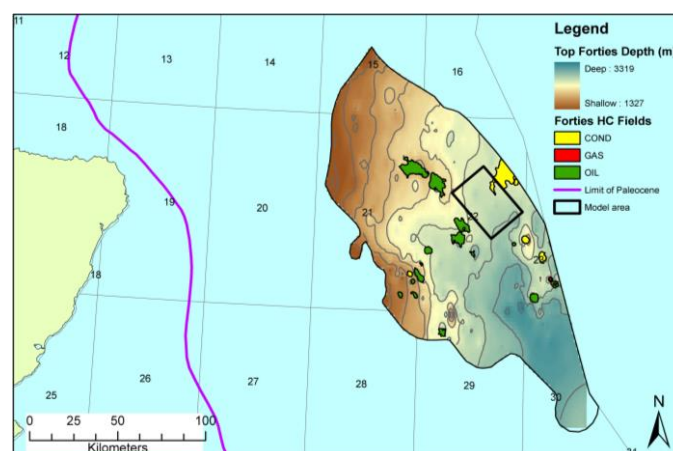


Figure 2-1 Location of the Forties Sandstone member and the Forties geological model (black rectangle). After ETI UKSAP Final Report (2011).

Table 2-1 Parameters from PBD and HW models and CO₂Stored website used for Forties models.

Parameter	Unit	PBD E100 MODEL	HW E300 MODEL	Forties 5 (372.000)
area	km ²			13,803
average thickness	m	275	171	98
model dimensions	km	42 x 48	20.8 x 35.6	
cell dimensions in x & y	m	400 x 400	400 x 400	
cell dimensions in z	m	4.5	9.5	
number of cells		105 x 120 x 61	52 x 89 x 18	
total number of cells		768,600	83,304	
number of active cells		331,180	83,304	
average porosity	frac.	0.185*	0.155	0.24
average horizontal permeability	mD	36	9.93	194
average vertical permeability	mD	28	9.93	
average net to gross	frac.			0.64
total pore volume	m ³	4.0 x 10 ¹¹ <i>P_{ref}=281 bar</i>	2.06 x 10 ¹¹ <i>P_{ref}=275 bar</i>	2.057 x 10 ¹¹
rock compressibility	1/bar	4.89 x 10 ⁻⁰⁶	5.57 x 10 ⁻⁰⁵	4.89 x 10 ⁻⁰⁵
water compressibility	1/bar			3.38 x 10 ⁻⁰⁵
initial pressure	bar	281*	290	288
datum depth	m	2,712*	2,840	2,336
fracture pressure	bar	405	390	425.2
water density	kg/m ³	1,065.0		
CO ₂ density	kg/m ³	1.87		630
brine viscosity	cP			0.36
CO ₂ viscosity	cP			0.0554
salinity	ppm	94,000	250,000	89,000
temperature	deg C	100	115	104
pore volume utilisation	frac.			0.54
theoretical capacity	Mt			1,859
dynamic utilisation	Mt			1,600
maximum injection rate	Mt/y	7	40**	
injection period	Y	40	40	
monitoring period	Y	3,500	1,000	

*from PBD report

** maximum injection rate used in UKSAP – this is included for completeness, not under the expectation that this injection rate will be used in any early or medium term CCS project

2.1 Development of Model-36mD

In the high permeability model named Model-36mD, a total of 40 horizontal wells were set in a relatively high permeability area, as shown in Figure 2-2. The well stock comprised 32 horizontal injectors and 8 vertical producers in 8 clusters. The placement of these wells was determined manually, aided by a detailed visualisation of the permeability distribution in each layer and the local dip angle, with a view to maximising injectivity but minimising post injection CO₂ migration, with consideration of the effect of water production and likelihood of CO₂ breakthrough. The number of injection wells and their locations were optimised by gradually increasing the number of injectors in each 10 year period, and adding or relocating water producers to maximize the benefit of water production.

Because of the high injectivity of the system, the maximum injection rate for each horizontal well is 1.5 Mt/y, higher than for the vertical injectors in the low permeability model where the maximum injection rate for each well is only 0.8 Mt/y. Producers were perforated across all layers contacted. The distance from any producer to its nearest injector is between 2000m and 6000m, as shown in Figure 2-3 in which the red crosses represent clusters of four horizontal injectors and the black dots represent the vertical producers.

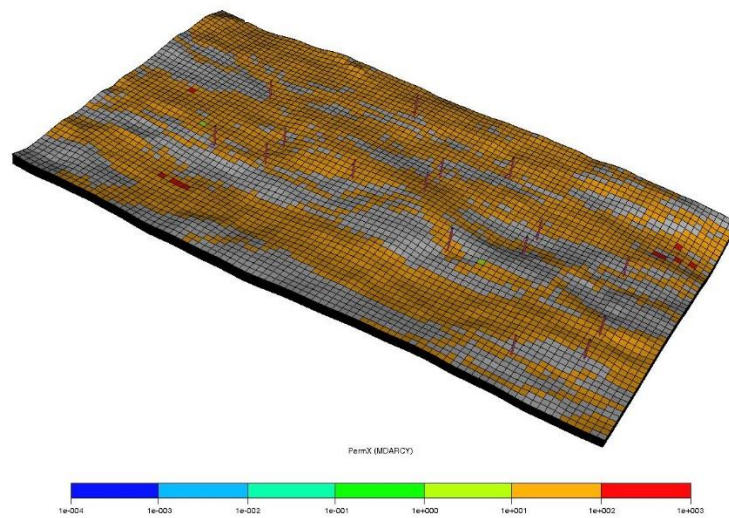


Figure 2-2 Permeability distribution and well locations for high permeability model.

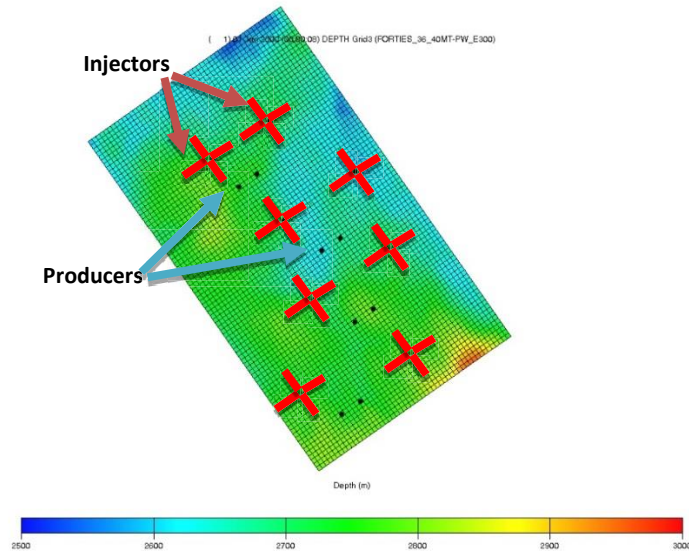


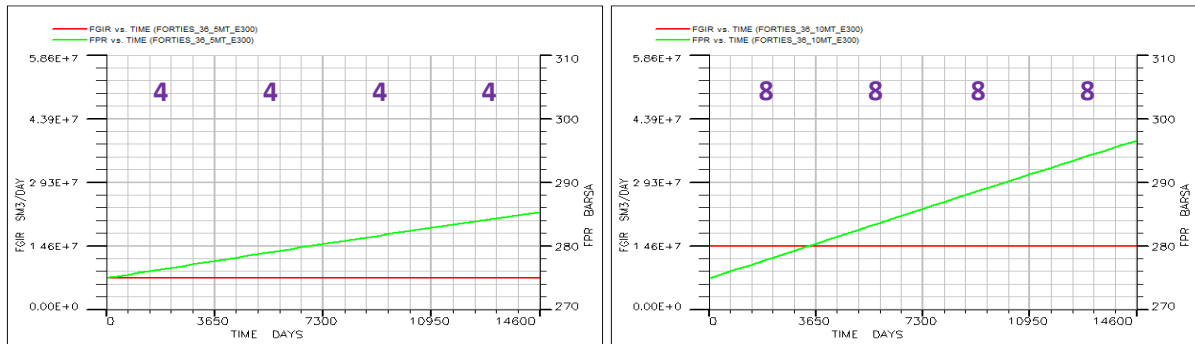
Figure 2-3 Injectors and producers on top structure depth map of Forties Model-36mD.

2.2 Results from Development Plan Three (Model-36mD)

As identified in Table 2-2, 14 simulations were run in total. Two water production scenarios were considered in the study. In the first scenario the number of injectors and producers was not changed from the beginning to the end of the injection period. In this scenario, for the cases with water production, the total number of wells is greater than for the cases without water production because the number of injectors was unchanged regardless of whether or not there was water production. In the second scenario the duration of constant CO₂ injection was increased by increasing the number of injectors in the 15 Mt/y and 20 Mt/y cases. In the other three cases the total number of wells for each water production case was the same as in the corresponding no water production case, and thus these results are not shown. Results are only shown for the two cases where the total well stock reduced.

Scenario 1: Constant number of wells

Five cases were run where the field injection rate was set to 5, 10, 15, 20 and 40 Mt/y, with no water production; these correspond to the injection rates in CO₂Stored. A further five cases with the same injection rates but now including water production were then run for direct comparison. For the cases where the field injection rate is less than or equal to 10 Mt/y, no comparison case proved necessary as a constant injection rate could be maintained without any water production, as shown in Figure 2-4. For cases with injection rates above 10 Mt/y water production was necessary to maintain the injection rate for longer.



5 Mt/y

10 Mt/y

Figure 2-4 Comparison of field CO₂ injection rate (FGIR) and field average pressure (FPR) for each case in base group. **Number of wells** required during each 10-year period identified. For injection rates of 5 Mt/y and 10 Mt/y it is possible to maintain the injection rate constant for 40 years.

Figure 2-5 and Figure 2-6 show comparisons of field CO₂ injection rates and field average pressures for each case in the base group (top row) and in the water production group (middle row). The bottom row of figures shows the water production rates (blue lines) vs time for each case with the CO₂ breakthrough (red) line. Figure 2-5 shows the case where the injector and producer well numbers are kept constant over the injection period, whereas Figure 2-6 shows the case where the well numbers increase over the 40 years.

The maximum water production rates and the total volume of water produced are also listed in Table 2-2. The duration of the constant rate period is listed in Table 2-2. From the output of the models without water production it can be seen that the duration of CO₂ injection is dependent on the injection rates, should the total number of injectors not be changed.

A mole fraction of CO₂ in the produced fluid of 2.5×10^{-5} was set as the limit at which production wells would be choked back, and this occurs after 40 years, 32 years, and 13 years for the 15Mt/y, 20Mt/y, and 40Mt/y cases, respectively. For each of these three cases, water production rate had reached its maximum as shown in the diagrams in the bottom row of Figure 2-5. However, the voidage replacement ratio, V_w/V_g , (which is the ratio of volume of water produced to volume of CO₂ injected at reservoir conditions) was just 0.14-0.18. Comparing the field average pressure, FPR, in the models without water production (top row of Figure 2-5) and the models with water production (middle row of the same figure) it can be seen that the field pressure was not significantly reduced by water production in these cases. An attempt was made to move the producers closer to the injectors, but this resulted in an early breakthrough of CO₂, which shortened the water production period and

reduced the capacity - these results are not shown. To maintain a constant injection rate for longer, the only solution was to use more water producers.

Scenario 2: Varying number of wells over time

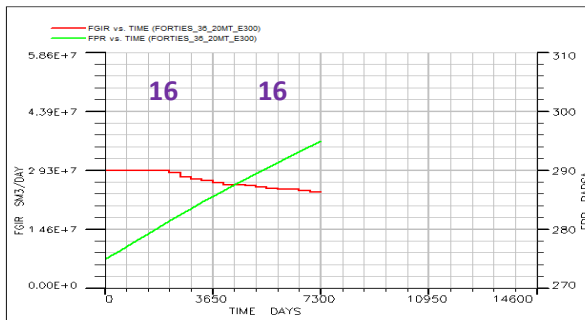
This scenario shows that in the 15 Mt/y and 20 Mt/y cases it is possible to achieve the same injection target with a similar or smaller total well stock, but replacing some CO₂ injectors with water producers. Further calculations were performed in an attempt was made to reduce the number of CO₂ injectors from 12 injectors to 9 in the first year of the 15 Mt/y case by increasing the number of water producers from 3 to 6. Thus the ratio of injectors to producers would be decreased from 4:1 to 3:2, and the total number of wells kept unchanged. However, this proved unsuccessful, indicating that there will be an optimum ratio of injectors to producers; this optimum may vary from case to case, and will depend on injectivity, communication between wells, balance between viscous and gravity forces and injection rate, amongst other issues.

Table 2-2 Model control parameters and output properties for Forties injection site

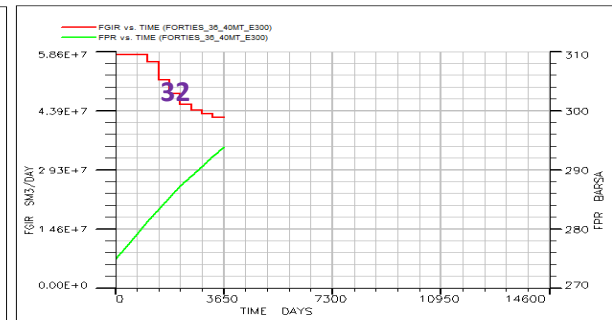
Case ID	Brine production	CO ₂ Injection Wells						Brine Production Wells						Output from Period of Constant Injection					
		10	20	30	40	Injection rate/well Mt/y	Max. WBHP bar	10	20	30	40	WBHP target bar	Production rate limit m ³ /day	Duration at max rate y	Total CO ₂ injected Mt	Max. production rate m ³ /day	Total brine produced × 10 ⁶ m ³	Voidage replacement ratio (V _w /V _{CO₂}) frac.	
Scenario 1: const wells																			
FORTIES-5MT	NO	4	4	4	4	1.5	390							40	200				
FORTIES-10MT	NO	8	8	8	8	1.5	390							40	400				
FORTIES-15MT	NO	12	12	12	12	1.5	390							7	105				
FORTIES-20MT	NO	16	16	16	16	1.5	390							6	120				
FORTIES-40MT	NO	32	32	32	32	1.5	390							3	120				
FORTIES-5MT-PW	YES	4	4	4	4	1.5	390							40	200				
FORTIES-10MT-PW	YES	8	8	8	8	1.5	390							40	400				
FORTIES-15MT-PW	YES	12	12	12	12	1.5	390	3	3	3	3	260	16000	12	180	7660	26.1	0.10	
FORTIES-20MT-PW	YES	16	16	16	16	1.5	390	4	4	4	4	260	16000	10	200	11570	31.8	0.11	
FORTIES-40MT-PW	YES	32	32	32	32	1.5	390	8	8	8	8	260	16000	5	200	15164	29.8	0.11	
Scenario 2: vary wells																			
FORTIES-15MT-var	NO	12	16	20	24	1.5	390							40	600				
FORTIES-15MT-PW-var	YES	12	14	16	20	1.5	390	3	3	3	3	260	16000	40	600	9865	116.4	0.14	
FORTIES-20MT-var	NO	20	24	28	32	1.5	390							40	800				
FORTIES-20MT-PW-var	YES	16	20	24	28	1.5	390	4	4	4	4	260	16000	50	1000	13183	184.0	0.14	



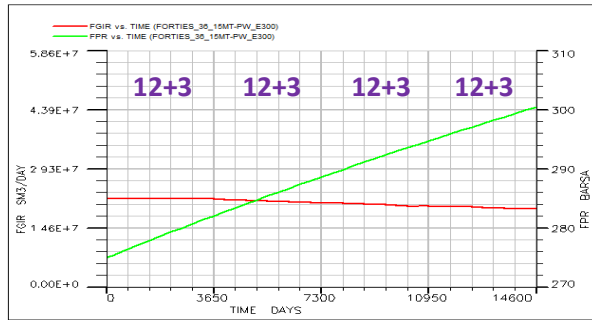
15 Mt/y without water production (base case)



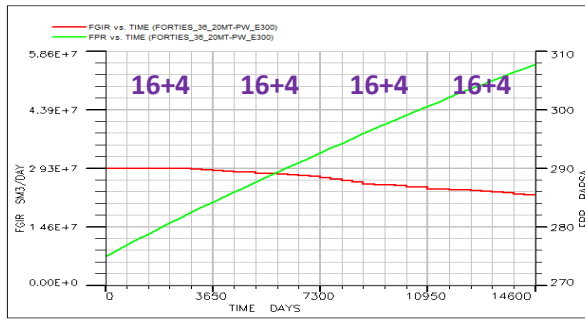
20 Mt/y without water production (base case)



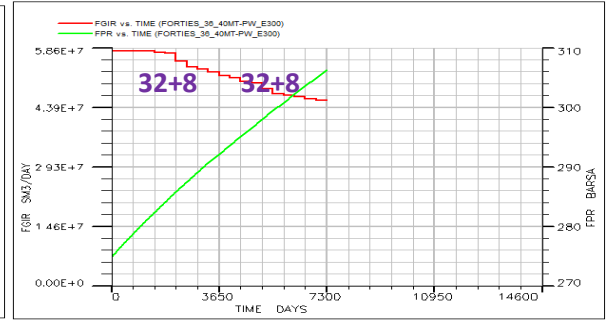
40 Mt/y without water production (base case)



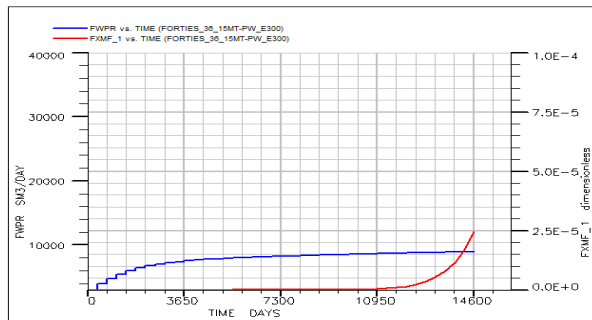
15 Mt/y with water production



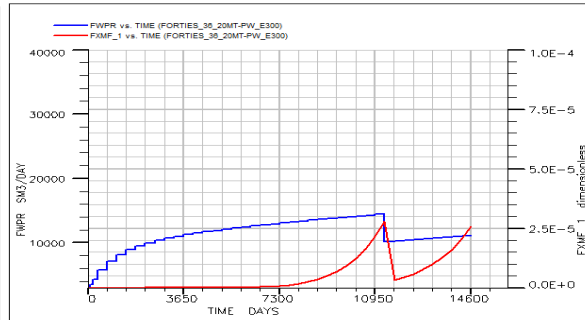
20 Mt/y with water production



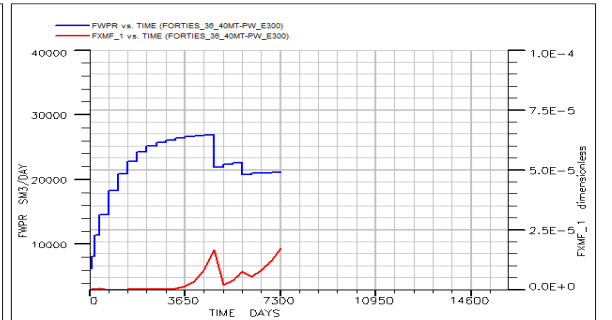
40 Mt/y with water production



15 Mt/y - water production rate & CO₂ mole fraction

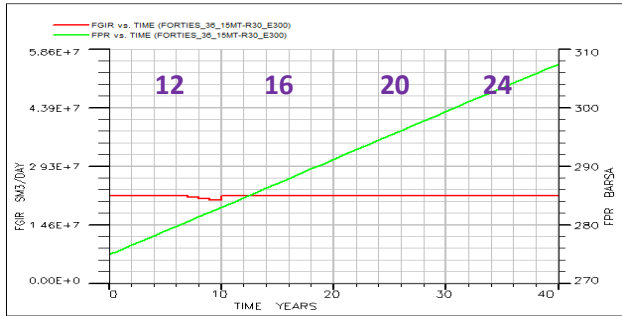


20 Mt/y - water production rate & CO₂ mole fraction

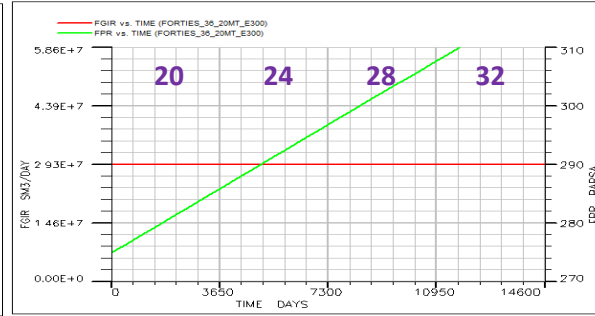


40 Mt/y - water production rate & CO₂ mole fraction

Figure 2-5 Comparison of field CO₂ injection rate (FGIR) and field average pressure (FPR) for each case in base group (top row) and water production group (middle row), and water production rates (FWPR lines in the bottom row) for each case with CO₂ breakthrough vs. time (FXMF lines in the bottom row).



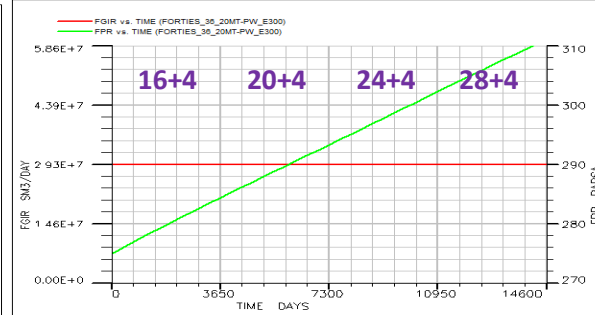
15 Mt/y without water production (base case)



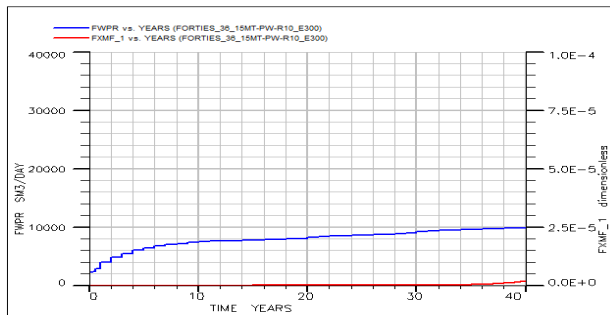
20 Mt/y without water production (base case)



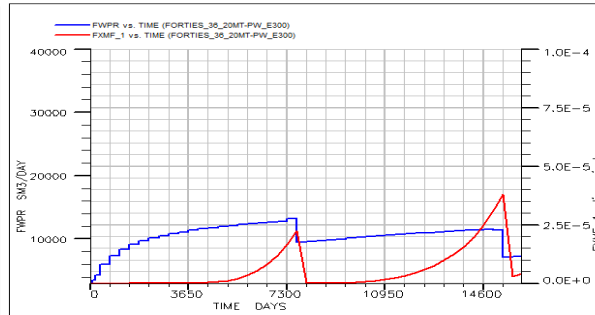
15 Mt/y with water production



20 Mt/y with water production



15 Mt/y - water production rate & CO₂ mole fraction



20 Mt/y - water production rate & CO₂ mole fraction

Figure 2-6 Comparisons for similar cases as for Figure 2-5, but with number of wells increasing with time.

Figure 2-7 shows the distribution of CO₂ after 40 years of injection at a rate of 20 Mt/y, with a constant 16 injection wells and 4 production wells. Cross section AB is identified, and in Figure 2-8 the pressure and dissolved CO₂ in the cross section may be seen.

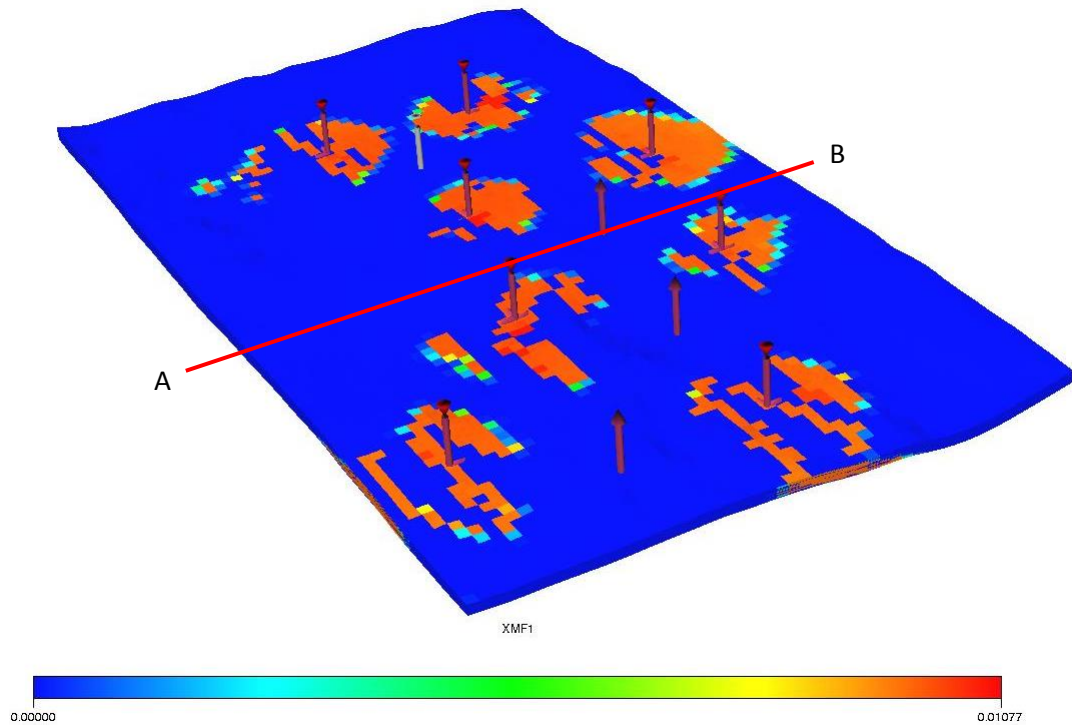


Figure 2-7 Top view (of the top layer of aquifer) showing distribution of dissolved CO₂ after 40 years of injection at a rate of 20 Mt/y with 16 injection wells (in pairs) and 4 production wells.

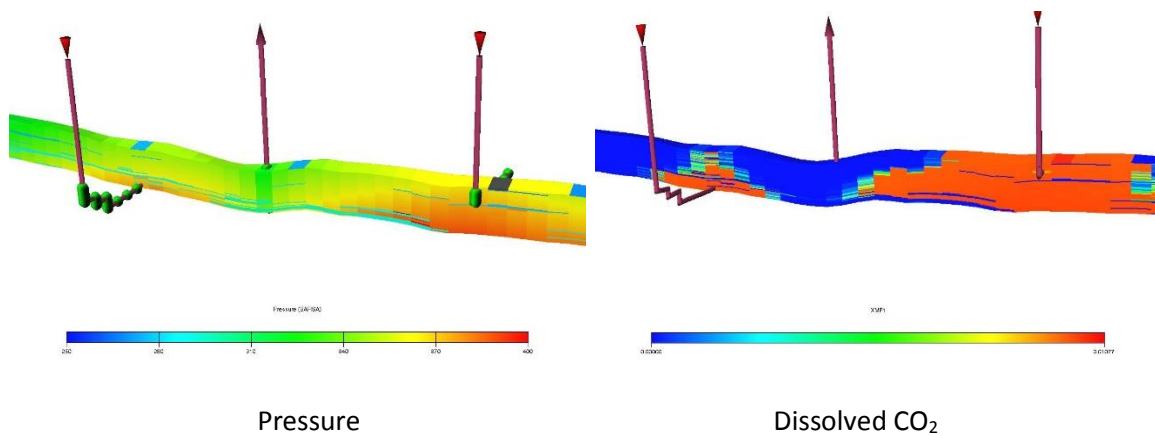


Figure 2-8 Pressure (left) distribution and dissolved CO₂ migration (right) at cross section A-B (shown in Figure 2-7) shortly before the water producer (centre well) was shut down after 30 years in the 20 Mt/y injection scenario.

2.3 Summary

The benefits of water production in the Forties system are evident from the results of these and other simulations conducted as part of this study. They may be listed as follows:

- The local pressure around the wells is reduced and a constant injection rate can be maintained for longer without addition of more wells.
- The average field pressure is reduced to the extent that the storage capacity of the Forties aquifer can be increased by two thirds (from 120 Mt to 200 Mt) in the high permeability model.
- It is most effective in the cases with intermediate injection rates (10-20 Mt/y).
- It is not necessary for the cases with low injection rates (≤ 5 Mt/y) because the aquifer is large enough that additional injectors may be drilled to maximise capacity.
- Quick breakthrough of CO₂ at the water producers reduces usefulness at high injection rates (≥ 40 Mt/y).
- Ratios of injectors to producers from 2:1 to 10:1 were tested in the study. The results show that a lower ratio is required for the cases with higher injection rates, especially at the beginning of the injection period - this may be attributed to a more rapid buildup in pressure and therefore production wells will produce at higher rates, relieving pressure more quickly; however, typically earlier breakthrough of CO₂ will occur.
- Converting producers into injectors when CO₂ breakthrough occurs is a way to reduce drilling costs, but if no additional producers are then added the newly converted injectors will only function for a short period because after years of injection the margin for allowable pressure increase is already low.

3 Bunter Model

Figure 3-1 shows the Bunter formation with structural closures, in which the red rectangle shows the region of study (including four closures) and the black boundary identifies a larger section thought to be in pressure communication and named Zone 4 (unit 139.000) in the CO₂Stored database that includes 50 closures. Closure 36 (within the red rectangle) is the injection site studied in Phase I and is assumed to be well connected with the other closures in the whole of Zone 4. The Bunter model used in Phase I was developed based on the geological model for the area within the red triangle, and included numerical aquifers at the boundaries so that the pore volume of the model is equivalent to the total pore volume of Zone 4. The constraint for the capacity of Closure 36 is thus not pressure (since the system permeability is high and the total connected pore volume is very large), but the leakage of CO₂ from the structural trap.

Closure 36 in the red rectangle in Figure 3-1 is the closure that the PBD model is based on. The HW model considers the whole volume within the red rectangle.

Even though the Bunter Sandstone is hydrostatically pressured and is assumed to subcrop to the sea bed to the south east of the area of investigation, as shown in Figure 3-1, there is the possibility that baffles are present, such as salt walls, fault zones, dykes, and cemented zones (as illustrated in Figure 3-2). In Phase II of the study being reported here, the uncertainty in the Bunter connectivity was simulated by modifying the model to add baffles between Closure 36 and its neighbours, and by adding a shale layer to separate the various vertical intervals. In the first case to be modelled a baffle was located between Dome 36 and Dome 37, the latter being to the north east of Dome 36, but CO₂ could still be displaced to the north west and to the south east. The second case is more severe, in which Dome 36 is completely surrounded by a permeable Dyke. The consequence would be a situation in which, after several years of injection of CO₂, further injection could not be maintained because the pressure in the dome would reach a predetermined limiting value. Thus the limit on storage capacity would cease to be the risk of CO₂ migration beyond a spill point, and would now become a pressure constraint. Evidently pressure management by water production might be a means of addressing this limitation on injection. In this second scenario a post injection brine production period was also considered to estimate the potential to reduce the risk of formation failure during the immediate period after CO₂ injection has ceased.

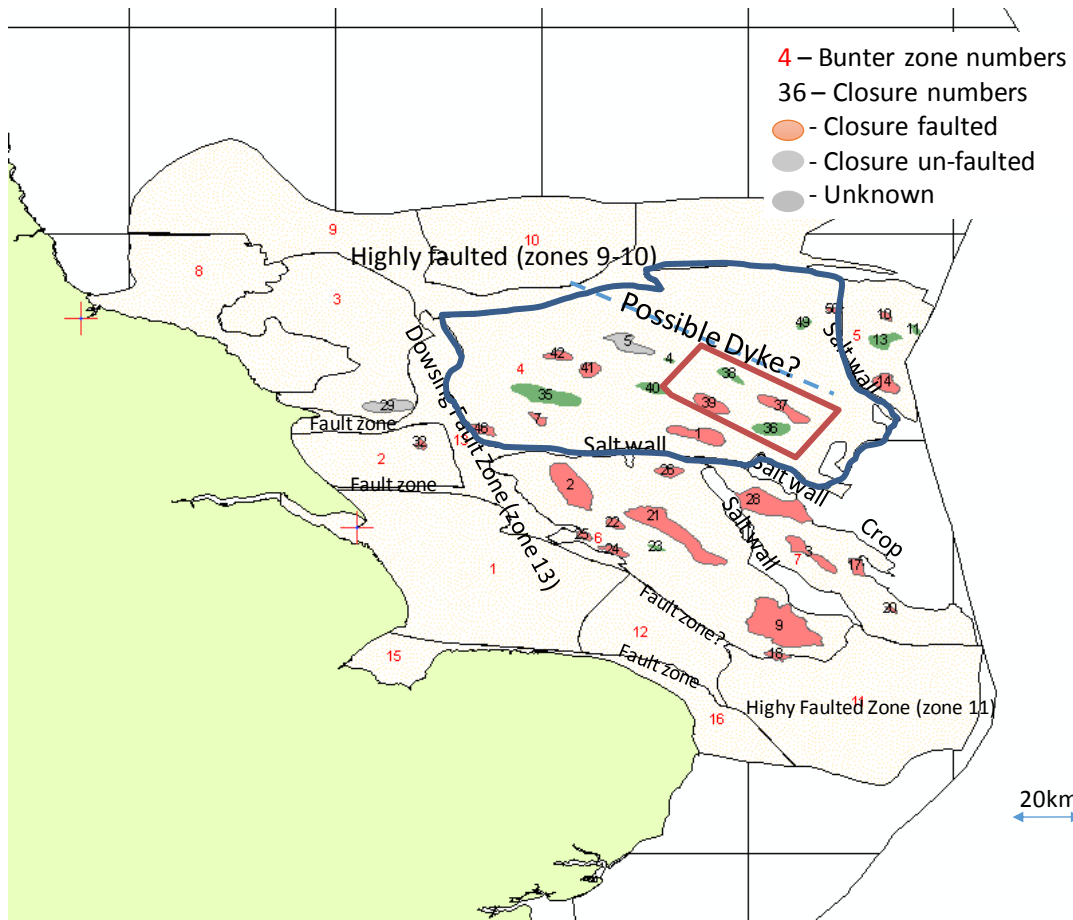


Figure 3-1 Bunter formation with structural closures, in which the red rectangle shows the area of study and the black boundary outside the section identifies a region thought to be in pressure communication, which is referred to as Zone 4 (unit 139.000) in the CO₂Stored database.

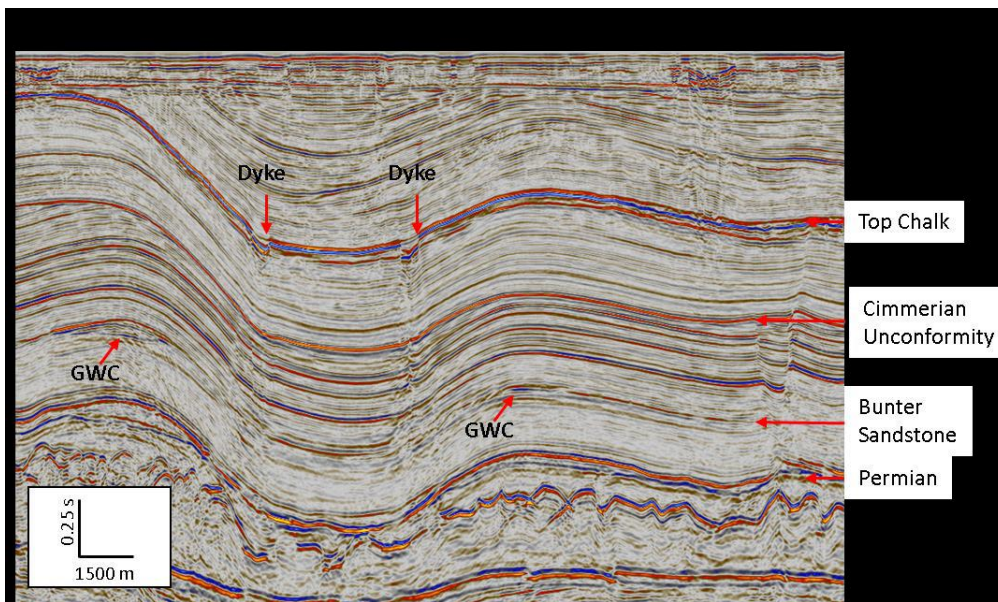


Figure 3-2 Seismic showing the existence of a dyke in the Bunter Sandstone. (GWC identifies a gas water contact, and thus the presence of a hydrocarbon trap.)

3.1 Modified Bunter Models with a Partially or a Fully Sealing Boundary

The Bunter model previously developed for this study was modified to include an internal vertical boundary to represent a fault. In the first instance this boundary was treated as partially sealing. As shown in Figure 3-3, permeability in some cells between Dome 36 and Dome 37 were set manually to be a low value so it formed a barrier between the two domes. Flow directly between the two domes were not possible, but flow round the barrier was still possible and the pressure could still be relieved by the volume of Dome 37.

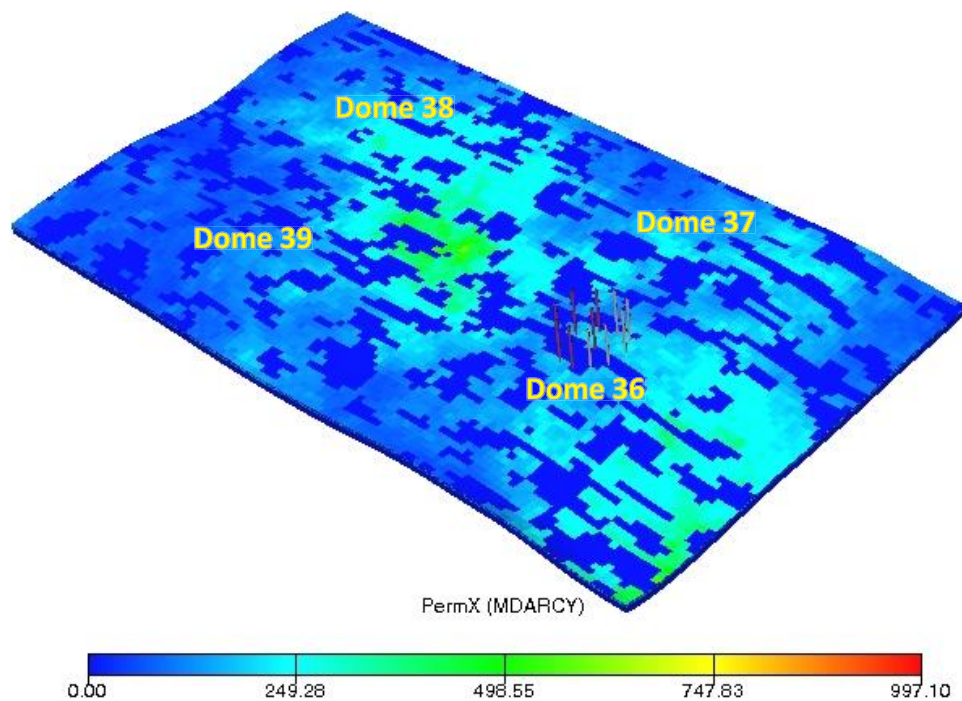


Figure 3-3 Permeability distribution in Bunter model: a low permeability barrier has been placed between D36 and D37, but the domes would remain connected through other domes.

Five injectors (I1-I5) were set in a half circle, as shown in Figure 3-3, with a well at the crest of the dome to monitor the pressure at the shallowest point, with a view to controlling injection rate and preventing failure of the cap rock.

Figure 3-4 shows the result from the base case without water production. Comparing it with the results from Phase I, in which only 4 injectors (I1-I4) were used for the first two decades, the impact of the barrier on pressure redistribution is such that more wells are required to (unsuccessfully) attempt to maintain the injection rate. Pressure build up was much quicker than in the case without the barrier, and due to a resulting convergence problem, brought on by the contrast of the high and low permeability cells, the simulation became very CPU intensive and was stopped after 30 years. The

presence of the partially sealing fault between domes D36 and D37 also causes the CO₂ to be displaced away from D37 (see Figure 3-5) to a greater extent that occurred in the Phase 1 modelling, where the limitation on injection was not pressure but CO₂ being displaced beyond the spill point separating D36 and D37.

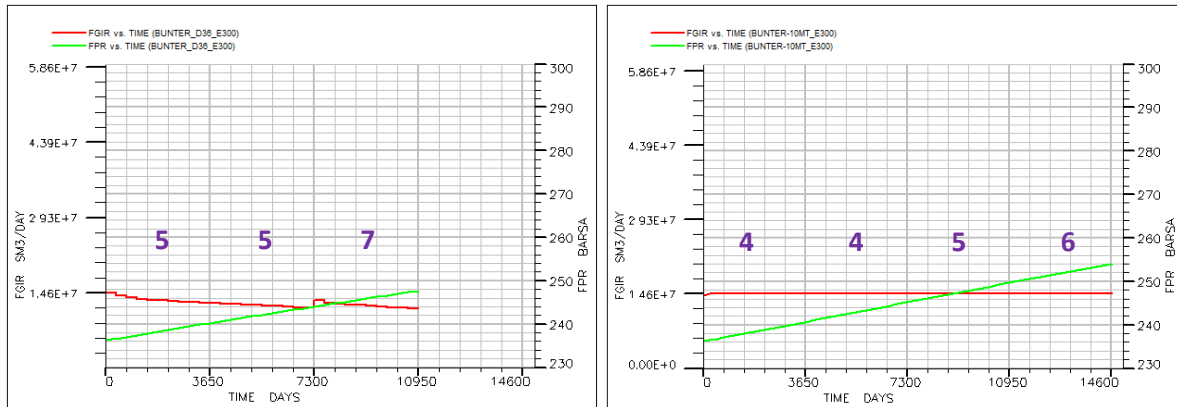


Figure 3-4 Field CO₂ injection rate (FGIR) and field average pressure (FPR), with the number of injectors in each 10 year period identified. The left diagram shows the result from the Phase II model with the partially sealing fault, and the right diagram shows the results from Phase I model with no fault. The presence of the partially sealing fault meant the injection rate of 10 Mt/y could not be maintained, even with a greater number of wells, whereas in the absence of the fault it could be maintained.

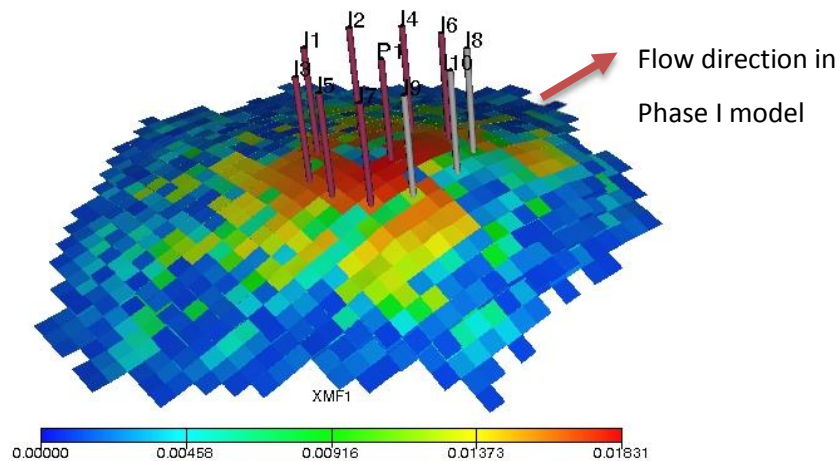


Figure 3-5 Zone where dissolved CO₂ (XMF1) is located after 30 years of injection in the scenario with a partially sealing fault. The flow towards D37 observed in the Phase 1 modelling is now blocked by the fault, and so there is more displacement in the opposite direction.

Table 3-1 shows the model parameters.

Table 3-1 Comparison of parameters in Bunter Models and CO₂Stored database

Parameter	Units	PBD E100 Model	Bunter Closure 36 (139.016)*	HW E300 Model	Bunter Zone 4 (139.000)
Area	km ²	664	71.1	1,108	11,640
average thickness	m	235	221	260	198
model dimensions	km	24.8x26.8		44x25.2	
cell dimensions in x & y	m	200 x 200		400 x 400	
cell dimensions in z	m	varying		varying	
number of cells		124x134 x41		110x63 x65	
total number of cells		681,256		450,450	
number of active cells		603,364		429,660	
average dip angle	deg.	7	6.6		4.64
average porosity	frac.	0.175	0.17	0.144	0.14
average horizontal permeability	mD	152	50	188	100
average vertical permeability	mD	35	50	188	100
average net to gross	frac.		0.91		0.91
total pore volume	m ³	2.68x10 ¹¹	2.40x10 ⁰⁹	3.07x10 ¹¹	2.798x10 ¹¹
rock compressibility	1/bar	5.57x10 ⁻⁰⁵	5.69x10 ⁻⁰⁵	5.57x10 ⁻⁰⁵	6.20x10 ⁻⁰⁵
water compressibility	1/bar			4.0x10 ⁻⁰⁵	3.54x10 ⁻⁰⁵
initial pressure	bar	121	158	155	160
datum depth	m	1,211	1,569	1,450	1,591
fracture pressure	bar	183.4	277	210	171
CO ₂ density	kg/m ³		847.5		325
brine viscosity	cP				0.39
CO ₂ viscosity	cP				0.0296
Salinity	ppm	200,000	180,000	213,500	180,000
temperature	deg C	45	43.3	62	62
pore volume utilisation	frac.		0.118		0.59
theoretical capacity	Mt		248		436
dynamic utilisation	Mt		200		400
maximum injection rate	Mt/y	7		40	
injection period	y	56		40	
monitoring period	y	0		1,000	

* Data from www.co2stored.co.uk, P50 value used

The closed boundary model was established by defining the cells in three quarters of the model to be inactive, as shown in Figure 3-6. The blue rectangle shows the boundary of the Phase I model before modification. The visible part of the model is the active part (inactive cells are not visible).

Since the boundary of the model is now closed, the total volume of the model is no longer the volume of Zone 4, but is the volume of the visible portion of the model only. Three injectors and three producers were used, as shown in Figure 3-6. As for the previous Bunter model, all wells are vertical wells. The injectors, located 2 km from the centre of the dome, were completed between layers 8 and 62, and the producers, 4 to 8 km from the centre of the dome, were complete at the bottom of the formation (layers 53 to 62). The field injection rate is 5 Mt/y, which is calculated accounting for the total pore volume of the model, the rock compressibility, and the allowable pressure increase.

Figure 3-7 shows a comparison of field CO₂ injection rate (FGIR) in surface volume units (sm³/day) for the model without water production (solid red) and with production (dotted pink line). Field total volume of injected CO₂ (FGIT) in surface units (sm³) for the model without water production (solid light green) and with production (dotted green line) are also shown in the figure. As shown in Figure 3-7 the constant injection rate can only be maintained for 8 years without water production, but with water production the CO₂ injection rate of 5 Mt/y was maintained for 40 years.

The field pressure curve coloured light green in Figure 3-8 shows a balance between injected volume and produced volume was reached so that the average pressure were not increased in the simulation of injection with brine production. This dynamic balance should be maintained at least until CO₂ breakthrough, since the leakage constraints at spill points were relevant in the closed site, but instead the limit on injection capacity was determined by the pressure response. The key water production rates in the closed structure are shown in Figure 3-8. With water production the total injected volume of CO₂ was increased by at least four times, but the field average pressure increase was only half that in the case without brine production.

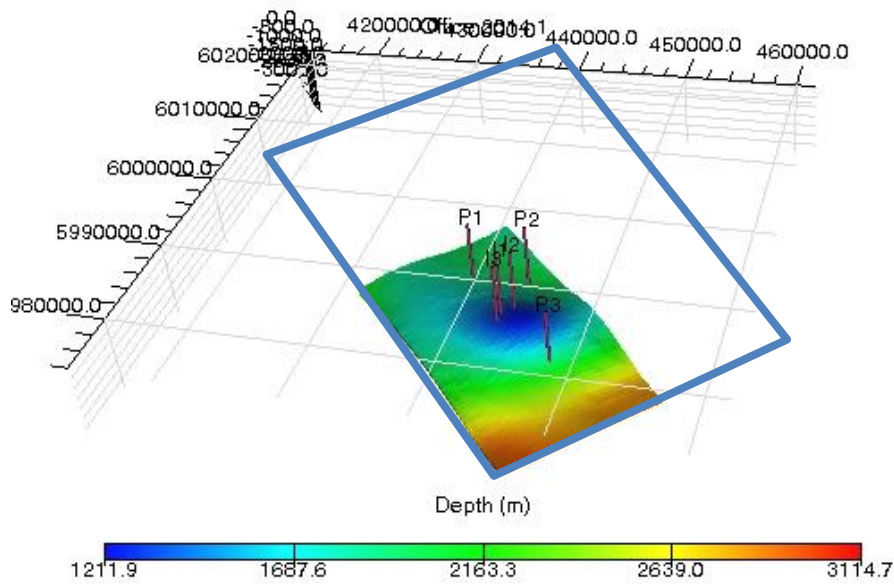


Figure 3-6 Depth map for the Bunter_D36 model, showing the shape of Dome 36 with a closed boundary. The injectors, 2 km from the centre of the dome, were completed between layers 8 and 62, and the producers, 4 to 8 km from the centre of the dome, were complete at the bottom of the formation (in layers 53 to 62). The blue rectangle identifies the boundary of the Phase 1 model, with the blank zone within the blue triangle now deactivated cells in this Phase 2 modelling - representing the impact of sealing faults between Dome D36 and all the neighbouring domes.

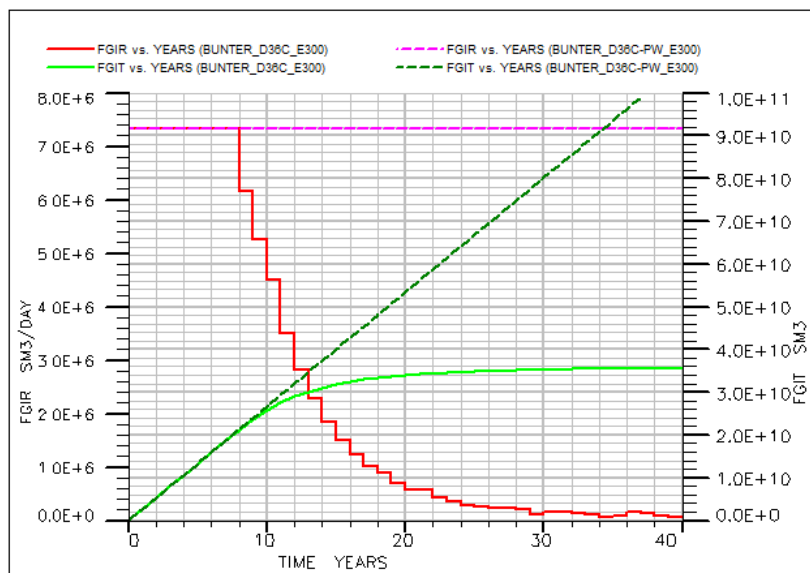


Figure 3-7 Field CO₂ injection rate (FGIR) in surface units (sm³/day) for the model without water production (solid red line) and for the model with production (dotted pink line). Field total volume of injected CO₂ (FGIT) in surface units (sm³) for the model without water production (solid light green) and for the model with production (dotted dark green line).

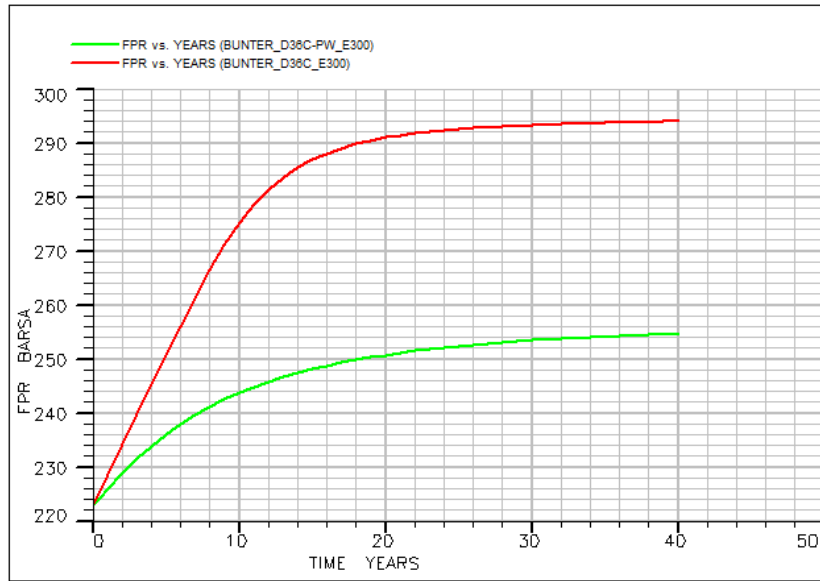


Figure 3-8 Field average pressure (FPR) for the Bunter-D36 model without (red) and with (green) water production. Note that water production significantly impacts the increase in pressure

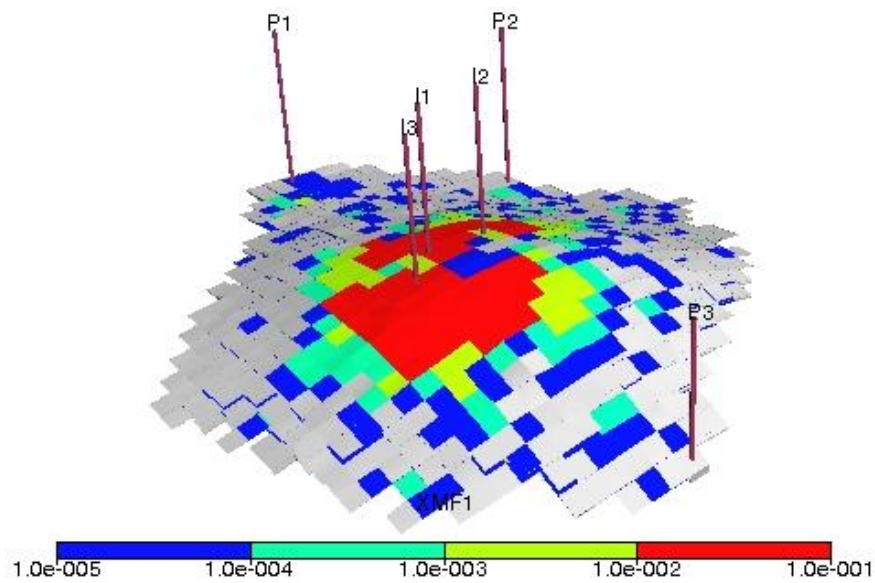


Figure 3-9 Distribution of dissolved CO₂ (XMF1) in the aqueous phase after 18 years of injection in the model with water production. Note the use of a log scale to show the location of the three producers P1, P2 and P3 to be within the zone of influence, but at this time CO₂ breakthrough has not yet occurred, as determined by the criterion that the model fraction of CO₂ in the aqueous phase must exceed 1×10^{-4} .

Two additional simulations have been completed using this model: one for the model without water production, and one for the model with water production. The purpose was to test the impact of

moving the injectors away from the crest of the dome to reduce the risk of failure of the caprock at the shallowest point. The shallowest point is chosen because this is where the confining pressure will be the lowest and potentially buoyancy effects will be greatest. As shown in Figure 3-10, when the total number of injectors is increased from 3 to 6 wells, and when all of the injectors are moved to deeper locations (from 1,300m to 1,600m), the period of constant rate injection increases from 8 to 12 years. In both models the injection wells cease injection because the pressure in the monitor at the crest of the dome reaches the predetermined limit.

The second model was developed to test the impact of reducing by one the number of producers in the water production case in order that the total number of wells (3 injectors and 2 producers) should become less than in the case with no producers (FILL-2 with 6 injectors). When only two producers were used the well production rates were increased for each well, but nonetheless the total field production rate was reduced since the wells are controlled by pressure, and one injector was not in sufficient communication with the producers to receive adequate pressure relief. As a consequence the constant injection rate of 5 Mt/y was only maintained for 23 years. Based on this simulation, the price to pay for the reduction in the number of producers is the loss of half of the storage capacity.

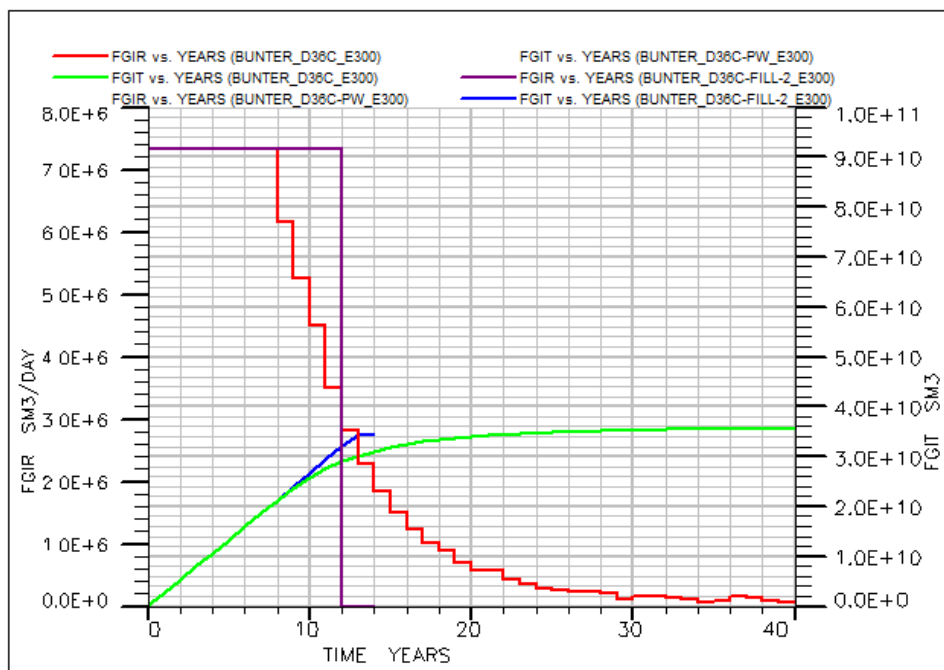


Figure 3-10 Field CO₂ injection rate (**FGIR**) and field CO₂ injection total (**FGIT**) for models without water production. When the total number of injectors is increase from 3 (BUNTER_D36C_E300) to 6 (BUNTER_D36C-Fill-2_E300), and when all of the injectors are moved to a deeper location (from 1,300m to 1,600m), the period of constant injection rate was extended from 8 to 12 years. The injection wells ceased operation when the well monitoring pressure at the top of the dome reached its preset limit. In both cases this occurs when nearly 60Mt has been injected.

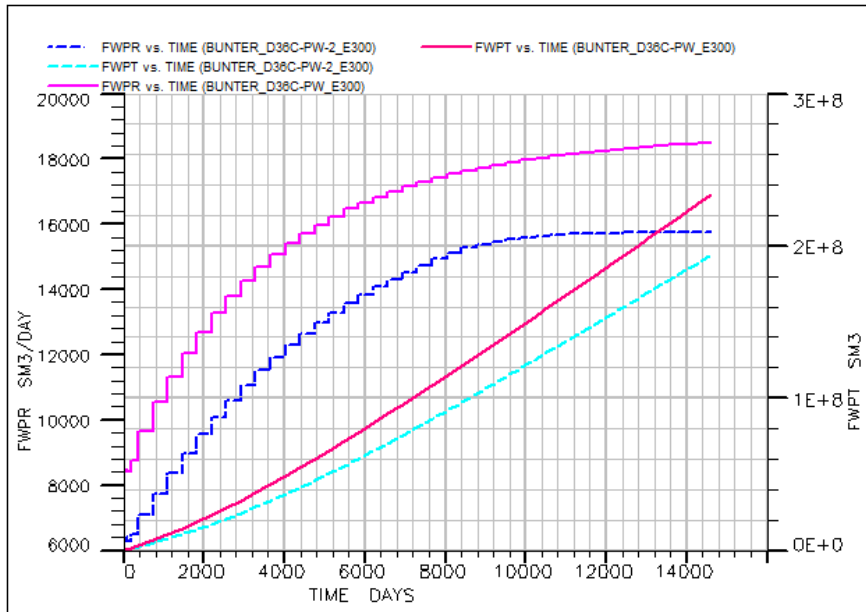


Figure 3-11 Comparison of field water production rate (**FWPR**) and field total water production (**FWPT**) for two cases in which there are three injectors, but in one there are three producers (BUNTER_D36C-PW_E300) and in the other only two producers (BUNTER_D36C-PW-2_E300). The former can inject 5Mt/y for more than 40 years, but the latter can only do so for 23 years.

3.2 Post Injection Brine Production (PIBP)

The value of post injection brine production (PIBP) is to reduce the risk of formation failure after CO₂ injection has ceased due to elevated pressure relative to the original reservoir pressure. Brine production in a model of the Bunter formation where poor connectivity is assumed has significantly increased the storage capacity, as shown in Figure 3-7, and reduced the impact of CO₂ injection on the field average pressure, as shown in Figure 3-8. If water producers are kept open for 10 years after CO₂ injection, then brine production continues to occur due to the over pressure, but serves to decrease the field average pressure. Figure 3-12 gives a comparison of the change in field average pressure (FPR) over 50 years for the CO₂ injection scenario without water production, including 40 years of CO₂ injection and then 10 years after CO₂ injection gas stopped, and compares this with a similar scenario, but where there is water production throughout the 50 year period. The ultimate change in average pressure over the 50 year period when there is water production is only about 8 bars, despite injection of 200 Mt of CO₂ into the formation. However, without water production, the pressure increase is 70 bars and only 60 Mt of CO₂ was injected. This 70 bars pressure increase is approaching the critical value (1.4 times of initial pressure) for rock failure.

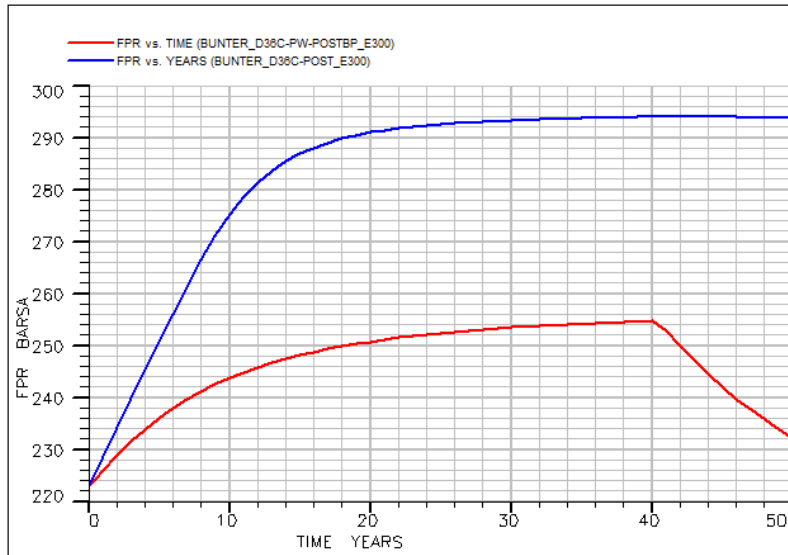


Figure 3-12 comparison of field average pressure (**FPR**) in the case without (**blue**) and with (**red**) water production and post-injection water production. The ultimate change in average pressure over the 50 year period is 8 bars when there is water production and 70 bars when there is not.

From the breakthrough and subsequent increase in mole fraction of produced gas, shown in Figure 3-13, it is evident that some dissolved CO₂ is displaced with brine towards the producer. However, only a small amount is produced, and the value is below the threshold set for the model (10^{-4}) at which the production well would be shut in, so the water producers can operate for the full 10 year post-injection period.

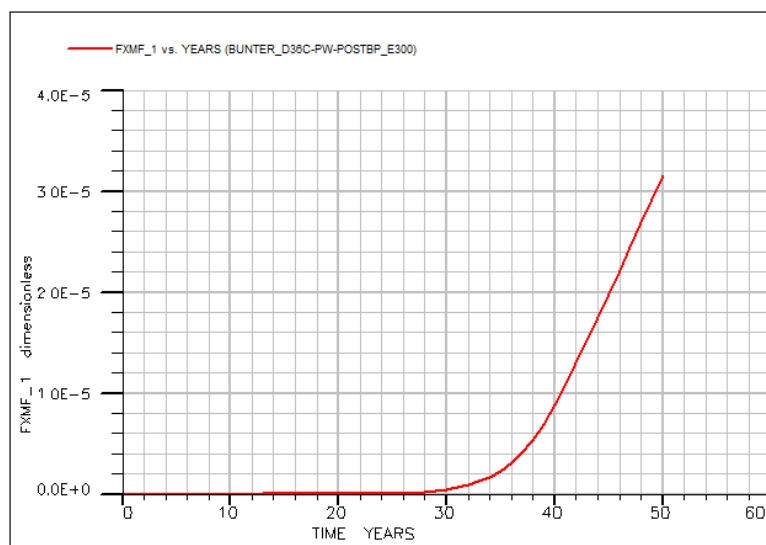


Figure 3-13 Total mole fraction of CO₂ in the produced water stream (**FXMF_1**) over 50 years, showing a potential for CO₂ breakthrough, but in such small amounts that the limit set of $FXMF_1=10^{-4}$ is not exceeded.

Because the field average pressure reduces to close to the initial pressure, there is decreasing energy available to lift the water to surface, and so the water production rate also reduces, as shown in Figure 3-14. This consequently also reduces the production of CO₂ compared to a scenario where the well would be flowed (by artificial lift) at a constant rate, say.

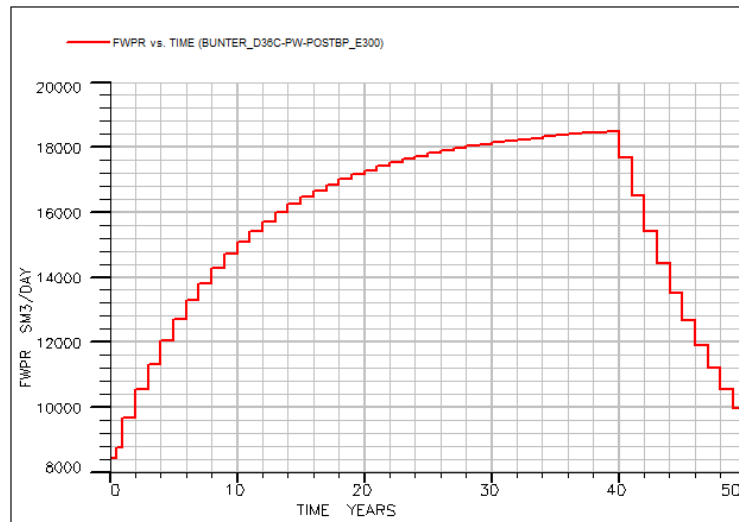


Figure 3-14 Field water production rate (**FWPR**) increases during CO₂ injection as there is increasing energy to lift the water to surface, but then reduces after the cessation of CO₂ injection because there is reducing energy in the system (and from Figure 3-13 it is evident that the reduction in water rate is not due to water production being replaced by CO₂ production).

3.3 Delayed Water Production

From Figure 3-14 it can be seen that the rate of water production is not high at the beginning of the CO₂ injection period - this being because the field average pressure has not increased greatly yet. Thus a delay in the commencement of brine production may not impact the effectiveness of brine production, but may improve the project economics. Simulations were performed using the Bunter model to compare the base case (brine production starts when CO₂ injection starts) with cases where water production starts after 5 years of injection, and separately after 10 years injection. Figure 3-15 shows water production rates in these simulations. Due to the pressure building up over time, the later the water production starts, the higher will be the initial production rate. Figure 3-16 shows the CO₂ injection rates in models without water production, when water production commences at the same time as CO₂ injection starts, when water production starts 5 years later and when it starts 10 years later. For a 10 year delay in brine production, the CO₂ injection rate profile will follow the profile from the model without water production for those 10 years, as would be expected, but then the

injection rate recovers within 2 years to the value it would have had if water production had commenced at the start of the simulation. This is important, because it means that if poor connectivity is identified *after* an initial period of injection, then brine production may be considered as an option to mitigate the resulting lowering of injectivity. The model with a 5 year delay in brine production is able to maintain a constant CO₂ injection rate and the maximum brine production rate is at no time greater than the maximum brine production rate in the model with brine production from the outset, so the brine production facilities can have the same specifications.

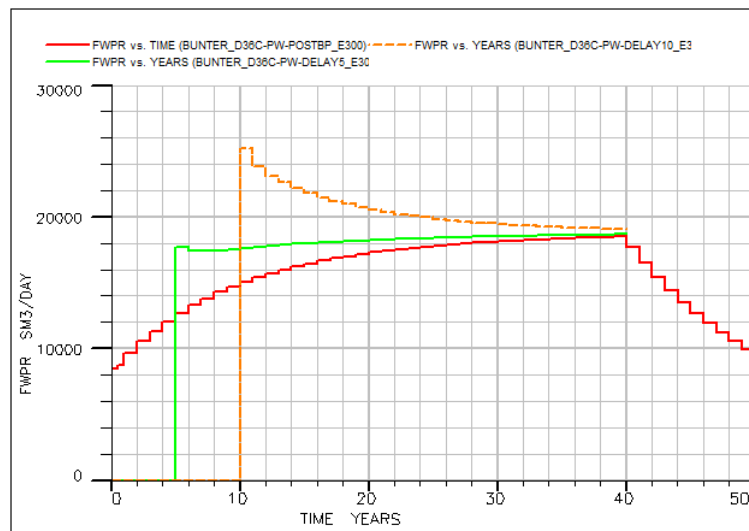


Figure 3-15 Field water production rate (**FWPR**) vs time in models where brine production commences at the same time as CO₂ injection starts (**red**), 5 years after CO₂ injection starts (**green**), and 10 years after CO₂ injection starts (**dashed orange**).

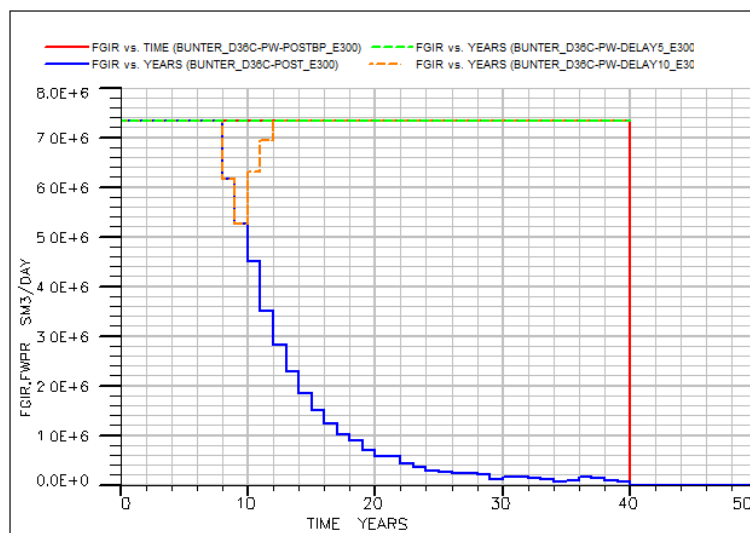


Figure 3-16 Field CO₂ injection rate (**FGIR**) in the model where there is no brine production (**blue**), and in models where brine production commences at the same time as CO₂ injection starts (**red**), 5 years after CO₂ injection starts (**green**), and 10 years after CO₂ injection starts (**dashed orange**).

The change of well bottom hole pressure in the injection well clearly indicates the impact of water production in the reservoir. Figure 3-17 compares well bottom hole pressure in injector I1 for the four scenarios illustrated in Figure 3-16. The maximum allowable pressure in the well is 210 bars: if the injector pressure reaches this value the well will be changed from rate control to constant pressure control, which explains why the injection rate subsequently declines (as was shown in Figure 3-16).

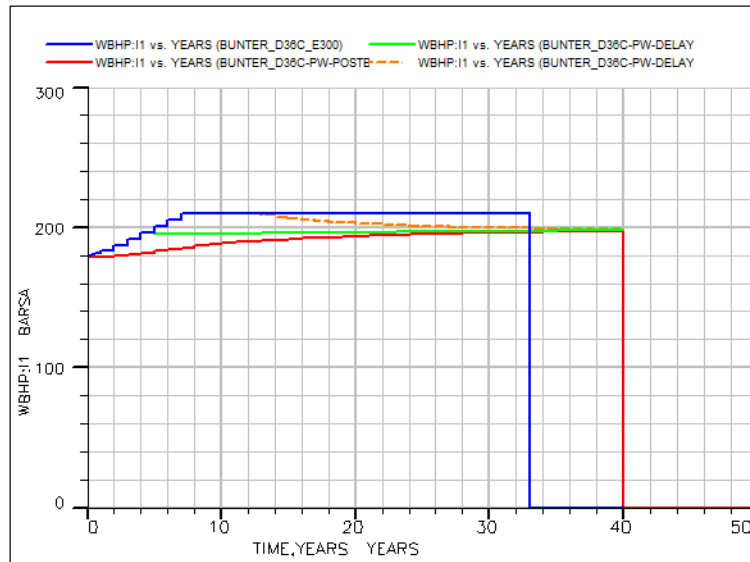


Figure 3-17 Well bottom hole pressure (**WBHP**) for injector I1 in the model where there is no brine production (**blue**), and in models where brine production commences at the same time as CO₂ injection starts (**red**), 5 years after CO₂ injection starts (**green**), and 10 years after CO₂ injection starts (**dashed orange**). The maximum allowable pressure is 210 bars.

These results clearly indicate that brine production in this scenario may be used very effectively to increase storage capacity, but that the decision to implement it may be left till *after* field data on CO₂ injectivity has been collected and the pressure response of the system assessed to identify whether in fact brine production is required or not.

3.4 Impact of Compartmentalisation on CO₂ Storage Characteristics in the Bunter Formation

It has been shown that brine production from the completely isolated Dome 36 can increase total CO₂ storage capacity by nearly four times while reducing final storage pressure. The CO₂ storage response

in Dome 36 could be different if this dome is not fully isolated and a degree of pressure communication between this structure and the rest of the Bunter formation can be established. The aim of the simulations conducted in this section is, therefore, to investigate the CO₂ storage characteristics in a compartmentalised Bunter formation with and without brine production. Compartmentalisation affects the net pore volume that is directly accessible for CO₂ storage by creating barrier between storage complex and the rest of formation's pore volume. Unexpected compartmentalisation, if it occurs, may dramatically increase the pressure response upon CO₂ injection and will adversely affect the storage potential. The uncertainty associated with compartmentalisation may be characterised by two important features; first, the size of the compartment i.e. the net pore volume of the storage complex and second, the sealing ability of the compartment i.e. the degree of hydraulic communication between either sides of a fault bounding the compartment.

To address the impact of compartmentalisation, CO₂ storage in Dome 36 is simulated when it is assumed two vertical faults limit hydraulic communication between Dome 36 and other surrounding structures. Figure 3-18 shows the location of these two faults; the faults pass through the spill points between Dome 36 and the nearby structures.

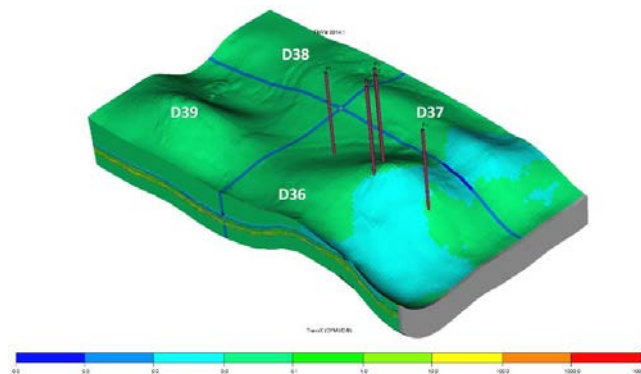


Figure 3-18: Location of the vertical faults in the Bunter model. The image of the model has been exaggerated by a factor of 3 in the vertical direction. CO₂ is only injected into Dome 36.

Different degrees of communication across the faults will be investigated, in models both with and without brine production. The fault transmissibility multipliers modelled are in the range 0 to 1, corresponding to complete barriers and perfectly conducting faults, respectively. Complete barriers will prevent all flow and all pressure transmission. Partial barriers (even very low values of the transmissibility multiplier) may allow some degree of pressure transmission but will very significantly impair flow. Other simulation parameters are as before. No aquifer is connected to this model; introduction of an aquifer would make the results less sensitive to compartmentalisation, as will be

illustrated later (Section 3.6). Another issue studied is the impact of fault locations relative to Dome 36 (by $\pm 800\text{m}$) - affecting the size of the compartment.

Figure 3-19 compares CO₂ injection rates and cumulative injected CO₂ for different magnitudes of fault transmissibility multipliers without (left) and with (right) brine production.

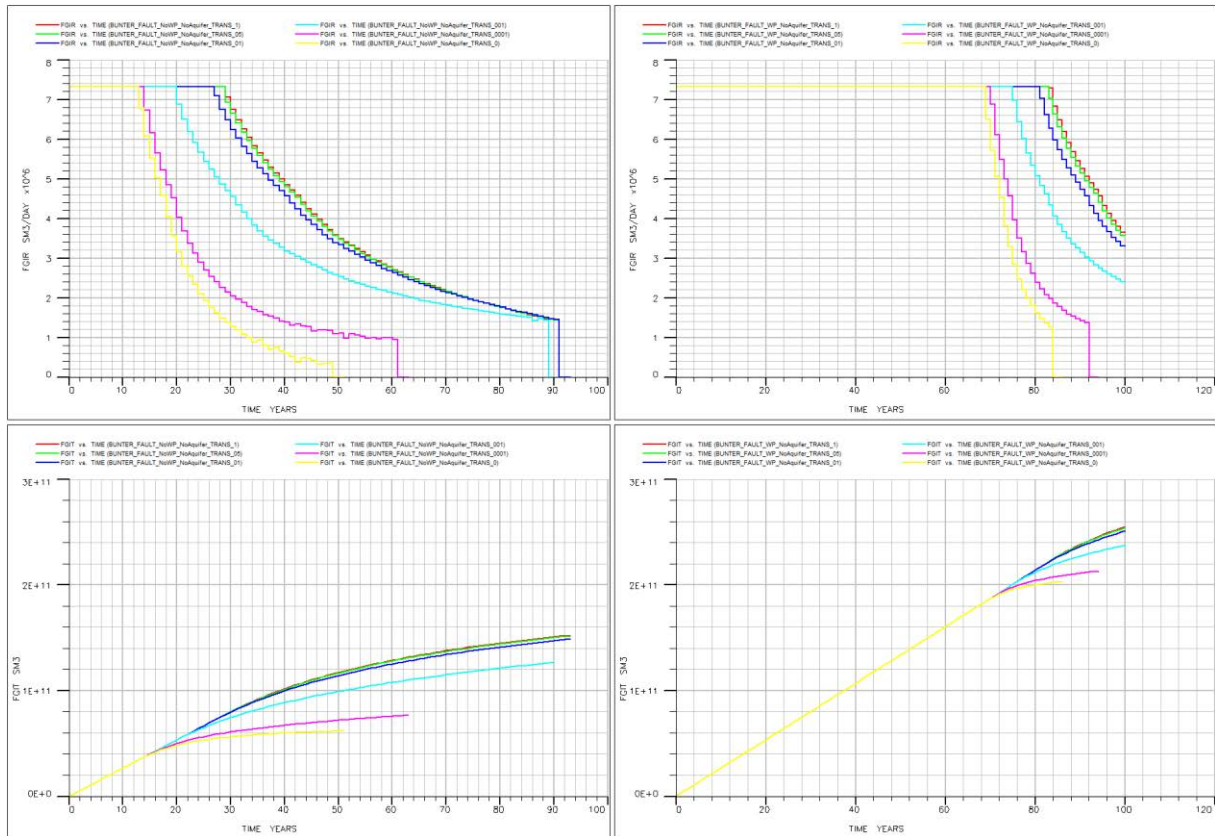


Figure 3-19: Field CO₂ injection rate (**FGIR** - top) and cumulative stored CO₂ (**FGIT** - bottom) without (left) and with (right) brine production, for various values of fault transmissibility multiplier ranging from 0 to 1.

Fault transmissibility significantly affects the overall storage of CO₂ for scenarios where there is *no brine production* and CO₂ storage is dependent on the pressure response of the formation. Fault transmissibilities become important only after a period of injection, once CO₂ storage capacity becomes dependent on the pressure response of the storage complex. Brine production significantly reduces the impact of low fault transmissibilities, which then only becomes apparent at even later times. For scenarios with brine production this dependency occurs after very long times e.g. beyond 60 years (possibly after CO₂ breakthrough in the brine production wells), whereas for scenarios without brine production, the impact of fault transmissibility is evident at much earlier times scales (after 20-30 years).

Figure 3-20 compares the ultimate stored CO₂ at the end of simulations both with and without brine production for the extremes values of fault transmissibility multipliers (i.e. 0 and 1). It can be seen that first, the cumulative stored CO₂ is significantly larger with brine production and second, the range of ultimate stored CO₂ is smaller which means that ultimate CO₂ storage is less sensitive to the degree of fault transmissibility.

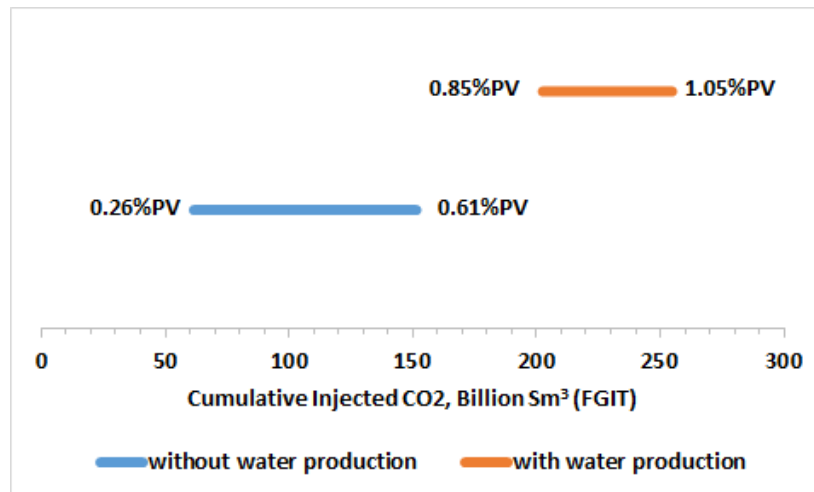


Figure 3-20: Ranges of stored CO₂ without (blue) and with (orange) water production. Individual numbers show cumulative injected CO₂ relative to the pore volume in Dome 36 for different magnitudes of fault transmissibilities ranging from 0 to 1.

Figure 3-20 shows that the ultimate stored CO₂ in Dome 36, when the fault transmissibility is set to zero but brine production has been undertaken (0.85% PV), is larger than the case where there is no brine production but full communication can be established between Dome 36 and other structures (0.61% PV).

Figure 3-21 compares the profiles of dissolved CO₂ in the brine phase at the end of the simulations and at the extremes of fault transmissibility multipliers (i.e. 0 and 1). While for the scenarios without brine production, a relative difference between the sizes of the plumes can be identified, they are almost identical when brine production has been undertaken.

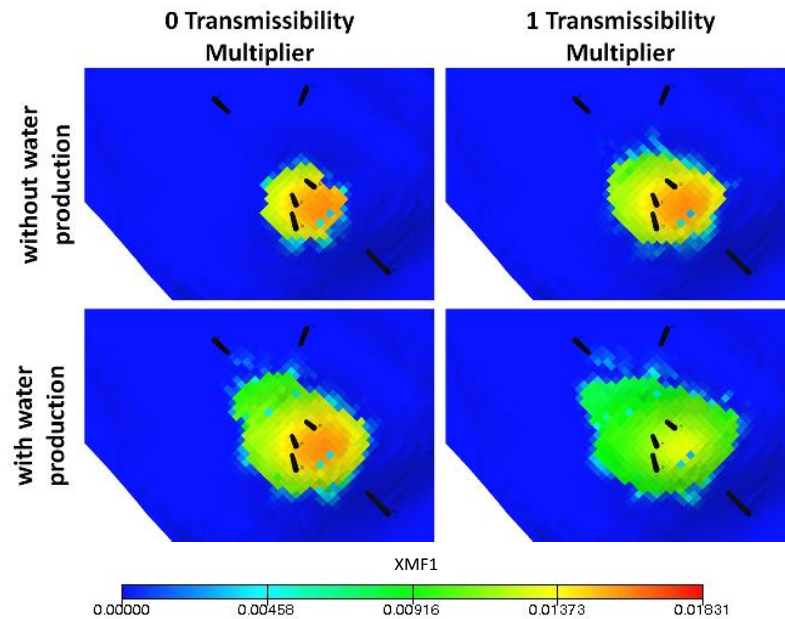


Figure 3-21: Profile of dissolved CO₂ in the brine phase; comparison at the end of the simulations. The top layer is viewed from directly above.

Brine production ensures sufficient voidage for the storage system, which consequently makes CO₂ storage less dependent on the characteristics of the compartment. This indicates that brine production is an effective measure in mitigating the risk associated with the uncertainty in characterising faults (i.e. their extent and sealing capacity) provided that brine production and CO₂ injection wells are in appropriate communication with each other.

Figure 3-22 compares the evolution of pressure in Dome 36 without (left) and with (right) brine production. Again the impact of fault transmissibility on the evolution of pressure is important when there is no brine production and CO₂ storage is only dependent on the pressure response of the storage complex. Note that, with brine production, the evolution of pressure in Dome 36 is not significantly different for various fault transmissibility scenarios *before* shutting-in of brine production wells (right image). However, after CO₂ breakthrough, the pressure profiles become quite different between different scenarios, indicating that storage is now dependent on the pressure response and that the fault transmissibilities are now important, similar to the scenario with no brine production from the outset.

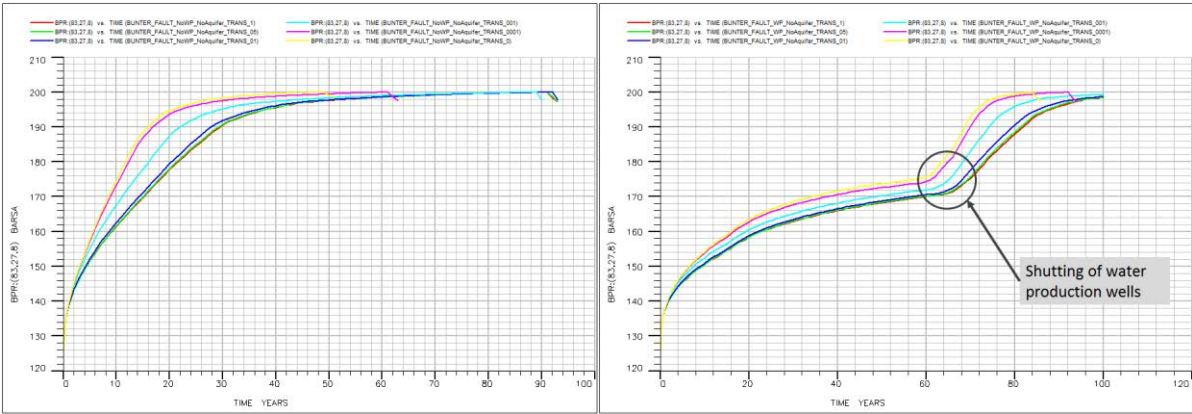


Figure 3-22: Evolution of field average pressure (FPR) in Dome 36 without (left) and with (right) brine production, for various values of fault transmissibility multiplier ranging from 0 to 1.

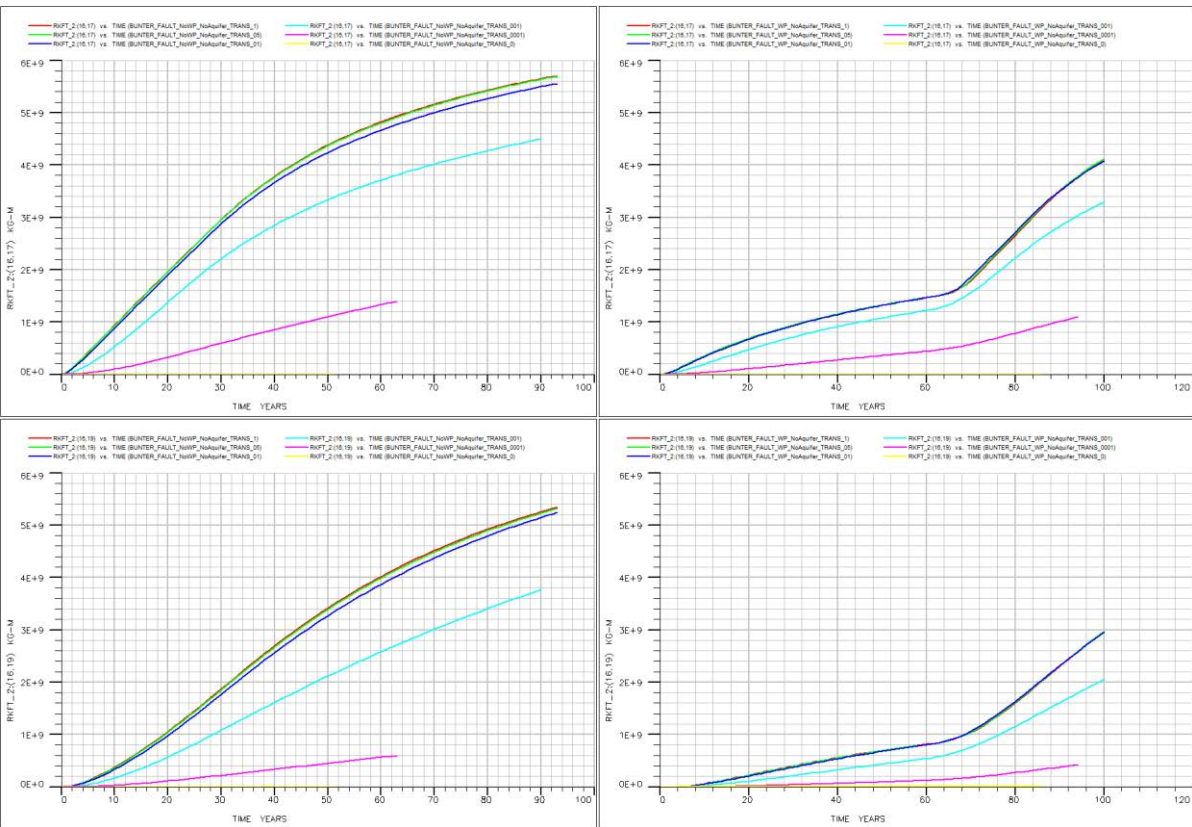


Figure 3-23: Brine migration, in kg-moles, into nearby Dome 37 (top) and Dome 39 (bottom) for scenarios without (left) and with (right) brine production, for various values of fault transmissibility multiplier ranging from 0 to 1.

Pressure increase in Dome 36 causes fluids (brine and CO₂) to migrate into other nearby structures. Figure 3-23 and Figure 3-24 compare the cumulative brine and CO₂, respectively, migration out of Dome 36 to nearby Dome 37 (left) and Dome 39 (right).

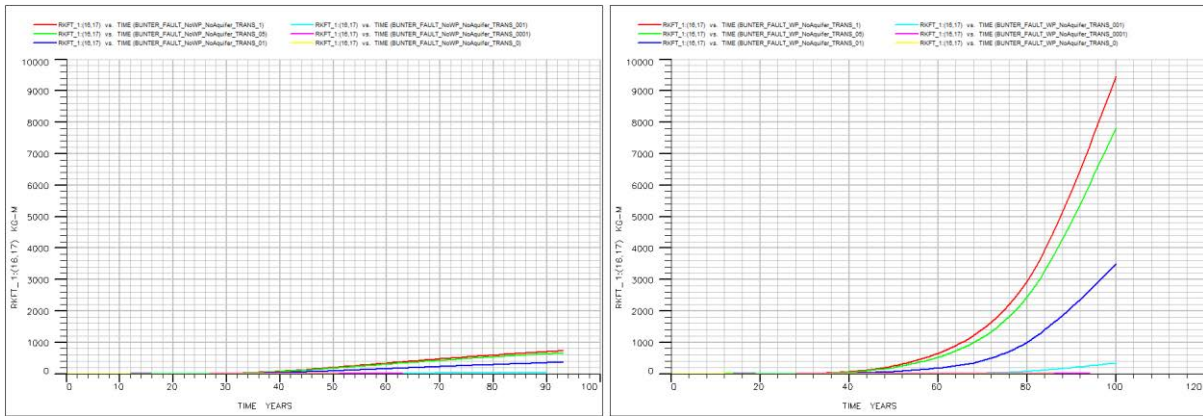


Figure 3-24: CO₂ migration, in kg-moles, into nearby Dome 37 for scenarios without (left) and with (right) brine production. (The CO₂ migration into Dome 39 was negligible and has not been illustrated.)

As expected, the greater the fault transmissibilities, the greater the amount of fluid migration out of Dome 36. In terms of brine migration, this is relevant both with and without brine production; nevertheless, the quantity of migrated brine is smaller when brine production is undertaken. However, CO₂ migration shows the opposite behaviour: when there is brine production, more CO₂ migrates to nearby structures than is the case without brine production. This is because brine production creates a drawdown which draws CO₂ toward brine producers located closer to the boundary of Dome 36. Since the net voidage replacement is still positive in Dome 36 (even with brine production), part of the injected CO₂ migrates out of this dome. This shows that while brine production can limit the quantity of migrated brine into nearby structures, the risk of CO₂ migration may increase simultaneously. Thus, this shows that the location and rate of voidage replacement should be carefully selected - i.e. the brine production wells should not be located very close to boundaries and high voidage rates should be avoided to allow gravity dominated CO₂ displacement. A voidage replacement rate where vertical equilibrium can be maintained (gravity stable CO₂ injection) is best as long as target injection rates can be maintained¹. The amount of CO₂ that migrates to Dome 39 is very small since the positioning of the production wells relative to the CO₂ injectors allows the mobilised CO₂ to be displaced towards production wells P1 and P2. Since there is no production well on the side where Dome 37 is located, the amount of CO₂ that migrates towards that dome is thus more significant. Nevertheless, the amount of CO₂ that is displaced out of Dome 36 is small, both with and without brine production, and is in the fraction range of 10⁻⁶ to 10⁻⁷ of the total mass of injected CO₂.

¹ The concept is very similar to gravity stable CO₂ injection for EOR purposes.

Figure 3-25 shows brine production profile in Dome 36 for different magnitudes of fault transmissibilities.

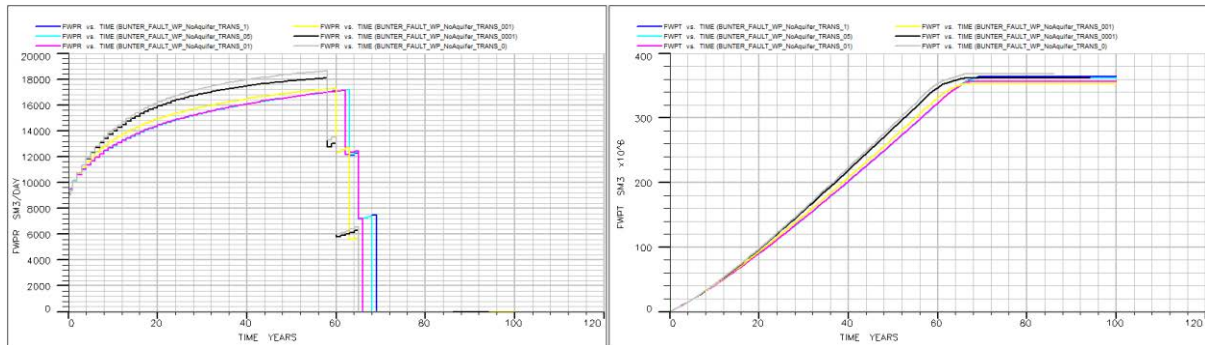


Figure 3-25: Brine production rate (**FWPR**, left) and cumulative brine produced (**FWPT**, right) from Dome 36 for the simulations with brine production; comparison between different transmissibility scenarios.

It can be seen the cumulative produced brine is nearly identical (less than 5% difference) for the entire range of fault transmissibilities, though individual brine production profiles are somewhat different. This indicates that the voidage created for CO₂ storage by brine production is almost identical, irrespective of the fault transmissibilities. The extent of the faults may also affect the CO₂ storage characteristics. Figure 3-26 compares the CO₂ injection profiles (rate) for different sizes of the fault (compartment) block, with (dashed data) and without (solid data) brine production.

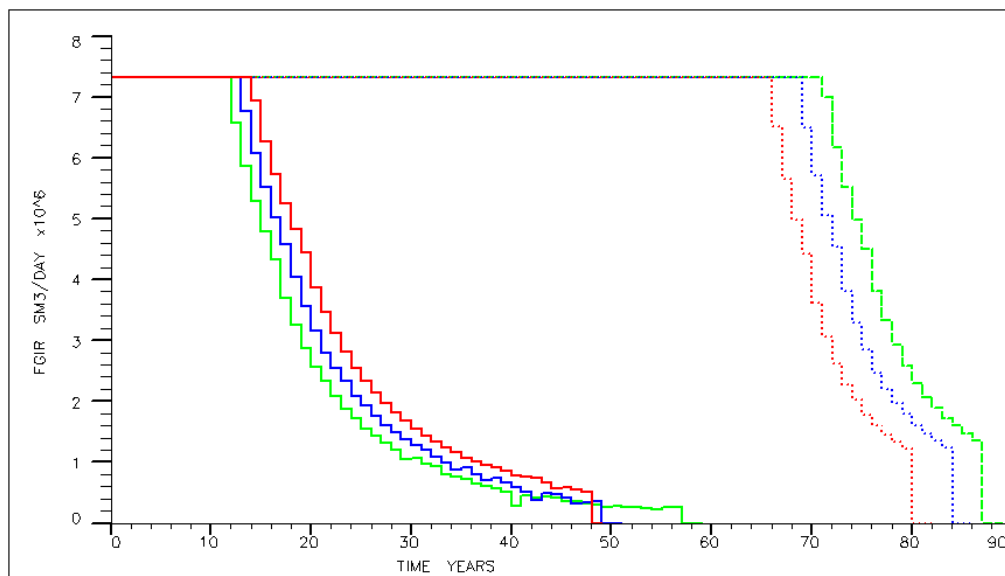


Figure 3-26: Impact of the size of the fault block on the rate of CO₂ injection (**FGIR**); comparison between with (dashed) and without (solid) brine production. Blue, red and green colours refer to fault locations at the spill point of Dome 36, 800m farther from the injectors and 800m closer to the injectors, respectively.

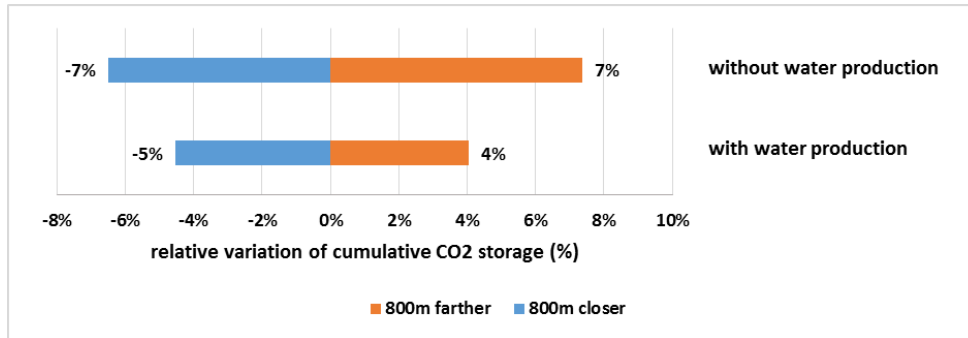


Figure 3-27: Sensitivity of cumulative stored CO₂ for various sizes of the fault block. Comparison between scenarios with (bottom) and without (top) brine production. Note the faults have zero transmissibility in these calculations.

Both with and without brine production, the size of the fault block affects the CO₂ storage response due to the change in the system volume that the CO₂ is being injected into. The ultimate cumulative stored CO₂ is more sensitive to the size of the fault block in the scenario where there is no brine production than in the scenario where there is brine production (Figure 3-27). In other words, brine production reduces the impact of uncertainty in the size of the fault block arising in uncertainty in the location of the bounding faults.

3.5 Limited Vertical Transmissibility

The presence of an impermeable or partially permeable shale layer may limit vertical fluid movement within the storage complex, and consequently can affect the CO₂ storage characteristics depending on the CO₂ injection and brine production strategy. To investigate this, the vertical transmissibility multiplier of the least permeable layer in the Bunter model (layer 38) was varied between 0 (complete barrier) and 1 (no barrier). In this set of calculations the same Bunter model as depicted in Figure 3-18 was used, but without horizontal fault blocks. Two injection strategies have been investigated for this section; injecting CO₂ into and producing brine from the intervals above the low permeability shale layer (the "above/above" scenario) and injecting CO₂ above and producing brine from below the shale layer (the "above/below" scenario). Note that, as before, there is no numerical aquifer connected to this model.

Figure 3-28 shows CO₂ injection profile for different values of shale layer vertical transmissibility multiplier for both above/above (left) and above/below (right) injection strategies.

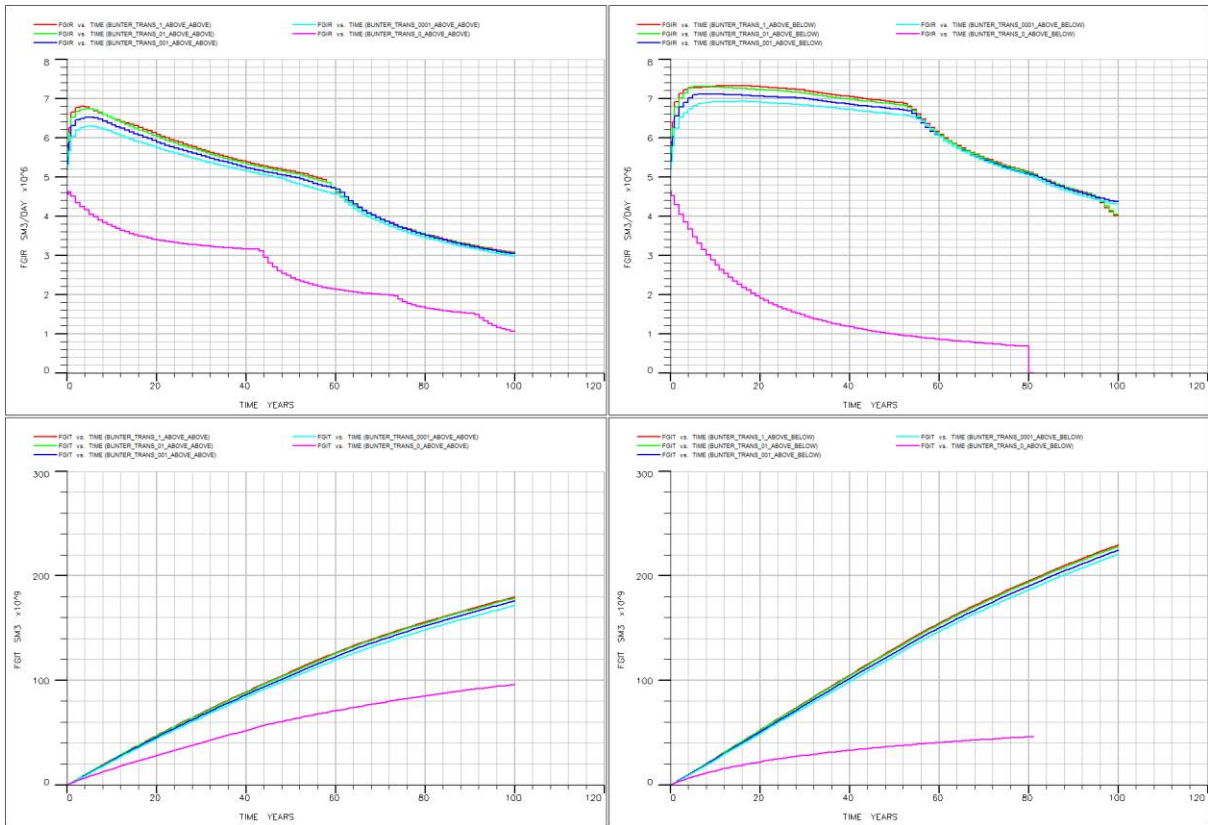


Figure 3-28: Impact of shale layer vertical transmissibility on CO₂ storage characteristics for above/above (left) and above/below (right) injection strategies. Top and bottom images respectively refer to CO₂ injection rate (**FGIR**) and cumulative stored CO₂ (**FGIT**). **Pink** lines correspond to zero crossflow, while for other lines there is finite communication and therefore crossflow potential.

It can be seen that the occurrence of crossflow within the storage complex (i.e. when the shale layer is permeable) significantly enhances CO₂ storage. Even limited crossflow capacity causes brine (and CO₂) to be displaced, but zero crossflow (pink lines) means no communication from above to below the shale layer, and thus the CO₂ storage potential will be reduced for both above/above and above/below injection strategies, with the above/below strategy being more significantly affected. Note in Figure 3-28 that there is virtually no difference, in terms of CO₂ storage characteristics, between any of the non-zero shale vertical transmissibility multiplier scenarios: i.e. all the non-zero transmissibility models follow the same storage profile irrespective of the degree of vertical shale transmissibility. This is because of the large surface area at the boundary relative to the model thickness for the Bunter structure (large LxW/H ratio) coupled with high k_v/k_h ratio ($k_v/k_h=1$), which makes storage performance insensitive to vertical shale transmissibility multiplier unless the shale layer is perfectly sealing (Figure 3-28), since even if brine is only displaced a short distance across this

boundary, because of the large surface area a large volume is displaced, creating voidage for the injected CO₂.

The vertical shale layer transmissibility can also affect the choice of injection strategy. If the shale layer is completely impermeable, then the pore volumes above and below the shale layer form two completely separate and isolated hydrodynamic systems, which may require an alternate injection strategy. Figure 3-29 compares the final gas (CO₂) saturation profile in Dome 36 for the above injection strategies. Note that the displacement is not perfectly gravity dominated in either of the models as CO₂ fronts show some propensity for channelling in all modelling scenarios.

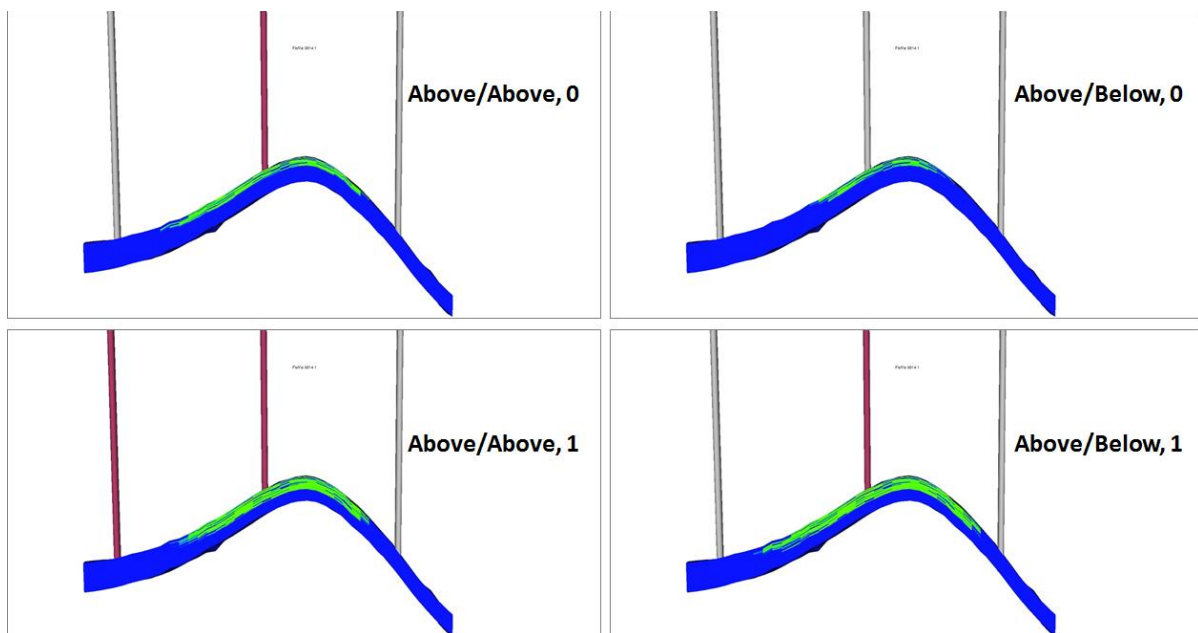


Figure 3-29: Gas (CO₂) saturation profile at the end storage operation for above/above (left) and above/below injection strategies. Top and bottom figures respectively show saturation profiles for 0 and 1 vertical shale transmissibility multipliers. **Green** blocks are those saturated with CO₂, and **blue** blocks are those saturated with water. Wells coloured in **red** were still operating up to end of storage operation, wells coloured **grey** were shut in earlier.

Figure 3-28 and Figure 3-29 show that when the shale layer is completely impermeable, the above/above injection strategy is the preferred injection strategy as it allows sufficient communication between (CO₂) injector and (brine) producers though, this injection strategy does not utilise the pore volume beneath the shale layer. However, when the shale layer is not perfectly impermeable, the above/below injection strategy is preferred, since it promotes further cross flow within system and utilises the entire pore volume to accommodate the pressure buildup.

Crossflow between layers also affects the extent of brine and CO₂ migration out of the Dome 36 region, depending on the choice of injection strategy. Figure 3-30 and Figure 3-31 shows brine and CO₂ migration out of Dome 36 for both injection strategies.

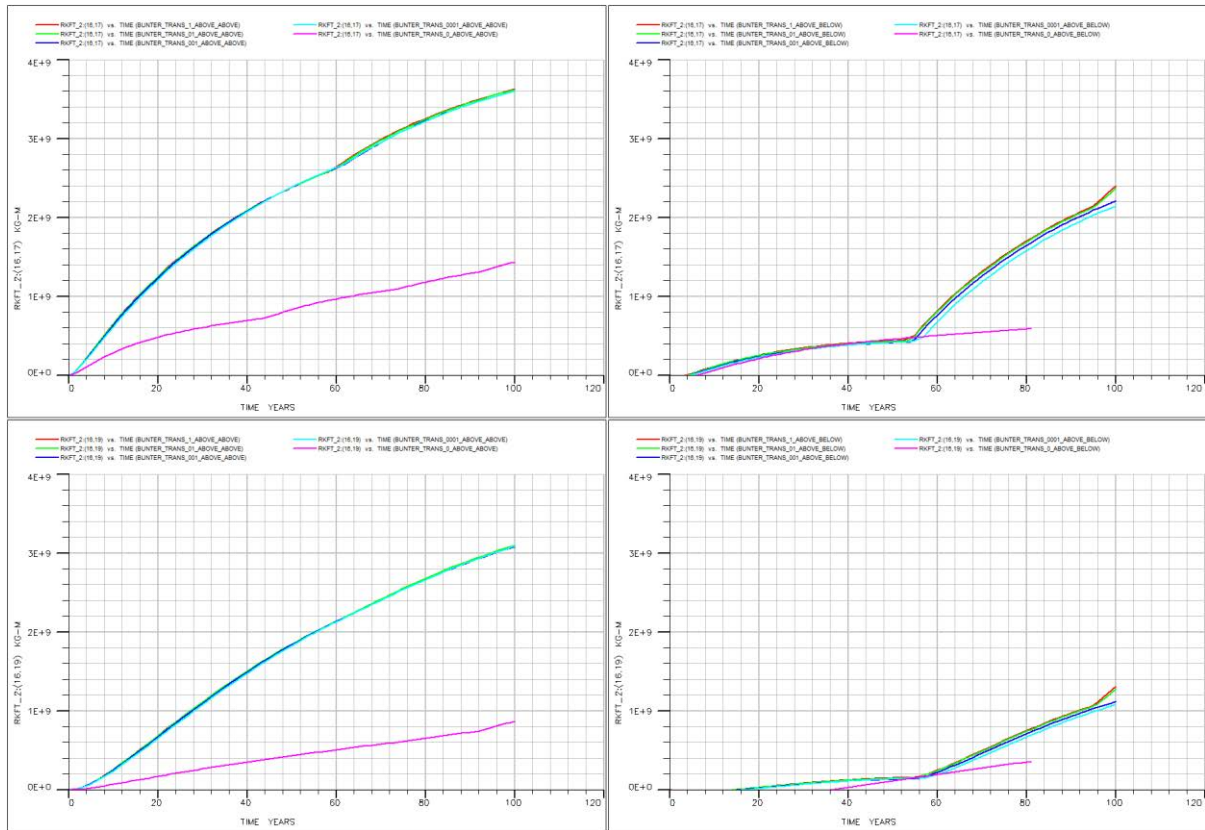


Figure 3-30: Brine migration (in kg-mole) into nearby Dome 37 (top figures) and Dome 39 (bottom figures) for above/above (left) and above/below (right) injection strategies.

It may be seen in Figure 3-30 that for all the non-zero vertical shale transmissibility cases, the quantity of migrated brine is not dependent on the magnitude of vertical shale transmissibility for both above/above and above/below injection strategies. The sharp rise in brine migration in the above/below (right images of Figure 3-30) is due to the closing of the brine production wells, which consequently diverts the mobilised brine towards other adjacent domes. Nevertheless, brine migration out of Dome 36 is more significant when the shale layer is *not* completely impermeable, since some of the mobilised brine (due to CO₂ injection) migrates to above or below the shale layer where it cannot be produced by the brine production well completed only on the other side of the shale layer, and consequently the CO₂ migrates to other adjacent domes. This suggests that when crossflow is high (i.e. if the shale layer is at all permeable) and the displacement is not gravity dominated, brine production wells should be completed across the full height of the target interval to capture all the mobilised brine.

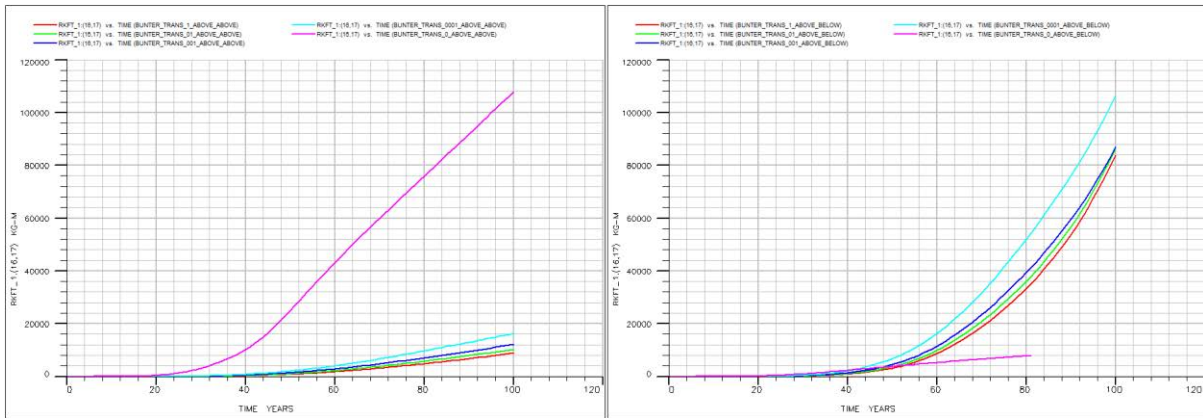


Figure 3-31: CO₂ migration into domes adjacent to 37 for above/above (left) and above/below (right) injection strategies. CO₂ migration into Dome 39 was negligible.

Figure 3-31 shows that while for the above/above injection strategy, CO₂ migration is more significant when the shale layer is completely impermeable, for the above/below injection strategy the opposite behaviour can be observed. An important observation in Figure 3-31 (right image, above/below scenario) is that while the quantity of migrated CO₂ is least when the shale layer is impermeable, for all other non-zero vertical shale transmissibility scenarios it continuously *increases* as the vertical shale transmissibility *decreases*. This can be explained by the fact that as the vertical transmissibility of the shale layer increases CO₂ can more readily be displaced below the shale layer and is thus being stored. As the transmissibility of the shale layer decreases, CO₂ has to travel further horizontally towards the brine production wells instead of being stored vertically beneath the shale layer. The more that CO₂ is transported towards the brine production wells, the more will be its migration into other adjacent structures. Once the shale layer becomes completely impermeable the brine production related drawdown cannot impact the injected CO₂ and its migration reduces to its minimum. Comparison of Figure 3-30 and Figure 3-31 also shows that the quantity of migrated CO₂ is more sensitive to vertical transmissibility of the shale layer than to brine production rate. This is expected, since CO₂ is more mobile than brine and is hence more sensitive to the degree of crossflow within system than is the brine. This indicates that while the degree of vertical transmissibility in the shale does not affect the ultimate cumulative stored CO₂, it certainly affects the distribution of CO₂ within the storage complex.

Finally, Figure 3-32 compares the brine production profile between above/above (left) and above/below (right) injection strategies. The stepwise reduction of brine production corresponds to sequential shut-in of brine production wells due to CO₂ breakthrough. Brine production is much higher for the scenarios with a higher permeability shale layer indicating that brine production is better supported by the pressure increase due to CO₂ injection and also flow above *and* below the shale layer. Note that there is a correlation between the cumulative amount of brine produced and the

cumulative amount of CO₂ stored (Figure 3-28). Based on this correlation, it can be inferred that maximum CO₂ storage can be achieved when the above/below injection strategy is undertaken provided that the shale layer is not completely impermeable. Or, in other terms, if the shale layer is sealing, brine production may be more of a necessity and have a greater impact because there is a smaller volume of rock available for injection into, but whether or not there is a sealing shale layer brine production will significantly increase injection capacity, and the scenario where there is not a sealing layer but there is the one that will allow for most storage, although the degree of transmissibility across the shale layer is not important, provided it is finite.

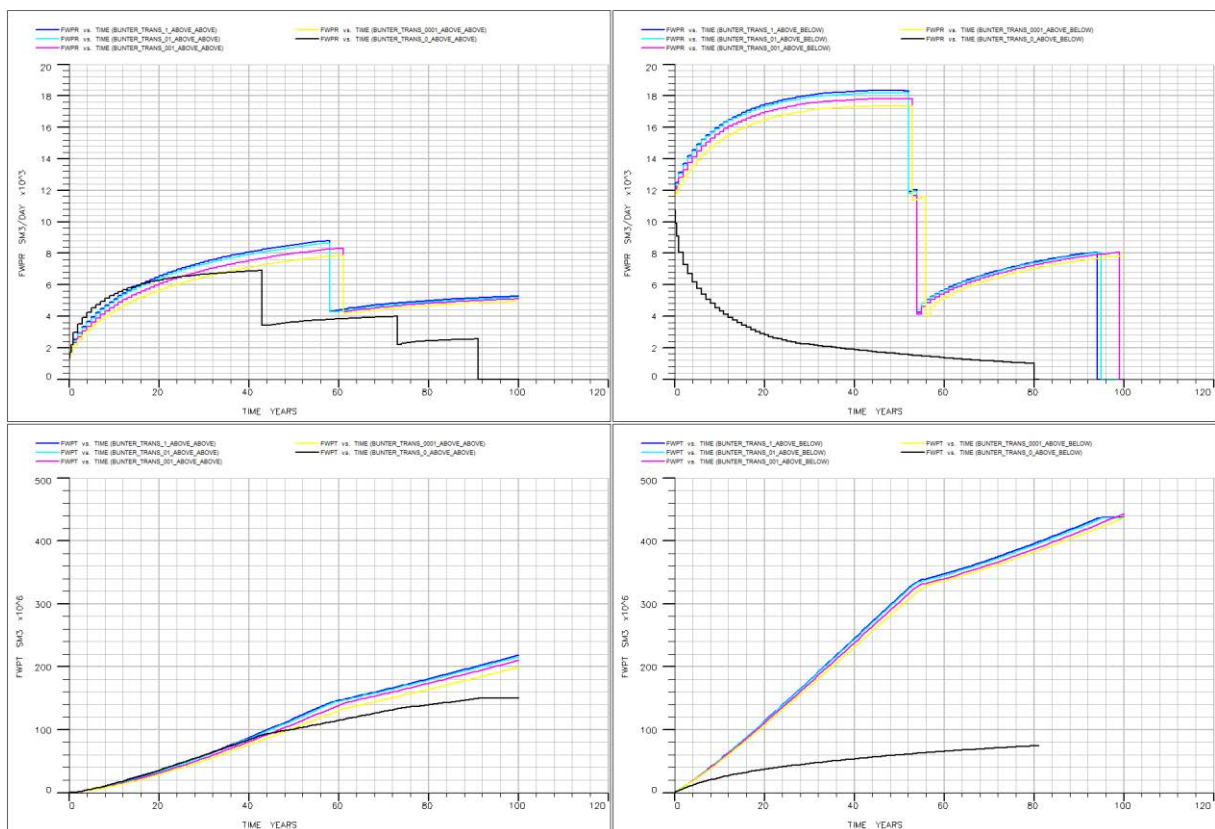


Figure 3-32: Comparison of brine production profile for above/above (left) and above/below (right) scenarios. The **black** lines correspond to the scenarios with a completely sealing layer, the coloured lines to scenarios with varying degrees of transmissibility all the way to no barrier at all (**blue**).

3.6 The Benefit of an Aquifer

The results presented in Sections 3.4 and 3.5 assume that the boundaries of the model represent sealing barriers (say due to faults, pinch out or an unconformity) - i.e. there is no aquifer volume connected to the edges of either of the models. The presence of a large connected aquifer would reduce the impact of compartmentalisation on the storage performance. Figure 3-33 compares the

cumulative amount of stored CO₂ within Dome 36 under four different storage scenarios; completely isolated and fully communicating Dome 36 both of which are assessed with and without a connected aquifer (modelled as a numerical aquifer connected to the boundary of the model). There is *no brine production* in either of these scenarios.

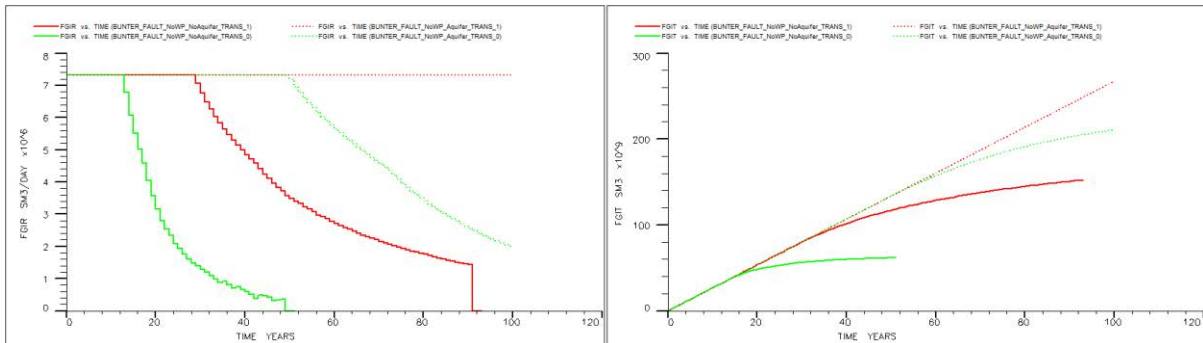


Figure 3-33: Impact of a connected aquifer on the CO₂ storage characteristics in Dome 36 on CO₂ injection rate (FGIR, left) and cumulative CO₂ stored (FGIT, right) in scenarios with no brine production.

The presence of an aquifer reduces the sensitivity of CO₂ storage to compartmentalisation provided that each compartment is connected to an aquifer. For this Bunter model, when an aquifer is connected to the models, storage performance is not sensitive to compartmentalisation for the first 50 years - i.e. the edge aquifer has the same impact as production wells in allowing water to be displaced away from the CO₂ injection zone. Additionally, it is expected that brine production coupled with the presence of an aquifer further reduces the storage sensitivity to compartmentalisation.

Table 3-2 The key technical input data for Bunter-D36 Model.

ID	Description	Flow rate (Mt CO ₂ /y)	Injection duration (years)	Brine production	Well type	Production wells converted to injection wells	Total CO ₂ injection wells	Total brine production wells	Bottom hole pressure (MPa)	Grid length (m)	Grid width (m)	Average well depth (m)	Maximum brine production (m ³ /d)
169	Bunter-D36	5	8	No	Vertical	No	3		21	1200	1800	1300	
170	Bunter-D36	5	20	No	Vertical	No	3		-	1200	1800	1300	
171	Bunter-D36	5	30	No	Vertical	No	3		-	1200	1800	1300	
172	Bunter-D36	5	40	No	Vertical	No	3		-	1200	1800	1300	
173	Bunter_D36-PW	5	10	Yes	Vertical	No	3	3	18.8	12000	5600	1650	14700
174	Bunter_D36-PW	5	20	Yes	Vertical	No	3	3	19.3	12000	5600	1650	17150
175	Bunter_D36-PW	5	30	Yes	Vertical	No	3	3	19.6	12000	5600	1650	18100
176	Bunter_D36-PW	5	40	Yes	Vertical	No	3	3	19.7	12000	5600	1650	18500
177	Bunter-D36	5	12	No	Vertical	No	6		25.0	5200	7200	1600	
178	Bunter-D36	5	20	No	Vertical	No	6		-	5200	7200	1600	
179	Bunter-D36	5	30	No	Vertical	No	6		-	5200	7200	1600	
180	Bunter-D36	5	40	No	Vertical	No	6		-	5200	7200	1600	
181	Bunter-D36-PW-post	0	50	Yes	Vertical	No	0	3	15.8	12000	5600	1650	18100
182	Bunter-D36-PW-delay5	5	5	No	Vertical	No	3	0	19.6	1200	1800	1300	0
183	Bunter-D36-PW-delay5	5	10	Yes	Vertical	No	6	3	19.6	12000	5600	1650	17558
184	Bunter-D36-PW-delay5	5	20	Yes	Vertical	No	6	3	19.7	12000	5600	1650	18188
185	Bunter-D36-PW-delay5	5	30	Yes	Vertical	No	6	3	19.8	12000	5600	1650	18504
186	Bunter-D36-PW-delay5	5	40	Yes	Vertical	No	6	3	19.8	12000	5600	1650	18669
187	Bunter-D36-PW-delay10	5	10	No	Vertical	No	3	0	21.0	1200	1800	1300	0
188	Bunter-D36-PW-delay10	5	20	Yes	Vertical	No	6	3	20.4	12000	5600	1650	20729
189	Bunter-D36-PW-delay10	5	30	Yes	Vertical	No	6	3	20.0	12000	5600	1650	19503
190	Bunter-D36-PW-delay10	5	40	Yes	Vertical	No	6	3	20.0	12000	5600	1650	19085

4 Firth of Forth Model with Brine Production

4.1 Geology of Firth of Forth Aquifer

The Firth of Forth (FoF) site was one of the two saline aquifer exemplars studied in the CASSEM Project (Smith, et al. 2012). As shown in Figure 4-1, it is located within a 75 km radius of what was a major CO₂ emitter at Longannet Power Station on the banks of the Firth of Forth. The primary saline aquifer targets are the fluvial and Aeolian sandstone of the Kinnesswood and Knox Pulpit formations (Ford and Monaghan 2009). The cap rock is the Ballagan formation. In terms of aquifer volume and depth criteria, the saline aquifer provides a potential testing site in the Midland Valley of Scotland with complex structural traps. Several anticlinal structural traps were identified with a deeper synclinal area. The main aquifer is identified at depths of 2000 to 2300 m on an anticline structure.

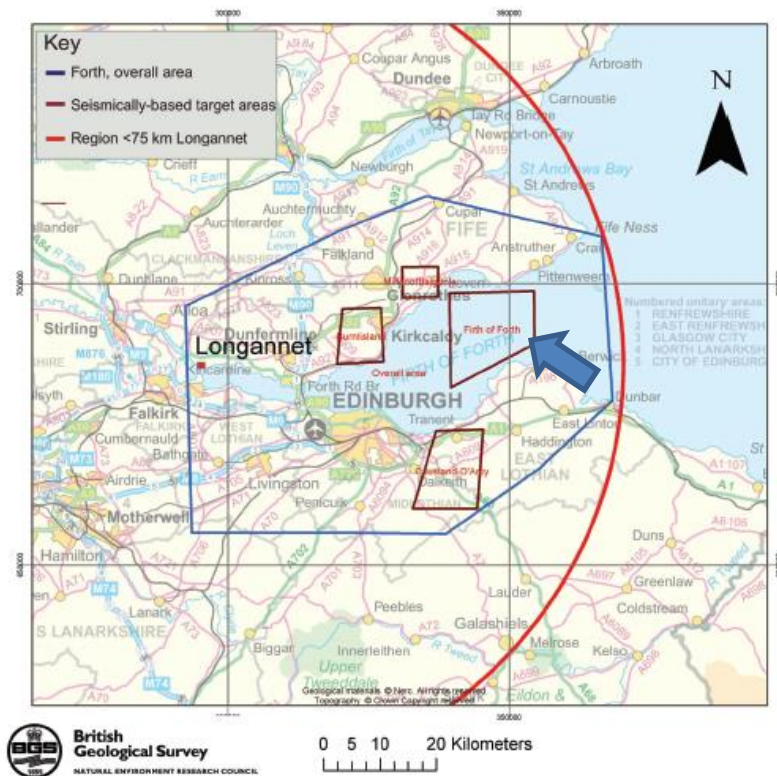


Figure 4-1 Location map for Firth of Forth injection site.

The geological framework and model is based on an interpretation of third-party 2D seismic data, limited downhole borehole/well data, subsurface mining data and BGS onshore mapping. No boreholes penetrate the target aquifer or caprock in the favoured sites, introducing considerable uncertainty in the geological interpretation, but reducing the risk of leakage due to drilled holes.

Analogue borehole core samples were collected from the BGS Glenrothes borehole where the primary aquifer/seal are at depths >200 m, with additional primary aquifer/seal material from shallow depths (<70 m) and outcrop. The geological interpretation and modelling are described in Monaghan et al. (2009) and Monaghan et al. (2012), and the porosity and permeability data entered into the stochastic geological model are summarized in Table 4-1. The data from CO₂Stored database is also listed in the table for comparison.

Table 4-1 The input parameters for the Firth of Forth Model.

Parameter	Units	HW E300 Model
Area	km ²	270
average thickness	m	150
model dimensions	km	17.6 x 15.8
cell dimensions in x & y	m	200 x 200
number of cells		88 x 79 x 20
total number of cells		139,040
total number of active cells		139,040
average porosity	frac.	0.125
average horizontal permeabilities	mD	61
average vertical permeability	mD	61
average net to gross		1.0
total pore volume	m ³	1.8 x 10 ¹⁰
rock compressibility	1/bar	5.57 x 10 ⁻⁰⁵
water compressibility	1/bar	4.0 x 10 ⁻⁰⁵
initial pressure	bar	300
datum depth	m	2,940
fracture pressure	bar	400
salinity (ppm)	ppm	100,000
Temperature	deg C	95
theoretical capacity	Mt	63
injection rate	Mt/y	40
injection period	y	40
monitoring period	y	1000

The petrophysical properties were generated stochastically using PETREL™. The structure in this region is more complex than other injection sites, with lower porosity and permeability and much more uncertainty. The average porosity of the aquifer is approximately 0.135, and the geometric average permeability is 12.6 mD. The porosity was modelled first using seismic analysis from SGS, with a vertical range of 0.1 m and a horizontal range of 2000 m. The permeability distribution was generated using “collocated co-kriging” (Journel and Huijbregts 1997), with a correlation coefficient of 0.6 obtained from log(k) crossplots of core data. A constant net to gross-ratio (N/G) of 0.8 was applied, estimated by Ford and Monaghan (2009). The k_v/k_h ratio was again taken as 0.1 to account for the discontinuous low permeability units (isolated mudstones). The rock compressibilities for the aquifer and caprock were set to $5 \times 10^{-4} \text{ MPa}^{-1}$.

In Figure 4-2 (a) the contour map shows the depth of the base Ballagan Formation, which is the base of cap rock or the top of saline aquifer. As shown in Figure 4-2 (b) the Forth Anticlines are in the area coloured in light blue, but the Leven syncline is at the bottom of the basin with a depth change from 300m at the south-east corner to 6000m in the west. The detailed regions of the model were extended laterally using numerical aquifers to cover the whole geological structure, while concentrating on the region of CO₂ migration.

Because the target area is between two syncline structures, the deepest part of the base of the storage formation is below 4000 m. The lateral extent of the model was $17.6 \times 15.8 \text{ km}$, and it was divided up into 88×79 grid cells with 200-m horizontal sides. The thickness of the model was approximately 300 m, and the cell thickness varied from 500 m in the underburden to 2.4 m at the top of the aquifer (Jin et al. 2010).

The sandstone has a porosity up to 0.26 in primary saline aquifer, with a relatively low permeability, with a mean permeability of 70-80 mD, and the maximum permeability is up to 1000 mD. The thickness of the sandstone is greater than 150 m for Knox Pulpit Formation, and is over 100 m for Kinnesswood Formation.

Relative Permeability and Capillary Pressure. There is a scarcity of measurements of CO₂/brine relative permeabilities. Many studies make use of data from Bennion and Bachu (2008). However, in the CASSEM project, relative permeabilities were measured on a single core sample from the Cleethorpes borehole (Smith et al. 2012). The resulting relative permeabilities are shown in Figure 4-3. These curves were also used for the Firth of Forth model. The dynamic reservoir simulations showed that CO₂ filled the structural trap and then spilled out of the anticline towards the North – dynamic trapping secured the finite volume that was injected. Thus the capacity estimate for the upper limit of the Forth may be significantly higher than the static estimate.

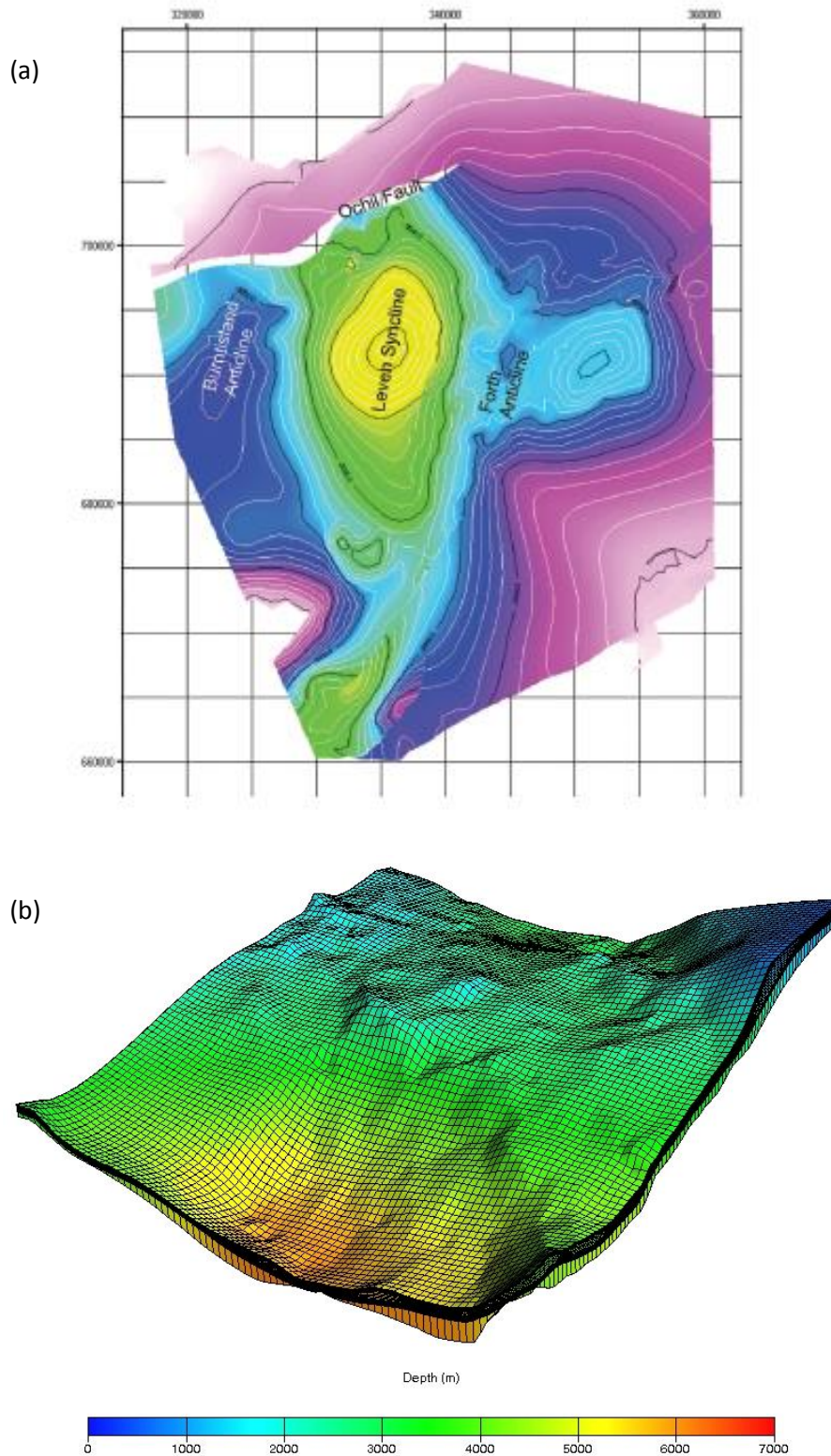


Figure 4-2 (a) Contour map (top) shows the depth of the base Ballagan Formation, which is the base of cap rock and the top of the saline aquifer. The Forth Anticlines are in the area coloured in light blue, but the syncline is at the bottom of the basin at a depth of 4000-5000 m. (b) ECLIPSE model (bottom) with grid size 200 m x 200 m.

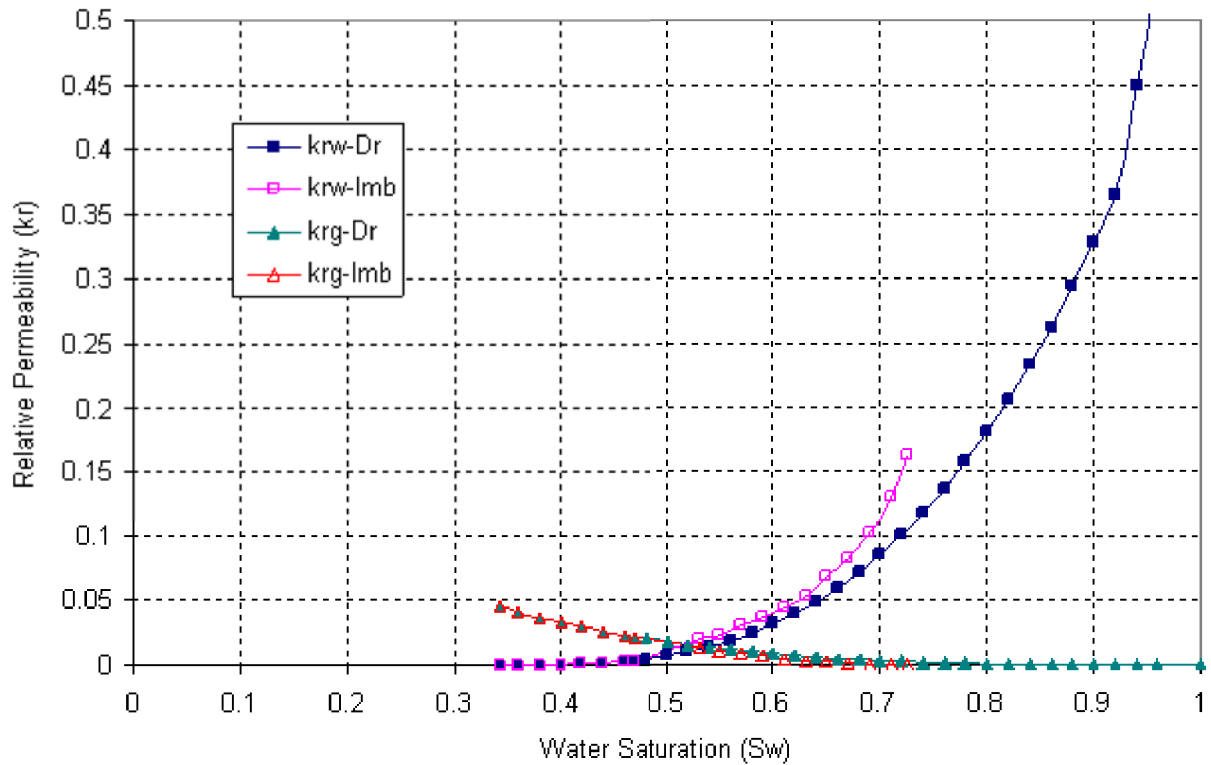


Figure 4-3 - Example of relative permeability results: k_{rw} is relative permeability to water, and k_{rg} is relative permeability to CO_2 . Drainage (Dr) curves correspond to decreasing water saturation, and imbibition (Imb) curves correspond to subsequently increasing water saturation.

4.2 ECLIPSE Model and Injection Plan

The flow calculations were performed using the compositional simulator ECLIPSE 300 (Schlumberger, 2014) with the CO2STORE option for CO_2 storage in saline aquifers. Two clusters with six vertical injectors in each cluster were used in the simulation. Two producers were set on the edge of syncline, but these were perforated in the bottom two layers, which is deeper than the injectors. In the cases that the injection rate is over 10 Mt/y four producers were used and the location of the producers was also adjusted. As the storage capacity was estimated about 100 Mt and the possible location for injectors is limited by the suitable depth (800 m – 3,000 m), the cases with high injection rate (20 Mt/y to 40 Mt/y) were not tested for the FoF model in the study.

Capacity

Before numerical simulation, initial simple analytical capacity estimates were performed, informed by typical values of porosity for analogous samples, using standard efficiency factors and dense phase

CO₂ densities to calculate the static capacity. It was assumed that the area of interest has a closed boundary.

From an analysis of the injectivity of the storage site and the calculation of the static capacity of the site based on the average input data, such as net-to-gross, porosity, and permeability, the type of injection well was chosen, and the spacing of the wells was estimated. The number of clusters was decided by estimation of the injectivity of a single well and the number of wells in a cluster, and the required field injection rate.

The total pore volume (PV) of the model is $18 \times 10^9 \text{ m}^3$ (at reference pressure 336 bars). The density of the CO₂ $\rho_{\text{CO}_2} = 700 \text{ kg/m}^3$. The total compressibility (C_p) is $5 \times 10^{-4} \text{ 1/MPa}$. The maximum field pressure increase (ΔP) is less than 4 MPa (van der Meer and Egberts, 2008).

$$\text{The static storage efficiency } E = V_{\text{CO}_2} / V_{\text{pore}} = (c_p + c_w) \Delta P = 0.004$$

$$\text{The storage capacity (in mass)} = E \cdot \text{PV} \cdot \rho_{\text{CO}_2} = 0.004 \times 18 \times 10^9 \times 700 = 50 \times 10^9 \text{ kg} = 50 \text{ Mt}$$

The maximum injection pressure depends on the formation fracturing pressure. The minimum *in situ* horizontal stress σ_h is taken as the fracture pressure under the normal formation stress condition. The gradient of σ_h 0.7 psi/ft and the gradient of initial pore pressure 0.45 psi/ft have been commonly used if the accurate formation stress/pressure gradients are not available. In the study, the maximum injection pressure $P_{\text{max}} = 0.7/0.45 \times 0.9 P_{\text{initial}} = 1.4 P_{\text{initial}}$.

The minimum production pressure of a producer was set to be the initial pore pressure at the datum depth of the producer. The production wells were controlled by two criteria. One is the maximum production rate (which is $16,000 \text{ m}^3/\text{day}$ in the study) if the well bottom hole pressure (WBHP) is over the minimum production pressure. The other is the produced mole fraction of CO₂ (WXM_{F_1}) and production rate of CO₂ (WGPR). A water producers is open when its WBHP exceeds the minimum pressure, and it is shut down when the produced CO₂ is over the limit (WXM_F>0.0001 or WGPR>28.3 m³/day in this study).

As shown in Figure 4-4 injectors were grouped in two clusters, one on the left of the model and the other on the right of the model. The spacing between the wells is 2,000 m and the distance between the centres of the two clusters is 6 km. The maximum injection rate of each well is 1 Mt/y, then from a case of 2 Mt/y to a case of 15 Mt/y the total number of injectors increases from 2 to 18. The left cluster was used first to avoid CO₂ reaching the shallowest part at the top-right corner of the system, even though the boundaries of the model were closed.

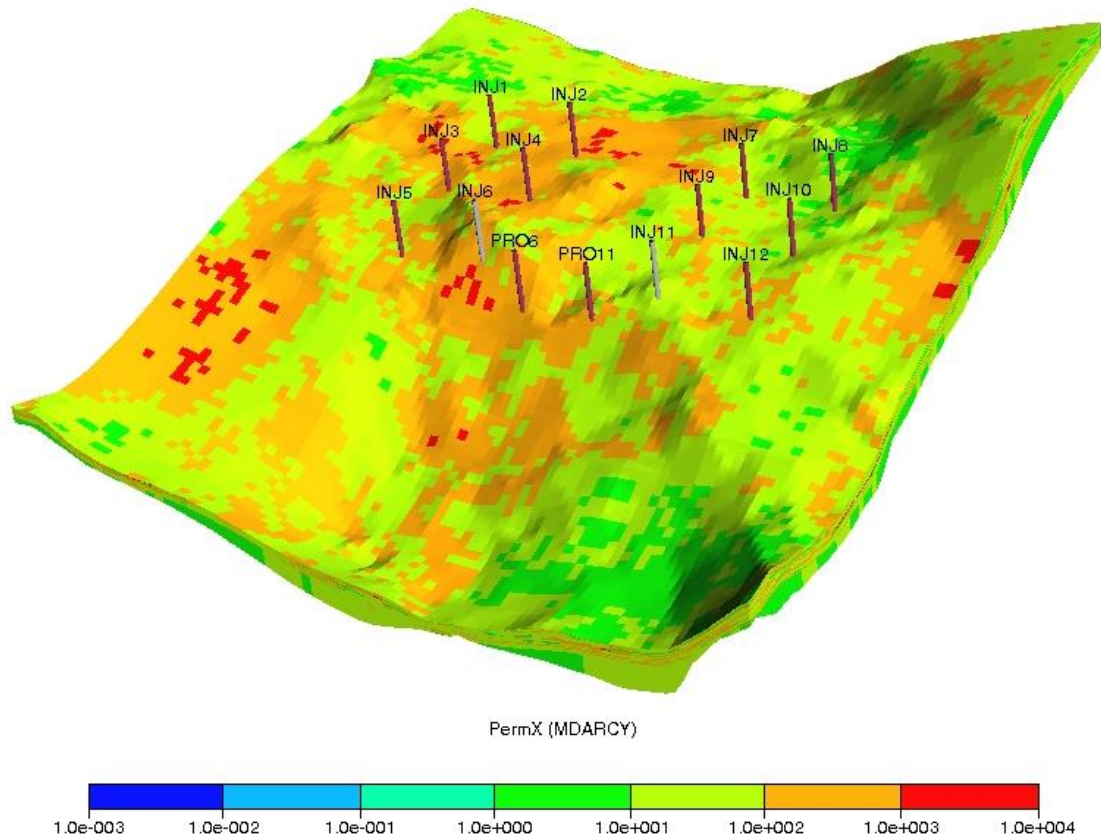


Figure 4-4 Permeability and well locations for the 10 Mt/y case as an example.

4.3 Simulation Results and Analysis

As listed in Table 4-2, nine simulations were run in the FoF study. Four base cases were run with the field injection rate equal to 2, 5, 10, 15 Mt/y, and five comparison cases were run with water production. In three out of the five comparison cases the total number of wells for each case was the same as its corresponding base case, but water producers were used, so that the number of injectors in each comparison case is less than that in its base case. Only for the first comparison case (2 Mt/y) and for the last comparison case (15 Mt/y (P-1)) were the number of injectors the same as their base cases, but producers were added.

Figure 4-5A and Figure 4-5B show comparisons of field CO₂ injection rate and field average pressure for each case in the base group (top row) and the water production group (middle row). The bottom row of the figure gives the water production rate (blue line) for each case with the CO₂ production vs. time (the red line). The values of the maximum water production rate and the total brine produced

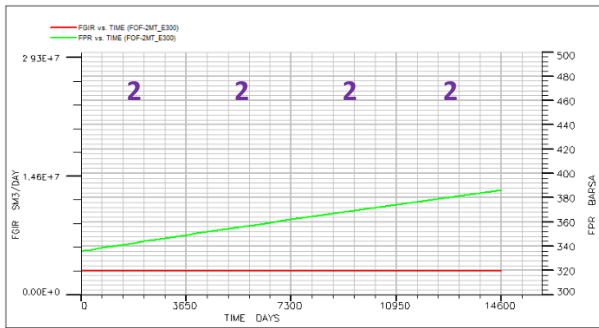
(in standard barrels per day) were also listed in Table 4-2. The durations of constant rate injection listed in Table 4-2 and shown in Figure 4-5 are also an indicator of dynamic capacity, which is one of the important properties for a storage site. From the output of the base case it can be seen that this property depends on the field injection rate without water production. The 2 Mt/y case is an exception, as its capacity had not been reached after 40 years of injection.

From the date when the constant injection rate changed to a reduced rate, it can be seen that with water production the capacity of the FoF site was increased in all cases. If pressure is the only restriction, by adjusting the location of the producers the time for CO₂ breakthrough, as shown in the bottom row of Figure 4-5, can be delayed further, and the storage capacity can be increased further. However, optimising well placement is outside of the scope of the study.

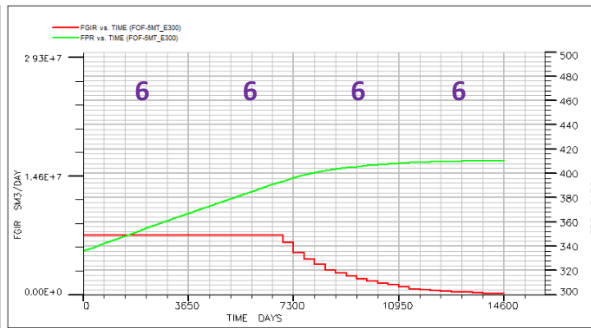
The distance between a producer and the nearest injector is a parameter that affects the time for CO₂ breakthrough; therefore, it affects the period of time that the producer can limit the rise in the injection pressure. This depends on the permeability of the formation and the injection rate. If the producers can be set at a distance that helps the injectors operate at a constant rate for 20-30 years, the storage capacity will be significantly increased according to this study.

Table 4-2 Key technical input of Firth of Forth Model

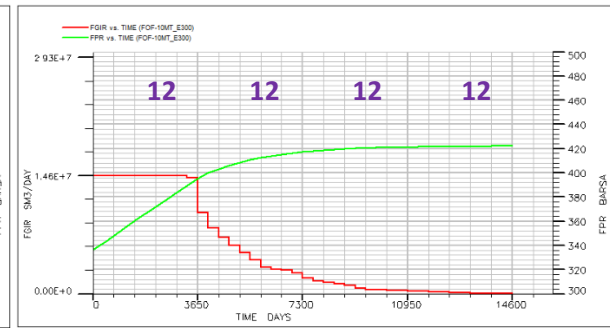
Case ID	Brine production	CO ₂ Injection Wells						Brine Production Wells						Output from Period of Constant Injection				
		Number of wells				Injection rate/well	Max. WBHP	Number of wells				WBHP target	Production rate limit	Duration at max rate	Total CO ₂ injected	Max. production rate	Total brine produced	Voidage replace ratio (V _w /V _{CO2})
		10	20	30	40	Mt/y	bar	10	20	30	40	Bar	m ³ /day	y	Mt	m ³ /day	× 10 ⁶ m ³	frac.
FOF-2MT	NO	2	2	2	2	1	290							40	80			
FOF-5MT	NO	6	6	6	6	1	290-350							19	95			
FOF-10MT	NO	12	12	12	12	1	290-400							9	90			
FOF-15MT	NO	18	18	18	18	1	290-400							6	90			
FOF-2MT-PW	YES	2	2	2	2	1	290	1	1	1	1	320-330	16000	40	80	6000	80.8	0.85
FOF-5MT-PW	YES	5	5	5	5	1	290-350	2	2	2	2	320-330	16000	31	155	9200	72.6	0.40
FOF-10MT-PW	YES	10	10	10	10	1	290-400	2	2	2	2	320-330	16000	17	170	16620	79.2	0.40
FOF-15MT-PW-1	YES	15	15	15	15	1	290-400	3	3	3	3	320-330	16000	18	270	36400	207.5	0.66
FOF-15MT-PW	YES	18	18	18	18	1	290-400	4	4	4	4	320-330	16000	22	330	41800	280.3	0.73



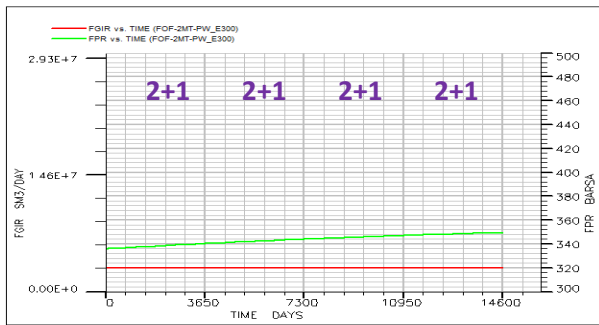
2 Mt/y without water production (base case)



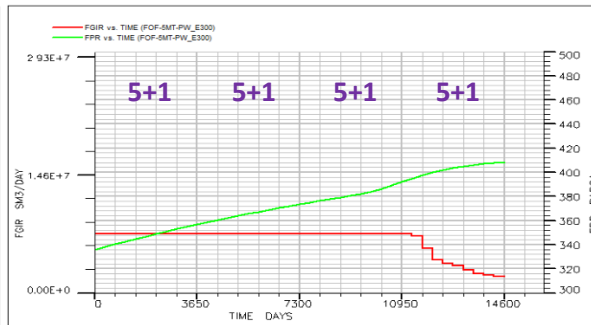
5 Mt/y without water production (base case)



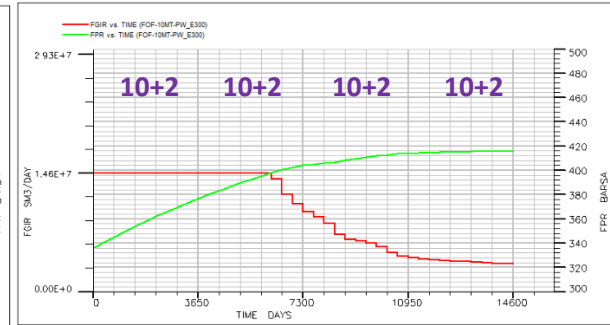
10 Mt/y without water production (base case)



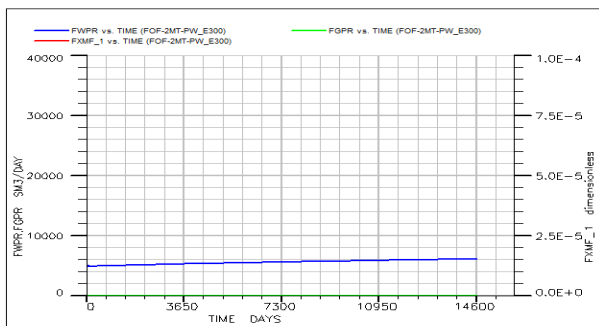
2 Mt/y with water production



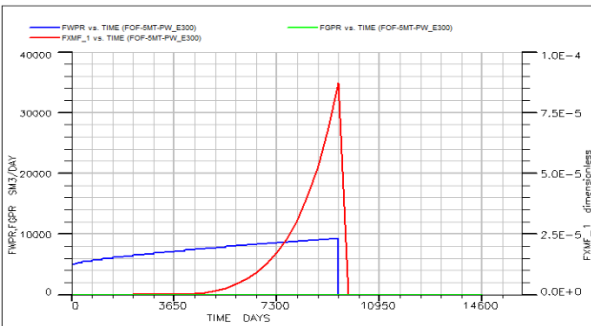
5 Mt/y with water production



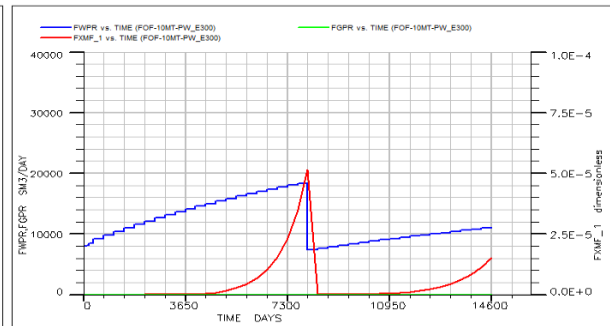
10 Mt/y with water production



2 Mt/y - water production rate & CO₂ mole fraction

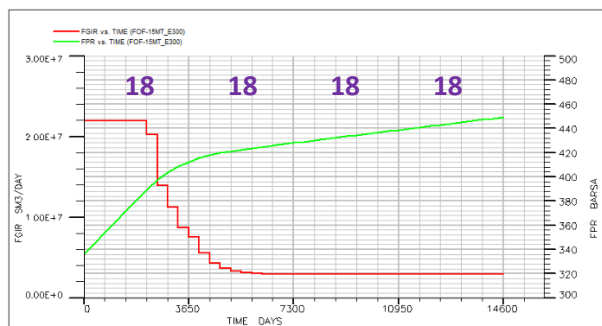


5 Mt/y - water production rate & CO₂ mole fraction

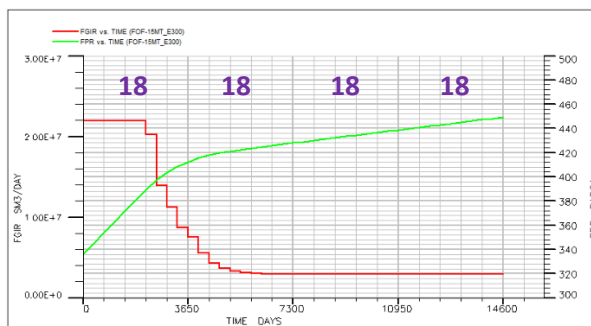


10 Mt/y - water production rate & CO₂ mole fraction

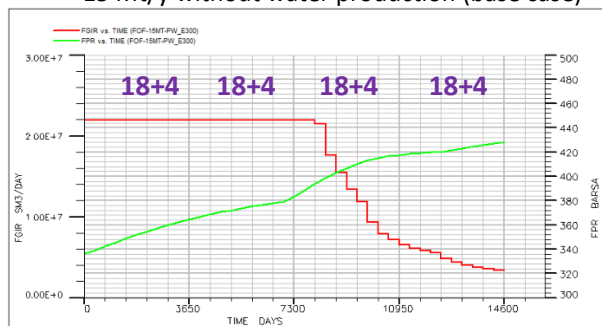
Figure 4-5A Comparison of field CO₂ injection rate (FGIR) and field average pressure (FPR) for each case in base group (top row) and water production group (middle row), and water production rates (FWPR lines in the bottom row) for each case with CO₂ breakthrough vs. time (FXMF lines in the bottom row).



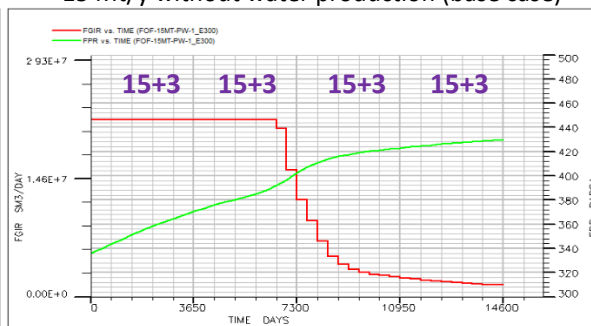
15 Mt/y without water production (base case)



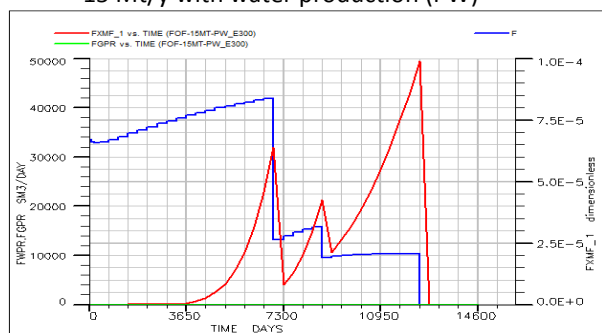
15 Mt/y without water production (base case)



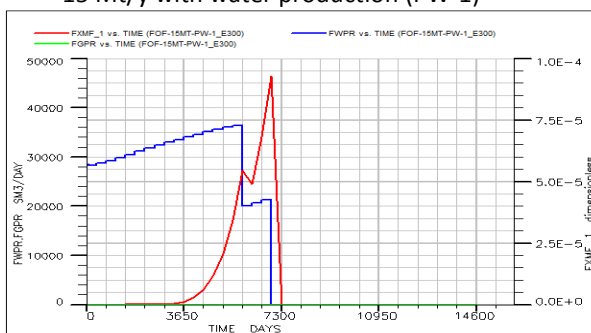
15 Mt/y with water production (PW)



15 Mt/y with water production (PW-1)



15 Mt water production rate & XMF (PW)



15 Mt-1 water production rate & XMF (PW-1)

Figure 4-5B Comparison of field CO₂ injection rate (FGIR) and field average pressure (FPR) for each case in base group (top row) and water production group (middle row), and water production rates (FWPR lines in the bottom row) for each case with CO₂ breakthrough vs. time (FXMF lines in the bottom row).

4.4 Value of Brine Production Later in the Life of the Project

Based on the previous simulations, the capacity of the formation allows CO₂ to be injected at the rate of 5 Mt/y for about 20 years without water production as shown in Figure 4-5A. The scenario presented here is where a decision is made to commence brine production after 20 years of injection in order to extend the life of the storage site (as opposed to, say, exploring for a second injection site).

Five injectors (INJ1 to INJ5) were operated at the total injection rate of 5 Mt/y, as shown in Figure 4-6. Because the pressure has built up over the 20-year injection period, two producers (PRO1 and PRO2) were created to provide pressure relief to ensure further injection could be achieved. One producer (PRO1) is set closer to the injectors at a shallower depth, while the other one (PRO2) is set farther from the injectors in a deeper location. Water production was controlled by pressure and the maximum production rate for each producer was set to 16,000 m³/day. Additional wells could be drilled in the locations shown (injectors INJ6 to INJ12 and producers PRO3 and PRO4).

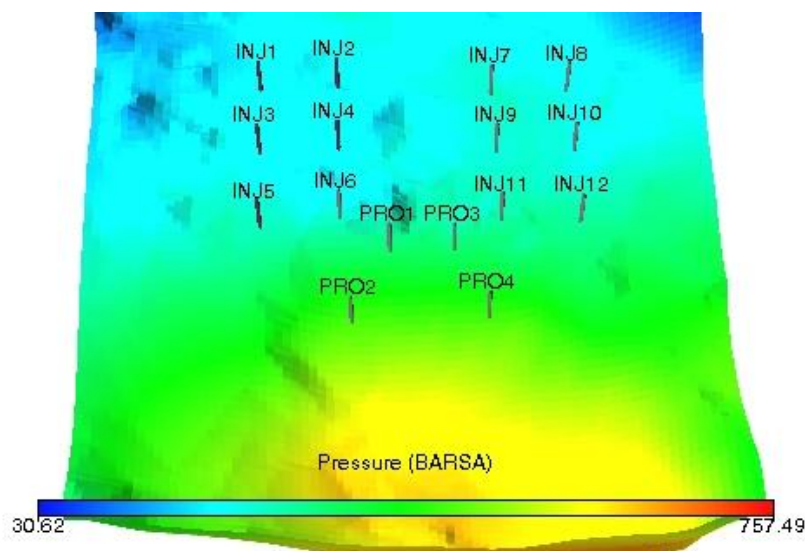


Figure 4-6 Initial pressure distribution and well locations.

In another scenario the site was developed in two stages. In the first stage, injection at a rate of 5 Mt/y was maintained for 10 years without brine production. Five injectors, designated INJ1 to INJ5, were used. Then, after 10 years, a group of injectors designated INJ7 to INJ10 and INJ12 (without INJ6 and INJ11) were used. The total field injection rate now increased from 5 Mt/y to 10 Mt/y with a total of 10 injectors being used. At the same time, four water producers (PRO1 to PRO4) were opened to relieve field pressure. As in the previous case, the producers were controlled by pressure and shut when the mole fraction of produced CO₂ exceeded a criterion.

It may be seen from Figure 4-7 and Figure 4-8 that brine production can be used to extend the life of the project and increase the storage capacity, even if brine production only starts 20 years after CO₂ injection started (green lines). This injection rate is maintained for longer than the injection rate (Figure 4-7) when there is no brine production at all (red line), and is comparable with the injection rate should brine production have started at the start of CO₂ injection (blue line). Thus early production confers no advantage in this case.

Additionally, the increase of CO₂ injection from 5 Mt/y to 10 Mt/y after 5 years of injection may be seen from the pink line, with brine production (Figure 4-8) also starting after 5 years being used to achieve this increased injection rate.

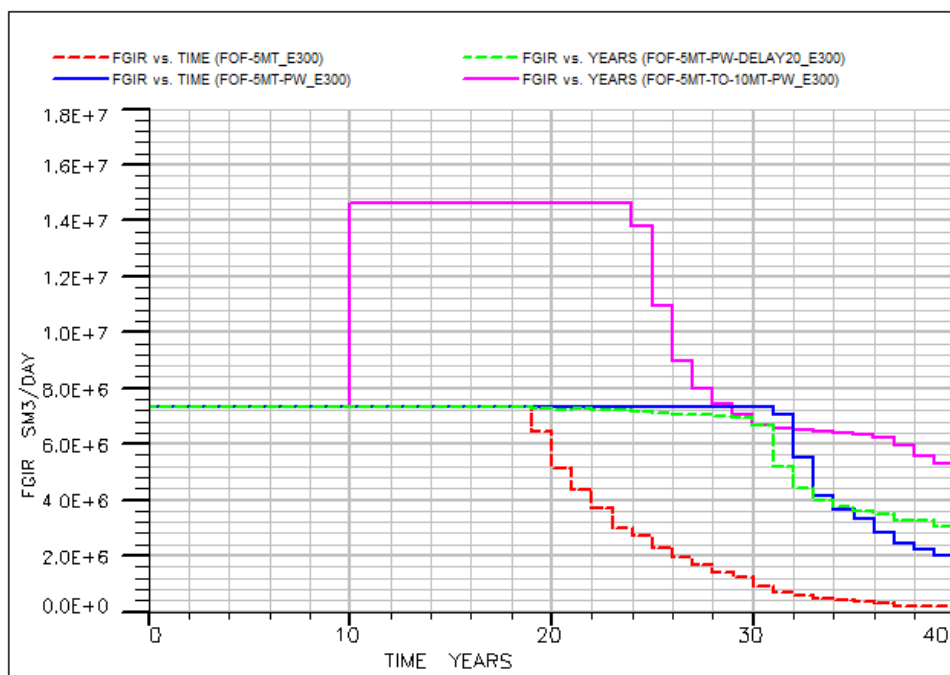


Figure 4-7 Comparison of field CO₂ injection rate (FGIR) vs. time for the base case without water production (red line), with water production at the beginning of injection (blue line), with water production commencing after 20 years of injection (green line) and the field injection rate increasing from 5 Mt/y to 10 Mt/y after 10 years with water production commencing in year 10 (pink line).

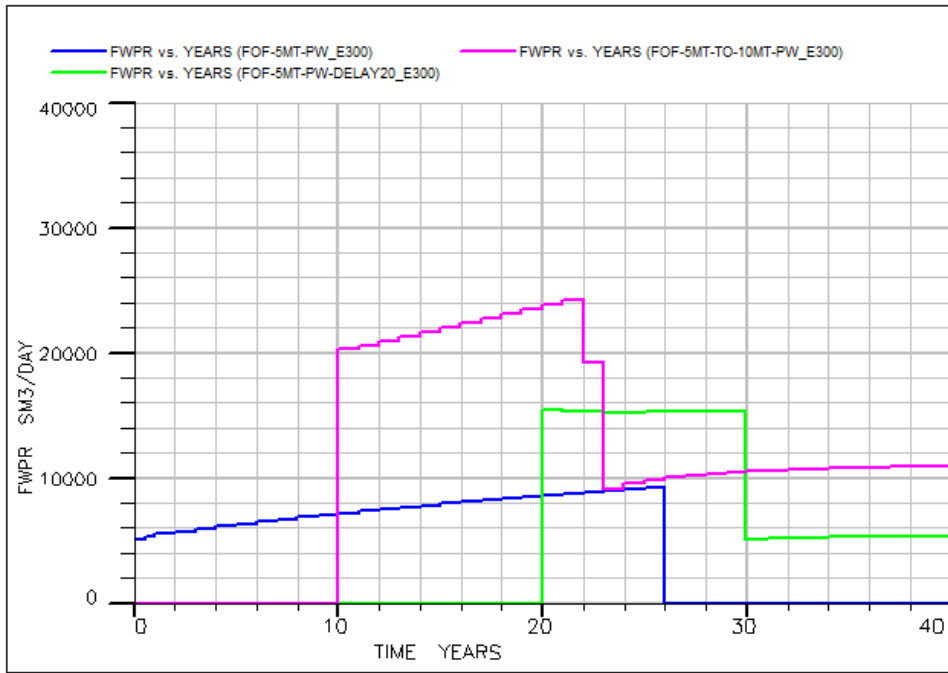


Figure 4-8 Comparison of field water production rate (FWPR) vs time for the base case with water production at the beginning of injection (blue line), with water production commencing after 20 years of injection (green line) and when the field injection rate increases to 10 Mt/y at year 10 with water production commencing at the same time (pink line).

Table 4-3 Key technical input data for the additional Firth of Forth modelling.

ID	Description	Flow rate (Mt CO ₂ /y)	Injection duration (years)	Brine production	Well type	Production wells converted to injection wells	Total CO ₂ injection wells	Total brine production wells	Bottom hole pressure (MPa)	Grid length (m)	Grid width (m)	Average well depth (m)	Maximum brine production (m ³ /d)
191	FoF-5MT-delay20	5	10	No	Vertical	No	5	0	27.0	4400	2200	2200	0
192	FoF-5MT-delay20	5	20	No	Vertical	No	5	2	30.0	4400	2200	2200	15420
193	FoF-5MT-delay20	5	30	Yes	Vertical	No	5	2	30.0	6200	3400	2600	15252
194	FoF-5MT-delay20	5	40	Yes	Vertical	No	5	2	30.0	6600	3400	2600	5347
195	FoF-5MT-to-10MT	5	10	No	Vertical	No	5	0	33.6	4400	2200	2200	0
196	FoF-5MT-to-10MT	10	20	Yes	Vertical	No	10	4	35.6	6200	8200	2600	23515
197	FoF-5MT-to-10MT	10	30	Yes	Vertical	No	10	4	37.5	6200	8200	2600	10436
198	FoF-5MT-to-10MT	10	40	Yes	Vertical	No	10	4	37.8	6200	8200	2600	10916

5 Tay Formation with Brine Production

5.1 Geology Data

The Tay Sandstone Member is located in the Central North Sea, at latitude 57.241, longitude 0.95325. The code for this aquifer in the CO₂Stored database is 235.000. It encompasses an area of about 3,000 km², with an average thickness of 75m. It is included in an integrated study of saline aquifers in the Central North Sea (Jennette et al., 2000). Based on a comprehensive data set, which includes 8,400 km² of 3D seismic, 11,100 km of 2D seismic, 350 well-logs and core data from 30 wells, new insights into the reservoir facies and architecture were obtained. The Tay basin-floor fan was characterized by using 3D seismic surveys calibrated to over 100 well-log synthetics by the British Geological Survey (Jin and Mackay, 2009).

As shown in Figure 5-1, the older Tay Sequences 1 and 2 (Middle and Lower) have greater basin-ward extent and the younger Tay sequences (Upper) are significantly smaller. Three sand developments are separated by laterally extensive shales (Armstrong et al., 1987). The Middle and Lower Tay Formation is dominated by clean, turbidite sandstones containing a high sand content. The thicknesses of the Upper Tay sandstones vary from thin to very thick with minor shales. No significant faults were found in the area.

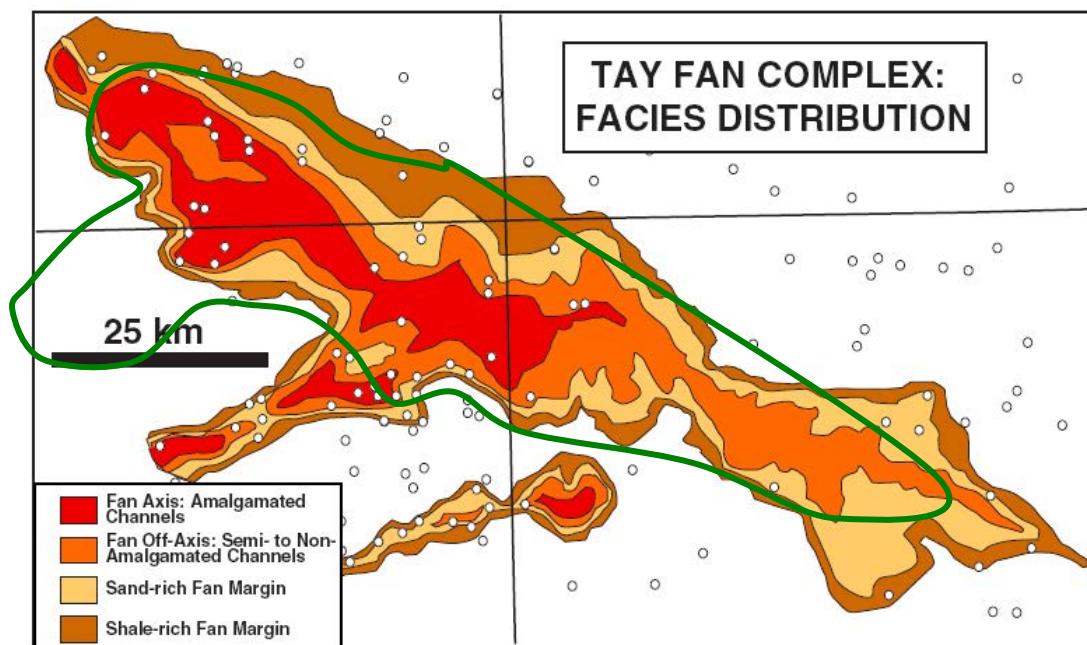


Figure 5-1 Detailed expression of the complete Tay Fan isochron and facies distribution map with the BGS Top-Tay surface overlaid in green.

5.1.1 Pressure and Temperature

The pressure gradient of the Tay formation shows a hydrostatic distribution. The Tertiary aquifers in the Viking Graben and in the Central Graben are expected to form 'open' reservoirs (Holloway, 1996). However, some oilfield data (Holloway and Vincent, 2006) show an overpressure. An average pressure and temperature are used in the references for most of fields, such as Teal, Cook, and Gannet, in and around the Tay formation.

The initial formation conditions thus include a hydrostatic pressure distribution which is dependent on the brine density and a geothermal temperature distribution. The average subsurface hydrostatic pressure increases with depth by 105 bar/km for aquifers that are in open communication with the surface water. The average geothermal gradient is approximately 30 °C/km. The major sedimentary basins of Western Europe, including the North Sea Basin, have geothermal gradients of 30 °C/km (Holloway, 1996). In this study, the initial pressure and geothermal gradients used for the Tay model were the following values:

The hydrostatic pressure gradient = 0.45 psi/ft = 102 bar/km

The geothermal gradient = 2.8 °F/100 ft = 30 °C/km

5.1.2 Porosity and Permeability

The average net sandstone thickness for the Upper Tay Formation is 163 ft (49.5m). The average core porosity is 0.346 (the CO₂Stored database (ETI, 2015) gives a range of 0.19-0.33). In Shell's Gannet A report (Donley, 2007), the porosity for the Upper Tay sand is 0.32-0.33 and the permeability is 500-2000 mD. The range of horizontal permeability varies between 10 mD and 6000 mD in the CO₂Stored database with a P50 value of about 410 mD. The ratio of vertical permeability to horizontal permeability is 0.8.

In this study, the porosity used in the HW model is 0.328 with an average horizontal permeability $K_h = 887$ mD and an average vertical permeability $K_v = 700$ mD.

5.1.3 Formation Compressibility

The compressibility of both the formation rock and the brine are important parameters for a 'closed' aquifer, in which the volume of CO₂ injected must be accommodated by compression of the reservoir. These data are required by the simulator as inputs, but are not included in the CO₂Stored database.

For typical North Sea conditions, the average pore compressibility is 1.5×10^{-3} 1/MPa, with an uncertainty of about 50% (Fatt, 1958; Hall, 1953). The compressibility of formation water for North

Sea aquifers will only vary between 3.9×10^{-4} and 4.5×10^{-4} 1/MPa (Holloway, 1996). Therefore, the total compressibility $C_t = C_f + C_w = 1.9 \times 10^{-3}$ 1/MPa.

5.2 Multiple Layers between Top and Base Surfaces

Well top data from well-logs and the then Department of Trade and Industry (DTI) database are used to create three zones in the model. The zones are Upper Tay, Tay Shale and Middle/Lower Tay. There are 5 layers in Upper Tay and 4 layers in Middle/Lower Tay, while there is only one layer in the Tay Shale. In order to better simulate the buoyancy effect of CO₂ during its migration, while using a limited number of cells to reduce computational overhead, a second model was developed where the ratios of each layer from the top to the bottom in each zone are 1:2:3:4:5 - so the thinnest layer is always at the top of each zone, to better capture CO₂ gravity segregation and propagation in the upper layers. The total number of cells is the same for the two models, but the number of active cells is different because of pinch out in the model. Figures 5-2 shows the three zones and 10 layers, with the Upper Tay becoming thinner moving down dip (from west to east, left to right in the figure).

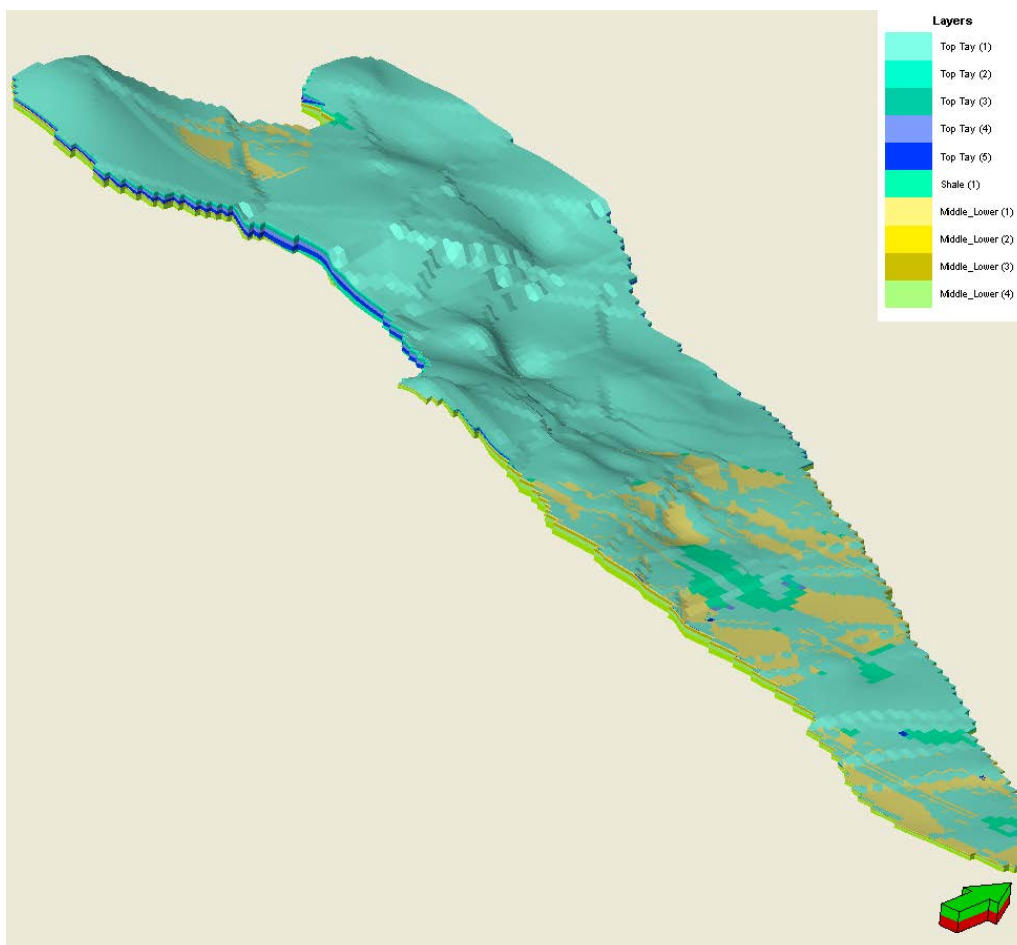


Figure 5-2 Zones and layers of Tay Formation model.

5.3 Reservoir Simulation Model (ECLIPSE)

The dimensions of the ECLIPSE model are 205 x 93 x 10 cells, with a total of 190,650. There are 67,454 active cells in the model, as shown in Figure 5-3. Each cell is 500m x 500m areally. As convergence difficulties were encountered for permeability and hysteresis sensitivity simulations, the pinchout thickness was set to be 1.0m to remove very thin cells which did not significantly affect the storage volume of the system but which made convergence more difficult due to a high throughput to volume ratio. There are 3600 non-neighbour connections (NNC) in the model after introducing this pinchout setting, and the numerical convergence performance was improved.

ECLIPSE E300 with CO2STORE module (Schlumberger, 2015) was used for all injection simulations. This option is typically used to study CO₂ storage in CO₂-H₂O system with salts. Three phases can be considered in the option; that is a CO₂ rich phase, which is labelled as 'gas', an H₂O rich phase labelled as 'water', and a solid phase – salt. The mutual solubility of CO₂ is based on experimental data for CO₂-H₂O systems at temperatures between 12 and 100 °C and pressures up to 600 bars. The brine density is calculated based on Ezrokhi's method, which accounts for the effect of salt and CO₂. The gas (CO₂) density is obtained by a tuned cubic equation of state (Peng-Robinson EoS). The partitioning of CO₂ and H₂O in liquid and gas phases follows the Spycher and Pruess method. The mole fraction of dissolved CO₂ and CO₂ rich phase can be output by ECLIPSE so the migration can be traced.

The Brooks and Corey method is used to calculate the water and gas relative permeability curves. The Brooks-Corey parameter λ is 2.0. The residual brine saturation is 0.2 and the residual CO₂ saturation is 0.05.

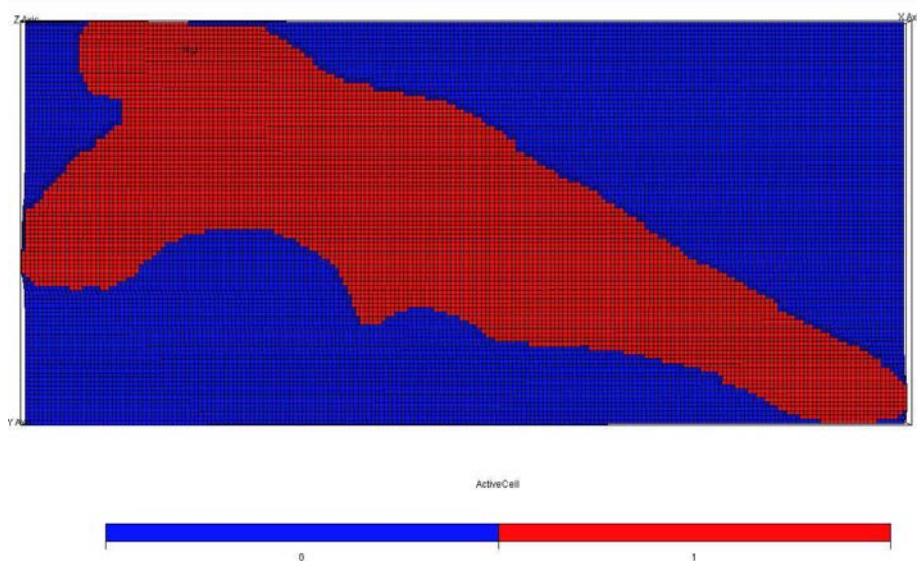


Figure 5-3 Active cells (in red) in the top layer of the ECLIPSE model (in red).

The first model geometry described above is used as the base case in this study. Model assumptions and parameters are as follows:

- The initial reservoir pressure gradient is 0.45 psi/ft (0.1 bar/m) and the temperature gradient is fixed at 30 °C/km.
- A closed boundary is assumed.
- The injectors are controlled at an injection rate of 1.5 Mt/yr, but with the maximum bottom hole pressure set to less than 70% of the Lithostatic pressure, which is ca. 1.0 psi/ft. The injectors are grouped and the group maximum injection rate was set to 5 Mt/year. The field injection rate was the target CO₂ injection rate, which was varied between 2, 5, 10, 15, 20, and 40 Mt/year in the sensitivity analysis. The period of injection was varied between 10, 20, 30, and 40 years.
- The locations for injectors is chosen where the formation has high injectivity (the thickest and highest permeability sands), and at existing well sites. The water producers are located at a distance of about 5 km from the injection cluster.
- The number of wells depends on the ability of injectors to achieve the desired injection rates, whilst ensuring that the bottom hole pressures do not exceed fracture pressure.
- Injection fluid temperature at the well head is 5 °C, assuming CO₂ cools to seabed temperature during transport.
- The mean horizontal permeability is 887 mD and the ratio of vertical permeability to horizontal permeability is 0.8 (giving a vertical permeability of 700 mD). The horizontal permeability varies between 500 mD and 2000 mD, with a standard deviation = 1.0.
- The mean porosity is 0.3 and varies from 0.2 to 0.4 with a standard deviation = 1.0.
- The mean net-to-gross (NTG) is 0.8 and varies from 0.6 to 1.0 with a standard deviation = 1.0.
- Reservoir initial water saturation $S_w = 1.0$ and the salinity of brine = 100,000 ppm (it is 60,600 ppm in the CO₂Stored database).
- Relative permeability and capillary pressure data from other published models of CO₂ injection in saline aquifers with no hysteresis are used.

5.4 Methodology

Because of the high permeability of the Tay formation, the injection rates for single wells were set higher than for the Forties formation. The locations of water producers were also set further away from the injectors because this way pressure relief could still be effectively provided whilst avoiding

early CO₂ breakthrough. As mentioned above, the maximum injection rate for each well was set to 1.5 Mt/y, while a group of 5 injectors might inject a maximum of 5 Mt/y. Vertical injectors were used.

Two group of models are used; one is the base case group, in which six cases were simulated with injection rates of 2, 5, 10, 15, 20, and 40 Mt/y, without water production, and the other is a comparison group in which model in the base case group is run again, but this time with water production.

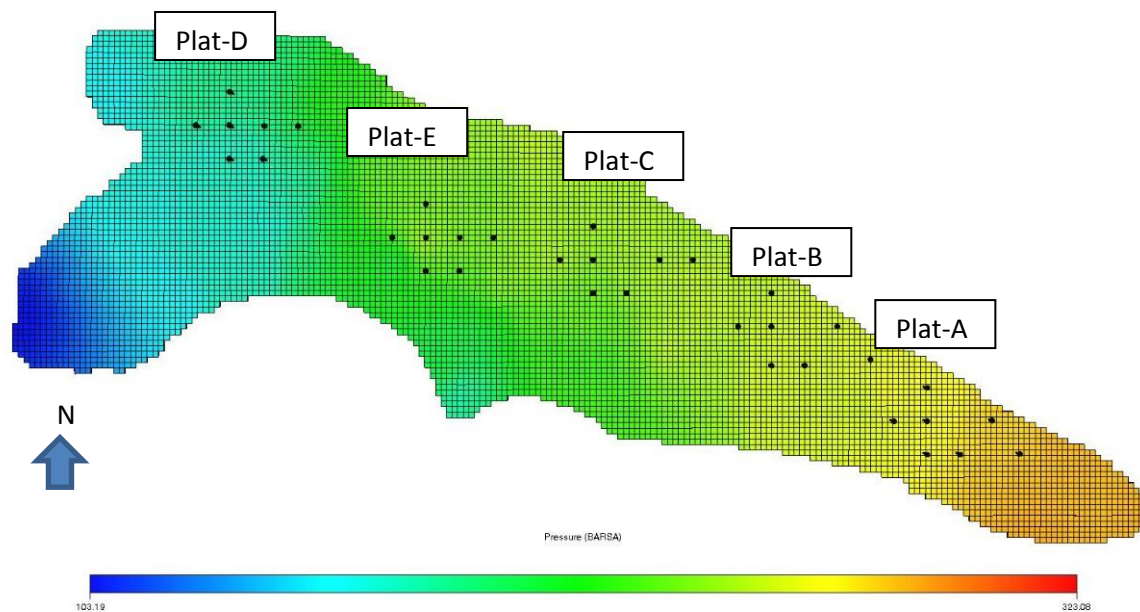


Figure 5-4 Depth of Tay formation with gridding and well locations.

As shown in Figure 5-4, each cluster has five injectors and two producers. The two water producers were the two in the most north-easterly part of each group. The distance between each of the injectors is 3 km (6 grid cells) and the distance between a water producer and the closest injector is between 3 and 6 km (6-12 grid cells). Based on a sensitivity study using a homogeneous model the breakthrough time in a formation with high permeability (>100 mD) is about 15 years if the spacing is 3.8 km. Because the Tay formation was shallower in the South-West, the producers were located towards the North-East of each group of injectors in order to delay the CO₂ breakthrough and to maximize the time for water production.

5.5 Static Storage Capacity

By definition, for the calculation of static storage capacity all aquifers have boundaries and are closed systems, regardless of the scale (i.e. reservoir scale, formation scale, or basin scale). Even though the initial reservoir pressure may be hydrostatic, the volume of CO₂ that is injected must displace a volume of water (brine or fresh water) which, because the system is closed, must result in an increase in pressure. Besides CO₂ migration and reservoir pressure changes, water displacement becomes one of the most important concerns in any storage project.

For a closed aquifer, the compressed volume of water and pore space is the volume (V_{CO_2}) that CO₂ can occupy as a consequence of increasing the average pressure Δp .

$$V_{CO_2} = V_w (C_p + C_w) \Delta p$$

Based on the Tay Aquifer model, the total pore volume initially occupied by brine $V_w = 55 \text{ km}^3$. The pore compressibility $C_p = 15 \times 10^{-5} \text{ (1/bar)}$ and the compressibility of water $C_w = 5 \times 10^{-5} \text{ (1/bar)}$. The allowed pressure increase may be defined as the maximum pressure that may cause a boundary (say a fracture) to leak or the maximum capillary pressure of the sealing rock, whichever is the lower. In this study, the fracture pressure is taken as 80% of the minimum horizontal in-situ stress of rock, which is assumed to be 0.8 psi/ft (0.178 bar/m) for this calculation. If the safety coefficient is 0.8, then the gradient of maximum reservoir pressure is 0.142 bar/m. At a depth of 2000 m, for example, the reservoir initial pressure is 220 bars and the allowed local reservoir pressure is 260 bars. The value of average pressure allowed should be lower than the local pressure value. The difference between the local pressure and average pressure depends on the permeability and pressure profile. Usually, 10% of initial pressure is used as the limit for the increase in average pressure for an aquifer where permeability is unknown.

Based on this calculation, the resource volume is:

$$V_{CO_2} = V_w (C_p + C_w) \Delta p = 55 (15 \times 10^{-5} + 5 \times 10^{-5}) \times 40 = 0.44 \text{ km}^3$$

If the density of CO₂ is 700 Mt/km³, the total mass of CO₂ that can be stored in the Tay Formation is 308 Mt without consideration of the sweep efficiency. If a Volumetric Sweep Efficiency of 0.33 (P50 in CO₂Stored) was used, the theoretical capacity is about 100 Mt (104 Mt in CO₂Stored P50).

5.6 Maximum Injection Pressure and Minimum Production Pressure

The maximum injection pressure depends on the formation fracture pressure. The minimum *in situ* horizontal stress σ_h is taken as the fracture pressure under the normal formation stress condition. A

formation stress gradient of $\sigma_h = 0.7$ psi/ft and a gradient of initial pore pressure of 0.45 psi/ft are commonly used if the precise formation stress and pressure gradients are not available. In the study, the maximum injection pressure $P_{\max} = 0.7 / 0.45 \times 0.9 P_{\text{initial}} = 1.4 P_{\text{initial}}$.

The minimum production pressure of a producer was set to be the initial pore pressure at the datum depth of the producer. A production well was controlled by two criteria. One is the maximum water production rate (which is 16,000 m³/day in this study) if the well bottom hole pressure (WBHP) is on or above the minimum production pressure. The other is the produced mole fraction of CO₂ (WXMF_1) and production rate of CO₂ (WGPR). A water producer opens for production when its WBHP exceeds the minimum pressure, and is shut down when the amount of produced CO₂ exceeds the limits set (WXMF > 0.0001 or WGPR > 28.3 m³/day in this study). It should be noted that these are very conservative constraints for CO₂ production.

As shown in Figure 5-4, injectors were grouped in association with five clusters. For each scenario the clusters were added beginning from the deeper end of the system. The first step was to find the impact of the pressure restriction on the injection rate whilst maintaining the number of wells constant during each period of injection. The injectivity would thus reduce with time and the storage capacity without water production could be evaluated. The next step would be to add injectors in the next period of injection to maintain the target injection rate.

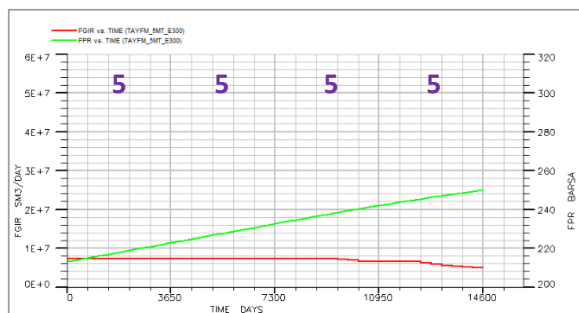
The spacing between the injection wells is 3000 m and the distance between the centres of any two adjacent clusters is about 15km. Since the maximum injection rate per well is 1.5 Mt/y, the minimum number of wells increases from 2 for the 2 Mt/y scenario to 27 for the 40 Mt/y scenario.

5.7 Simulation Results and Analysis

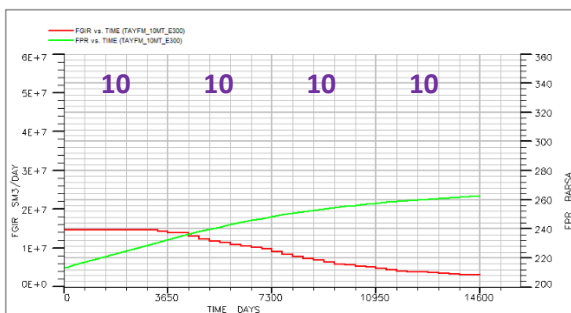
Twelve simulations were run: six cases with the field injection rate varying from 2 Mt/y to 40 Mt/y with no water production, and six cases for the same injection rates, but with water production. Except the case with an injection rate of 40 Mt/y, in all of the cases with water production the total number of wells was the same as for the corresponding case without water production. The cases with water production wells thus used fewer injection wells, such that the total well stock of injectors and producers was the same as for the corresponding injection only cases. Only in the 40 Mt/y cases were the well stocks different, there being the same number of injectors in both cases, but 2 new production wells were added to each cluster of 5 injection wells; thus the ratio of injectors to producers was 5:2 in the 40 Mt/y case, whereas in all the other cases the ratio was 4:1.

Table 5-1 Key technical input for the Tay Model.

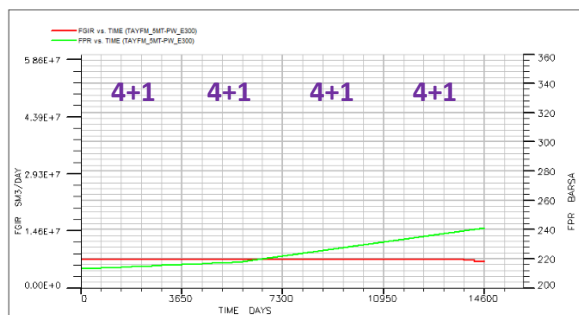
Case I/D	Brine production	CO ₂ Injection wells						Brine Production wells						Duration for const. inj rate	Total CO ₂ injected	Max. brine production rate	Total brine produced	Void replace rate (V _w /V _{co2})
		Number of wells				Injection rate/well	Max. WBHP	Number of wells				WBHP target	Production rate limit					
		10	20	30	40			Mt/y	bar	10	20							
TAY-2MT-PLAT	NO	2	2	2	2	1.5	320					220		40	80			
TAY-5MT-PLAT	NO	5	5	5	5	1.5	320					220		26	130			
TAY-10MT-PLAT	NO	10	10	10	10	1.5	320					220		9	90			
TAY-15MT-PLAT	NO	15	15	15	15	1.5	320					220		6	90			
TAY-20MT-PLAT	NO	20	20	20	20	1.5	320					220		6	120			
TAY-40MT-PLAT	NO	25	25	25	25	1.5	320					220		3	120			
TAY-2MT-PLAT-PW	YES	2	2	2	2													
TAY-5MT-PLAT-PW	YES	4	4	4	4	1.5	320	1	1	1	1	220	16000	38	190	13870	72.4	0.23
TAY-10MT-PLAT-PW	YES	8	8	8	8	1.5	320	2	2	2	2	220	16000	34	340	29640	269.2	0.48
TAY-15MT-PLAT-PW	YES	12	12	12	12	1.5	320	3	3	3	3	220	16000	39	585	45350	486.5	0.50
TAY-20MT-PLAT-PW	YES	16	16	16	16	1.5	320	4	4	4	4	220	16000	20	400	47770	305.0	0.47
TAY-40MT-PLAT-PW	YES	25	25	25	25	1.5	320	10	10	10	10	220	16000	23	920	136820	931.7	0.66



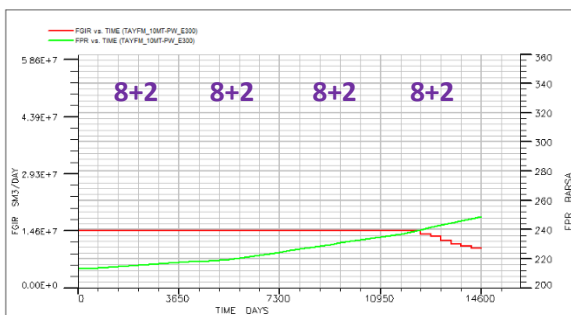
5 Mt/y without water production (base case)



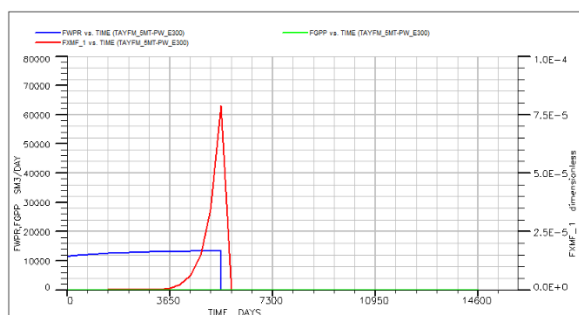
10 Mt/y without water production (base case)



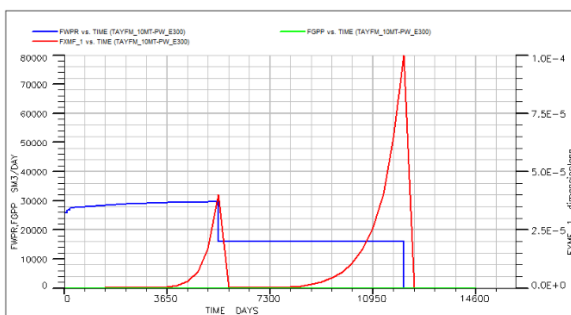
5 Mt/y with water production



10 Mt/y with water production



5 Mt/y - water production rate & CO₂ mole fraction



10 Mt/y - water production rate & CO₂ mole fraction

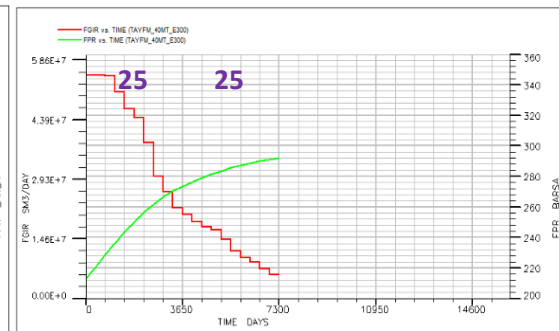
Figure 5-5A Comparison of field CO₂ injection rate (FGIR) and field average pressure (FPR) for each case in base group (top row) and water production group (middle row), and water production rates (FWPR lines in the bottom row) for each case with CO₂ breakthrough vs. time (FXMF lines in the bottom row).



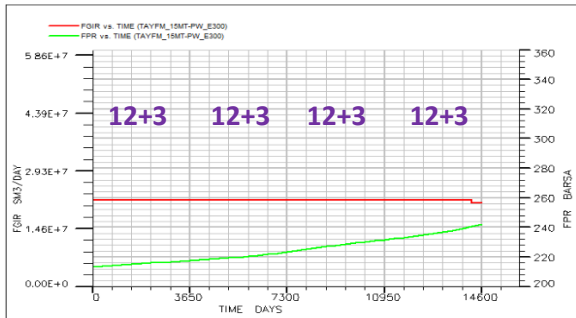
15 Mt/y without water production (base case)



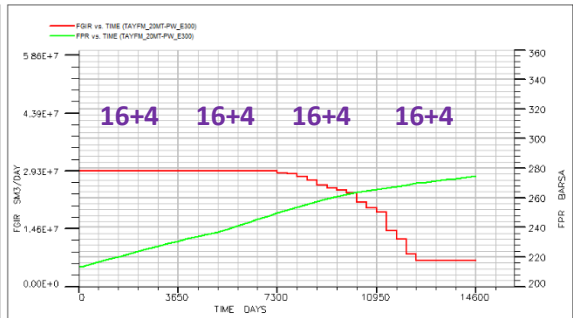
20 Mt/y without water production (base case)



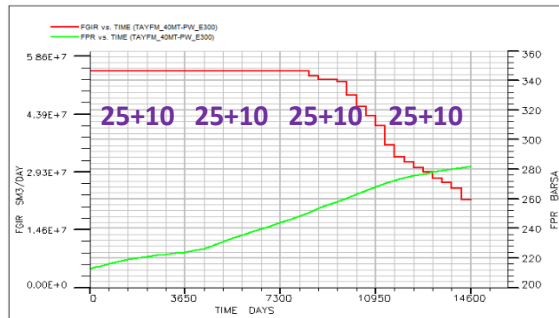
40 Mt/y without water production (base case)



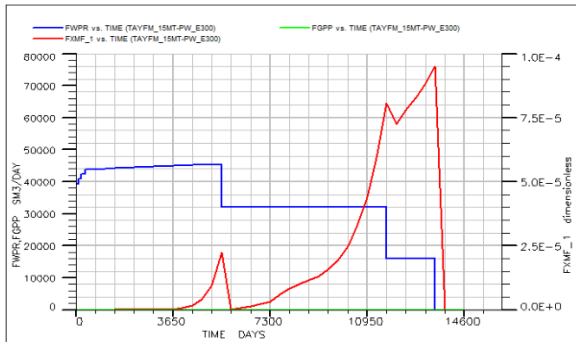
15 Mt/y with water production



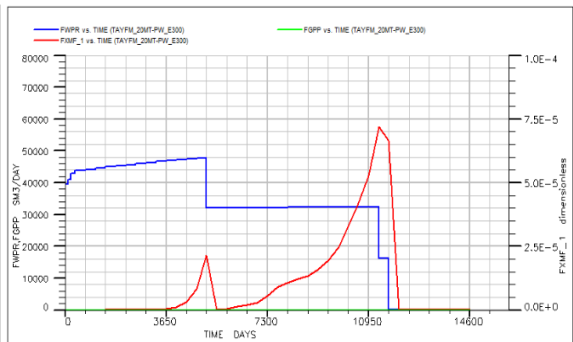
20 Mt/y with water production



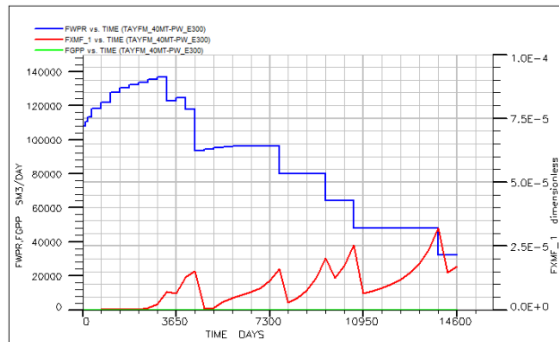
40 Mt/y with water production



15 Mt/y water production rate & XMF



20 Mt/y water production rate & XMF



40 Mt/y water production rate & XMF

Figure 5-5B Comparison of field CO₂ injection rate (FGIR) and field average pressure (FPR) for each case in base group (top row) and water production group (middle row), and water production rates (FWPR lines in the bottom row) for each case with CO₂ breakthrough vs. time (FXMF lines in the bottom row).

The results are listed in Table 5-1, including the total number of injectors and producers in each case, the maximum well bottom pressure used for injector control, and the minimum well bottom pressure for producer control. Both injector and producer bottom hole pressures were varied depending on the depth of each injector or producer. All producers were also limited by gas production rate and CO₂ mole production rate. Any producer would be shut down once these criteria were exceeded.

Figure 5-5a and Figure 5-5b show a comparison of the results from the base case with the results from water production case. The diagrams on the top row are field CO₂ injection rate (FGIR) and field average pressure (FPR) for each case with different injection rates. The results from the comparison group with water production are shown in the middle row. The duration of the period with constant injection rate reflects the capacity under that certain injection scenario, i.e. the capacity with that specified number of injectors/producers and the given injection/production rates. It can be seen from the two groups of curves that the effect of water production is significant in terms of reducing the field pressure, extending the period of stable injection, and therefore, enhancing the storage capacity. The reason the Tay formation is amenable to this type of improvement is its high permeability. The producers were set at a distance of 3 to 6 km from the nearest injector, and on the deeper side of each cluster. Thus pressure communication and relief was effective due to the high permeability, but gravity could be used to delay the CO₂ breakthrough. The capacity was increased by up to five times due to water production in the cases with a ratio of injectors to producers of 4:1, without increasing the total well stock.

In the 40 Mt/y case, by setting two producers in a line pointing away from the cluster of injectors, the task of water production could be taken over by the more distant producer when the producer closer to the injection cluster was shut down due to CO₂ breakthrough - thus maintaining a constant offtake rate for longer. The total volume of water produced was doubled, improving the efficiency of the storage; the injected CO₂ ultimately occupied some 2.4% of the total pore volume. This value is similar to the storage efficiency of an open aquifer. This means that with brine production, pressure ceases to be the constraint that limits storage capacity, but instead the extent of CO₂ migration will be the restriction that determines when injection must stop.

The diagrams on the bottom row of Figure 5-5b show, for each case, the water production rates (blue line) together with the mole fraction of CO₂ in the production brine (red line) and

the rate of CO₂ production as a free gas under surface conditions (green line). It can be seen that:

- CO₂ is produced mainly dissolved in water, rather than as a CO₂ rich gas phase. This means that while the CO₂ injected as free phase moves toward to the top of reservoir due to buoyancy, and while any CO₂ dissolved in water will sink down to the bottom of the reservoir, since the water producers were perforated in the lower layers, the CO₂ that is produced is predominantly that which has dissolved in water that is subsequently displaced towards the producers.
- If voidage replacement is almost established - i.e. the brine is produced from the reservoir at almost the same volume rate as CO₂ is injected into the reservoir, as measured at reservoir pressure, as is the case during the first 10 years in the 15 Mt and 40 Mt cases, the field average pressure increases only very slowly compared with the case where there is no brine production. This balance is only broken when the producer shuts down as a result of CO₂ breakthrough, as shown in the figure.

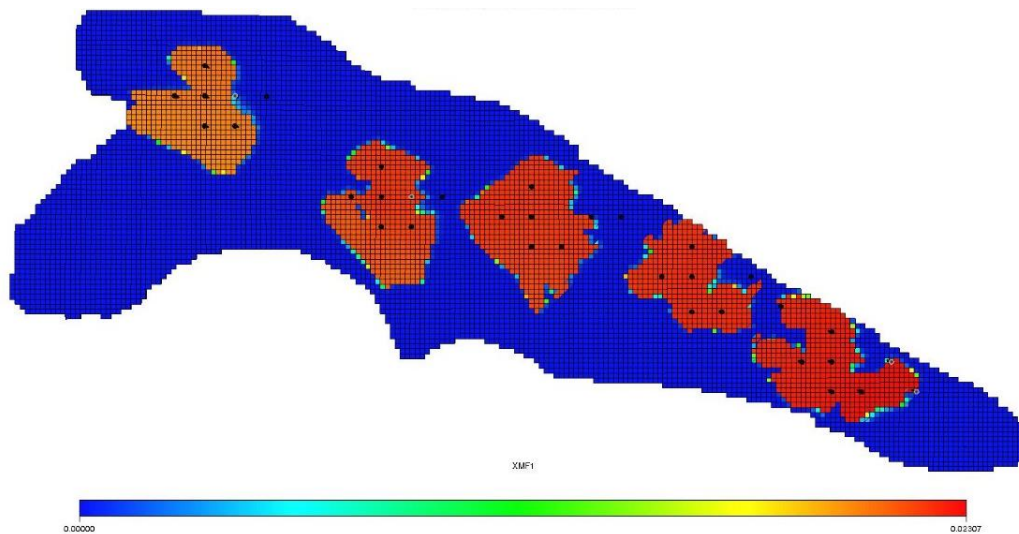


Figure 5-6 Distribution of dissolved CO₂ after 20 years of injection at 40 Mt/y.

Figure 5-6 shows the distribution of dissolved CO₂ after 20 years injection in the 40 Mt/y injection rate scenario. In this case there were two producers in each cluster, so that when one producer was shut down the other one, which is twice as far as the first producer from the nearest injector, could still work properly. Even though the field pressure increases after

the first producer was shut due to the less effective pressure relief because of the greater inter-well distance, the storage capacity would still be increased significantly.

5.8 Conclusion

If 60% of Lithostatic pressure is used as the maximum injection pressure, then injection rate will be pressure limited after 6 years of constant rate injection when the total injection rate is over 15 Mt/y; i.e. the capacity for CO₂ storage in the Tay formation aquifer will be reduced unless water production is used to provide pressure relief.

In the worst case scenario studied, where the Tay aquifer is treated as being a closed system and when the lowest pressure constraint was applied, only 0.33% of total pore volume can be used for storage, a storage volume of 100 Mt.

Assuming again that the site is closed, but now extracting 40,000 sm³/d of water, without increasing the total number of wells the Tay aquifer can readily store 400 Mt of CO₂.

When the ratio of injectors to producers is increased from 4:1 to 5:2, pressure may never be the constraint that limits capacity, and thereby the storage efficiency can be increased significantly.

6 Impact of Grid Resolution

6.1 Grid Resolution Sensitivity in a Flat Homogenous Model

In order to investigate the relation between reservoir parameters, such as permeability, dip angle, and engineering parameters such as inter-well distance and injection and production rates, and the relation between depth of perforations for producers relative to injectors, a quarter five spot model was used. (This is a standard configuration for sensitivity calculations, and entails placing two vertical wells at opposite corners of a rectangular cuboid shaped model. A sensitivity study investigating grid resolution was carried out to evaluate the effect of grid resolution on timing of CO₂ breakthrough and on pressure response.

6.1.1 Lateral and Vertical Grid Resolution Sensitivity

The developed model has dimensions of 1215 m X 1215 m laterally and 216 m vertically, with a numerical aquifer connected to the two boundaries opposite the injector to enable the total pore volume to be enlarged by 17 times the volume of the study region. The model is homogeneous, with a porosity of 0.15 and permeability in the horizontal directions of 10 mD, and 1.0 mD vertically. The total pore volume of the study area of the model is $47.83 \times 10^6 \text{ m}^3$, and $835 \times 10^6 \text{ m}^3$ including the volume of the numerical aquifer. The depth of the top of the model is 2840 m. The pore compressibility is $5.5675 \times 10^{-5} \text{ 1/bar}$.

The brine producer was controlled by pressure and limited by the maximum production rate. The CO₂ injection rate is 0.2 Mt/y and the injection period is 30 years. The initial pore pressure is 290 bars at the datum depth at the top of the reservoir. The maximum allowable injection pressure is 390 bar. The minimum production pressure is 260 bar, with the maximum production rate limited to 16000 m³/d. The producer will shut down if the produced CO₂ mole fraction in the water phase exceeds 0.0001, i.e. 0.01%, or the gas production rate is over 28.3 m³/d, i.e. 1 Mscf/day.

The models for the grid resolution study were refined by a factor of three, starting from a cell size of 405 m X 405 m. Model parameters are listed in Table 6-1. One injector, identified as I1, was located at a position 202.5 m from one edge and 202.5 m from the adjacent edge (thus in the centre of a cell in the corner of the coarsest model) and perforated from layer 1 to layer 14. One producer, identified as P1, was perforated from layer 15 to layer 18, and was located at a position 1012.5 m from the first edge mentioned above, and also 1012.5 m from the other edge (thus in the centre of a cell in the opposite corner of the coarsest model). In all the

sensitivity studies the wells would be placed in grid blocks selected such that their absolute position, and hence the inter-well distance, would remain unchanged.

Table 6-1 Model parameters and results

Model	405M-18	135M-54	45M-162	15M-468
Cell length and width (m)	405	135	45	15
Cell thickness (m)	12	4	1.333	0.444
Number of cells horizontally	3	9	27	81
Number of cells vertically	18	54	162	468
Total number of cells	162	4,374	108,098	3,070,548
Time to run simulator (s)	34.4	256	8,885	274,247
CO ₂ breakthrough time (FXMF1>0.0001)	5844	5844	6575	6940
Pressure at injector after 10 years (bar)	343.4	337.2	328.6	321.8
Total produced water after 10 years (x10 ⁶ m ³)	0.962	0.985	0.985	0.984

Table 6-2 Models used in the study of grid resolution. The models marked by a circle on the diagonal show those cases where the cells are refined both laterally and vertically compared to the next coarsest one. The models marked with a cross are those where the cell aspect ratio was changed.

Number of layers (and thickness)	Lateral cell size (m)				
	405	135	45	15	5
18 (12 m)	o	x	x	x	x
54 (4 m)	x	o	x	x	
162 (1.333 m)	x	x	o	x	
486 (0.444 m)	x	x		o	

Table 6-2 shows all the models used in this study. As also shown in Table 6-1 the lateral cell dimensions changed from 405 m to 5 m in decreasing steps by a factor of three each time.

(The cell sizes were used in the definition of each model's name.) The vertical cell size was also changed by a factor of three, in steps from 12 m to 0.444 m. (Because the decimal point cannot be used in the file name root in ECLIPSE, the *number* of layers was used as the second part in constructing each model's name.) The total thickness of all the models is 216 m, so that the thickness of any cell can be calculated by dividing the total thickness of the model by the number of layers in that model. The models marked by a circle on the table diagonal show those cases where the cells are refined both laterally and vertically compared to the next coarsest one, thus preserving their aspect ratio. The models marked with a cross are the ones where the cell aspect ratio was changed. For example, model 405M-18 and model 135M-54 have the same aspect ratio ($405:12 = 135:4$). However, the aspect ratio of a cell in model 15M-18 is 15:12. The range of the aspect ratios in these models is from 5:12 to 405:0.444, i.e. between 0.417 and 912. The aim of this is to analyse the effect of aspect ratio on CO₂ migration.

Table 6-3 Properties of model geometry (cells sizes in X, Y and Z directions, aspect ratios and bulk volumes, total number of cells in grid and CPU time required to run calculation over 16 years timeframe.

	Model name	Dx (m)	Dy (m)	Dz (m)	Dz/Dx aspect ratio	Cell bulk volume (m ³)	Total number of cells	Elapsed CPU time after 16 years simulation time (seconds)
1	5P-405M	405	405	12.0	0.030	1,968,300	162	51.69
2	5P-405M-54	405	405	4.00	0.010	656,100	486	28.67
3	5P-405M-162	405	405	1.33	0.003	218,700	1,458	98.11
4	5P-135M	135	135	12.0	0.089	218,700	1,458	114.6
5	5P-135M-54	135	135	4.00	0.030	72,900	4,374	207.1
6	5P-405M-486	405	405	0.44	0.001	72,900	4,374	763.0
7	5P-135M-162	135	135	1.33	0.010	24,300	13,122	345.4
8	5P-45M	45	45	12.0	0.267	24,300	13,122	249.0
9	5P-135M-486	135	135	0.44	0.003	8,100	39,366	4,194
10	5P-45M-54	45	45	4.00	0.089	8,100	39,366	1,250
11	5P-45M-162	45	45	1.33	0.030	2,700	118,098	3,632
12	5P-15M	15	15	12.0	0.800	2,700	118,098	10,202
13	5P-15M-54	15	15	4.00	0.267	900	354,294	45,355
14	5P-15M-162	15	15	1.33	0.089	300	1,062,882	did not complete
15	5P-5M	5	5	12.0	2.400	300	1,062,882	222,219
16	5P-15M-486	15	15	0.44	0.030	100	3,188,646	693,811

Figure 6-1 draws a correlation between CPU time used for simulation of a 16 year injection period and the number of cells in the model. For models with more than 1 million cells, calculations were performed in parallel using up to four cores. Regardless of whether or not parallel calculations were used, the CPU time increase is linear with the number of cells.

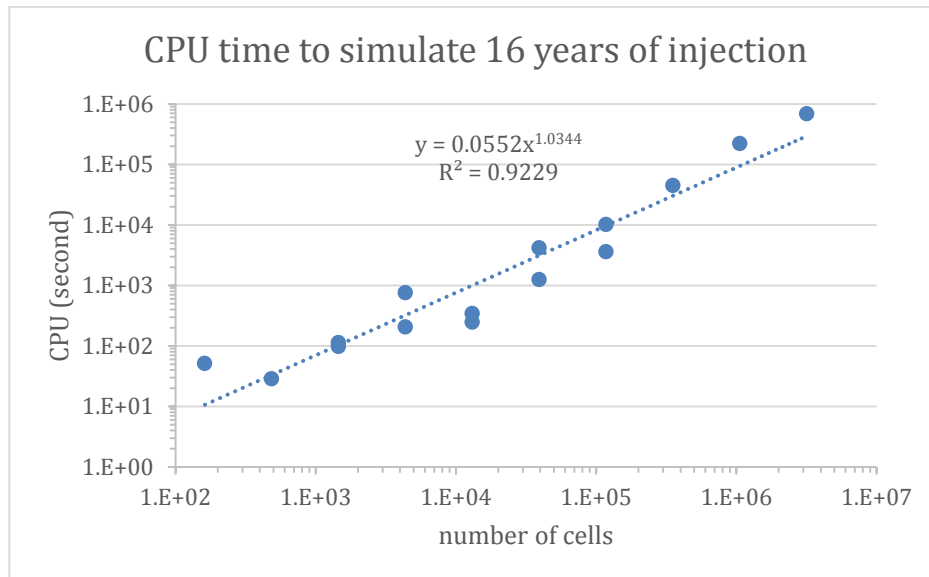


Figure 6-1 Correlation between CPU time (in seconds) used in simulation of 16 years of injection and the number of cells in the ECLIPSE E300 models using one processor (except for the finest two models, for which 4 cores were used).

The study of the sensitivity to grid resolution was carried out in three stages. First, the series of simulations starts with the coarsest one, 405M (18). The number of layers was kept constant at 18 layers, but the sizes of the cells in the lateral direction were reduced by a factor of three each time to study the effect of lateral size, i.e. to evaluate the models in row one of Table 6-2.

Next, case 135M (18) was chosen. Lateral dimensions of the cells were kept unchanged, but the vertical size was reduced by a factor of three each time, i.e. to evaluate the models in column two in Table 6-2. In the final stage, the cell sizes were reduced in all directions, lateral (x and y) and vertical (z), by a factor of three, i.e. the diagonal direction in Table 6-2. For each node on the diagonal, the rest of the simulations along the vertical and horizontal directions were compared with the result from the diagonal node to check whether the simulation can be replaced by a model with fewer cells.

6.1.2 The Impact of Grid Resolution on Pressure

The response of the water producer to the pressure increase due to CO₂ injection is reflected by changes in the water production rate; the production rate was determined by the local pressure and was limited by the maximum production rate. As in return the water production rate affects the pressure at the injector, and thus the CO₂ injection rate, CO₂ storage is dependent on the connectivity between the two wells. The connectivity between wells is affected by grid resolution, even if all other physical properties (inter well distance, formation permeability, fluid viscosity, etc) remain the same, and thus grid resolution has an impact on the estimation of storage capacity.

Figure 6-2 shows the water production rate for the first 1000 days for models with cells with the same thickness, but different lateral sizes. In all cases the initial water production rate cannot be maintained: this is because pressure support from the injection well takes time to be fully established. Thereafter, as flow becomes fully established, pressure at the producer gradually builds up over time, and thus the flow rate also increases over time. The figure also shows that the coarsest model (405m) has a much higher production rate than the other models. This means that the pressure response of the coarse model is faster than that of the fine models, such that a higher production rate was required to maintain the bottom hole pressure at its initially set value. Figure 6-3 shows the bottom hole pressure for the injector after 16 years for all the models in this sensitivity study. The x-axis is the cell bulk volume, which reflects the resolution of the model, as shown in Table 6-3. The bottom hole pressure in the CO₂ injector after 16 years of injection tends to be higher for coarser models, consistent with these models also producing more water.

In summary, the effect of grid resolution on pressure is mainly that at lower resolution there is a greater pressure increase in the injection well, and this translates to more water production. A higher water production rate may lead to faster CO₂ migration and can cause an earlier CO₂ breakthrough, but as shall be seen next the effect of grid resolution on CO₂ breakthrough is more than just because of the pressure response observed here.

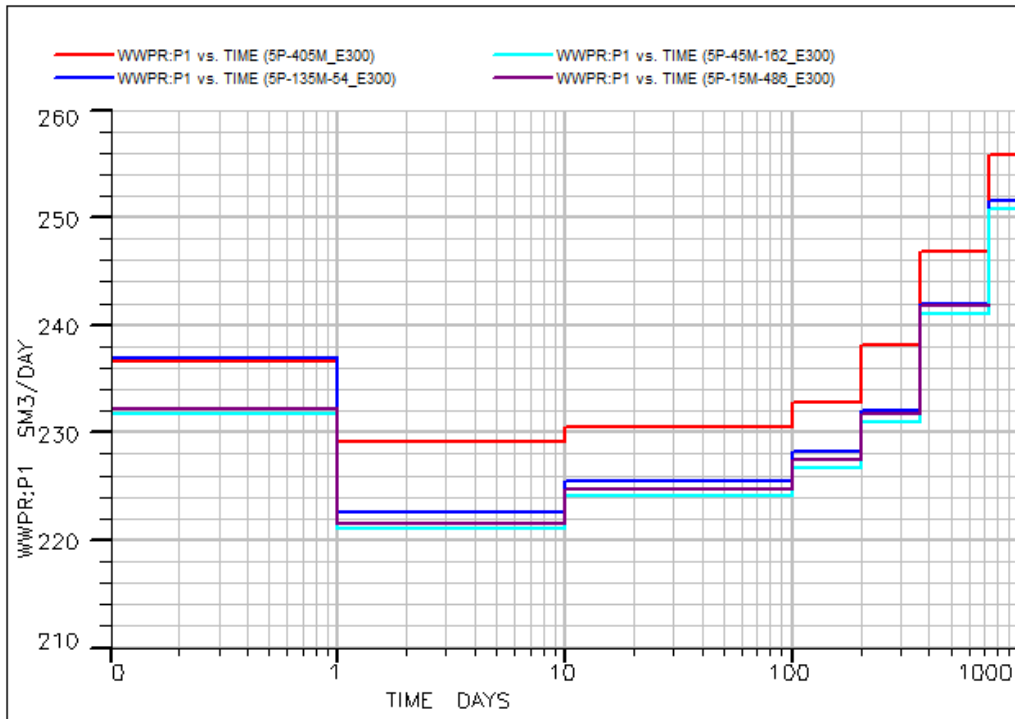


Figure 6-2 Well water production rate (WWPR) vs time for the first 1000 days for models with grid blocks lengths of **405 m (red)**, **135 m (blue)**, **45 m (light blue)** and **15 m (purple)**.

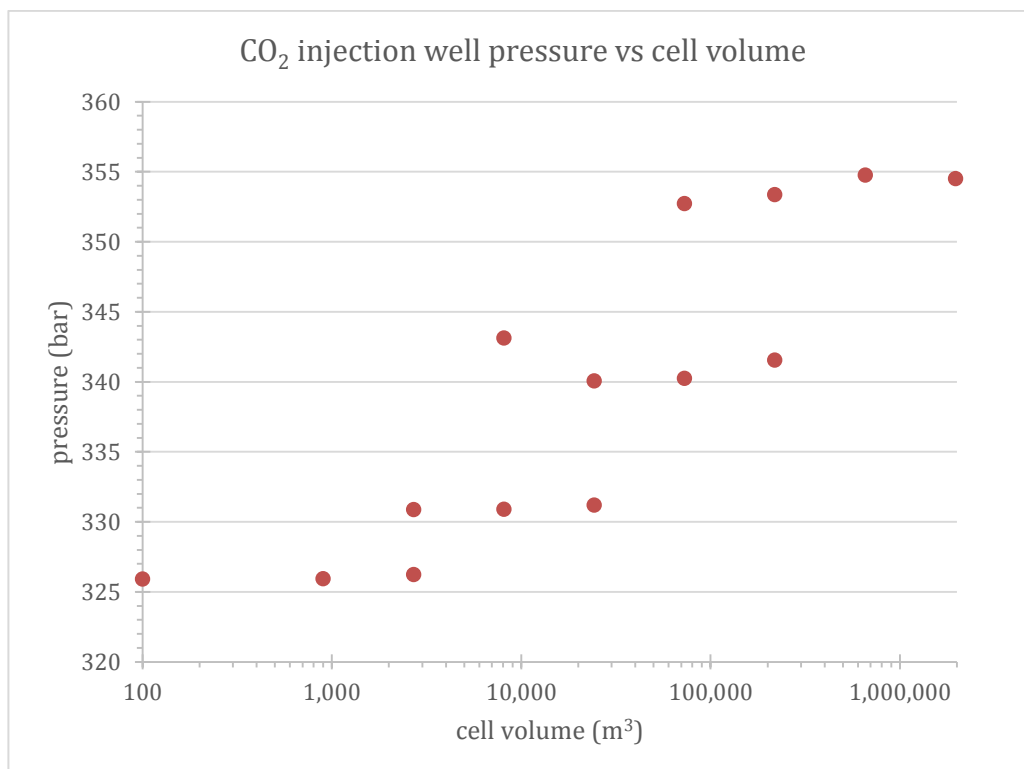


Figure 6-3 Well Bottom Hole Pressure (WBHP) in CO₂ injector after 16 years vs cell volume.

6.1.3 The Impact of Grid Resolution on CO₂ Migration

Due to gravity, the injected free phase CO₂ will rise towards the upper layers initially, but will then dissolve in brine, making the brine denser than the unsaturated brine, and so it will gradually drop down to the lower layers. The top layer and the third layer from the bottom were chosen to compare CO₂ free phase saturation (or gas saturation – SGAS, as it is labelled by the software, and referred to hereafter) and CO₂ mole fraction (XMF1), respectively.

Figure 6-4 shows the distribution of gas saturations at the same time step (3 years into the injection period) in models with different grid resolutions but with the same aspect ratio. The resolution changes from coarse to fine as we move from the top graph to the bottom graph. The simulations are based on the homogenous model. Since the water producer was perforated only in the bottom layer of the models, the less dense free phase CO₂ breakthrough was not observed in any of the models. The models were constructed with the injector in the first cell and the producer in the last cell in both I and J directions in the coarsest model. In order to keep the inter well distance the same, the well locations in physical space would remain the same, but in the finer models they would no longer be in the grid cells at the edge of the models, but there would be some cells between the wells and the edge, as can be seen from the figure.

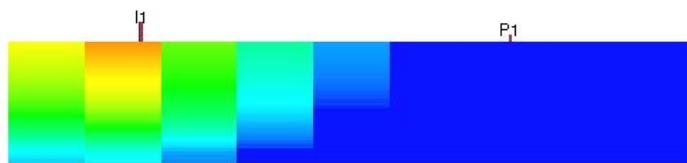
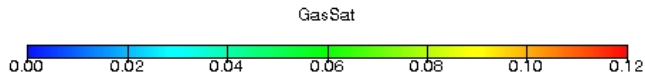
As a result, the gas plume would migrate away from the injection well asymmetrically, as can be seen from Figure 6-5 and Figure 6-6. Figure 6-7 shows the gas saturation in the grid block containing the water producer for three of the models. A spike in gas saturation is evident in model 405M-18 after about 35 years of injection, followed by a drop in gas saturation thereafter.

It is evident from these figures that the model with 405 m grid resolution behaves markedly differently from the other finer models, and is thus unlikely to be representative. On the other hand, refining to a higher degree than in the 135 m grid resolution model shows little further impact, and thus for this homogenous model there is unlikely to be much advantage in further refinement – as far as saturation based calculations are concerned. It should be noted that saturation calculations are based on two phase flow, and the mobility of the phases may be controlled by alteration of the relative permeability functions. However, dissolved CO₂ concentration within the brine phase cannot be controlled by relative permeability functions, as this is single phase compositional behaviour, and so this should be assessed also.



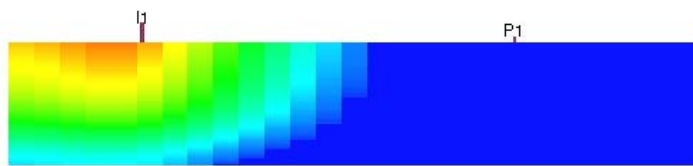
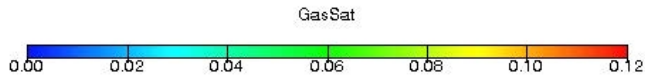
405m x 405m x 12m

(162 cells)



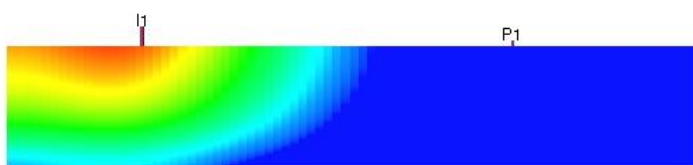
135m x 135m x 4m

(4,374 cells)



45m x 45m x 1.333m

(118,098 cells)



15m x 15m x 0.444m

(3,188,646 cells)

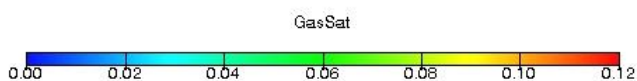


Figure 6-4 Gas saturation distributions after three years of injection in models with different grid resolutions; increasing resolution from top to bottom.

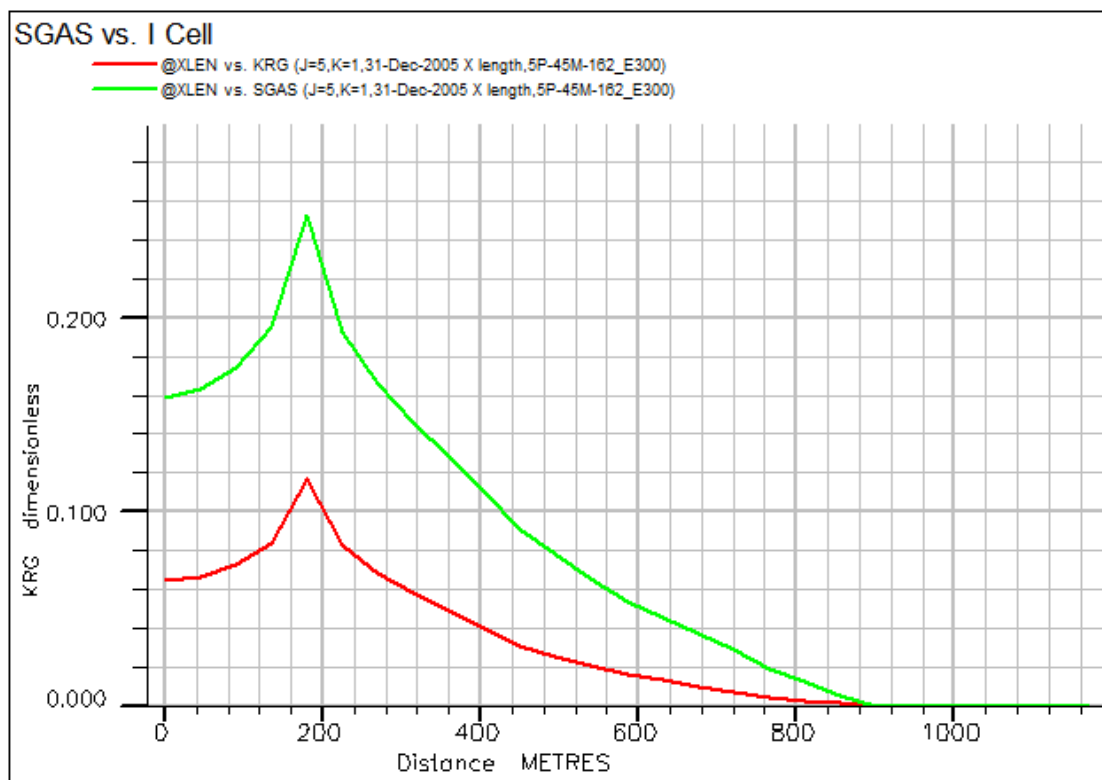


Figure 6-5 Plot of **relative permeability (red line)** and **gas saturation (green line)** after six years of injection for the cells in the top layer of the model with 45 m resolution, along a section in the x direction that includes the injection well (180 m from the left hand edge).

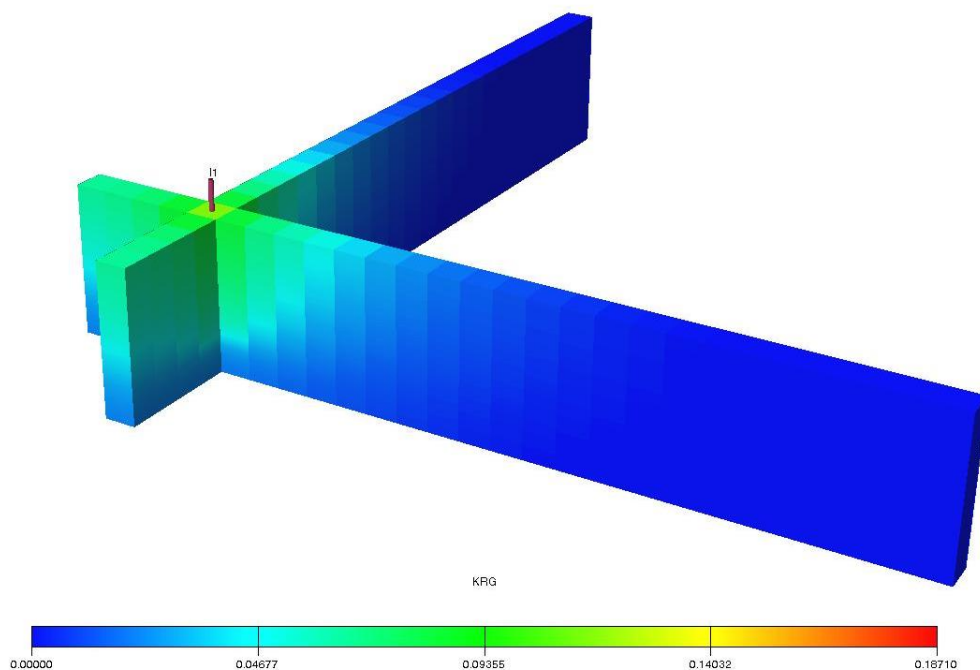


Figure 6-6 Fence diagram of gas saturation after three years of injection, showing vertical sections in x-z plane and y-z plane for the model with 45 m resolution.

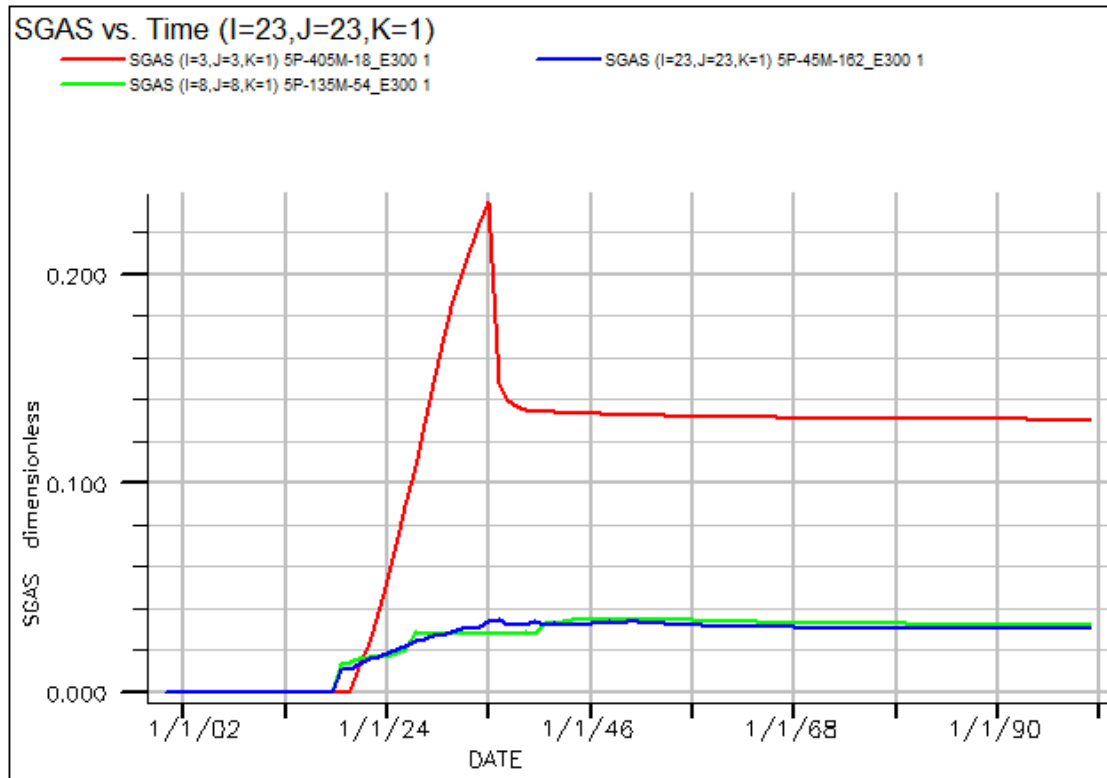


Figure 6-7 Gas saturation vs time for the grid cell containing the brine producer in models with different grid resolutions: **405m (red)**, **135m (green)** and **45m (blue)**.

To address the issue of CO₂ concentration in the brine phase, and the impact of grid resolution on this calculation, Figure 6-8 is plotted to show the amount of CO₂ dissolved in the aqueous phase (FXMF) after 18 years of injection. All of the models shown in the figure have 16 layers (as listed in Table 6-2 row 1).

Again, grid refinement beyond 135m does not show much change in the distribution of dissolved CO₂, although the front is sharper in more refined models.

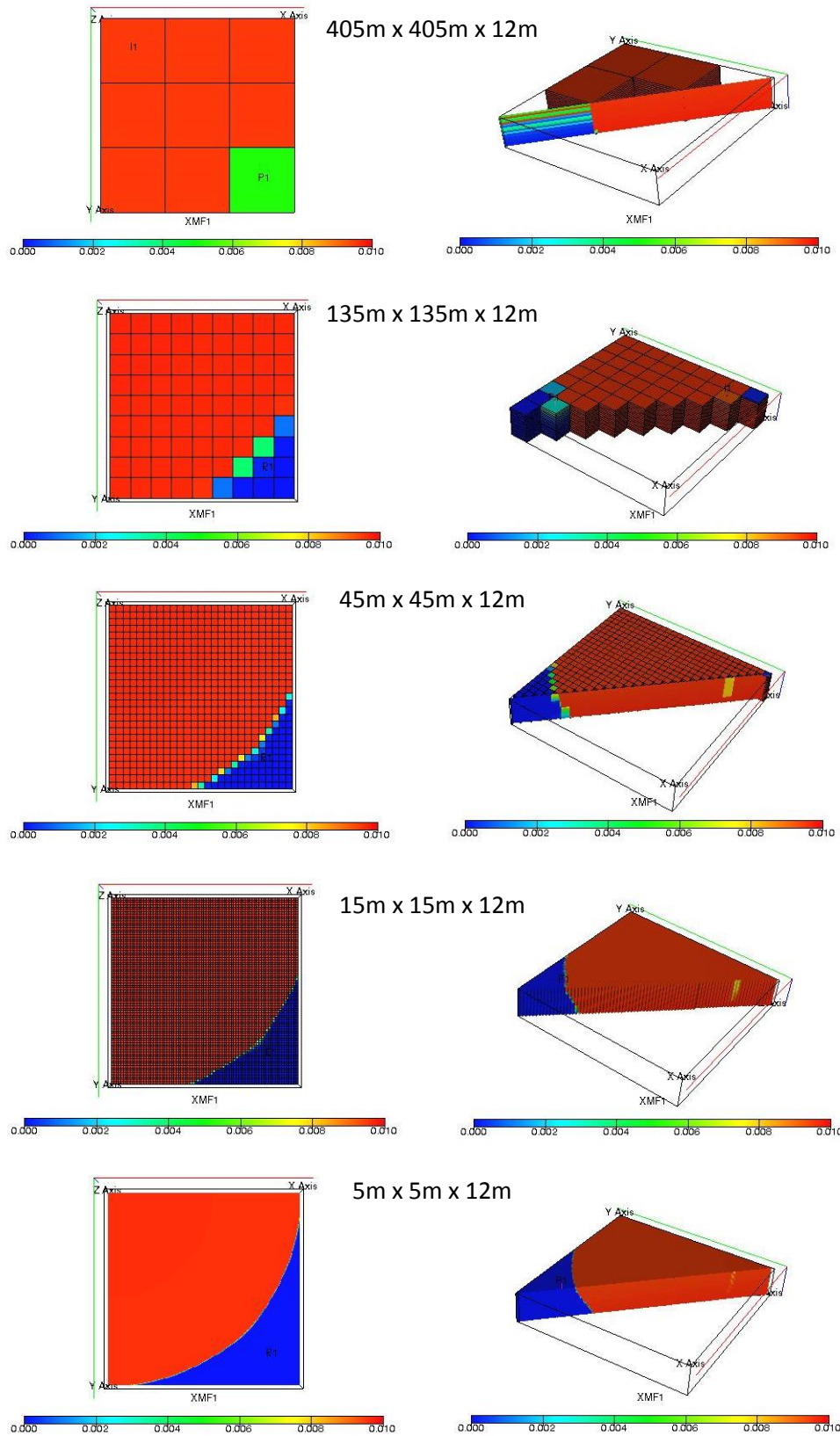


Figure 6-8 Plot of CO₂ dissolved in water (XMF1) after 18 years of injection, showing layer 16 (left) and a diagonal cross section view (right).

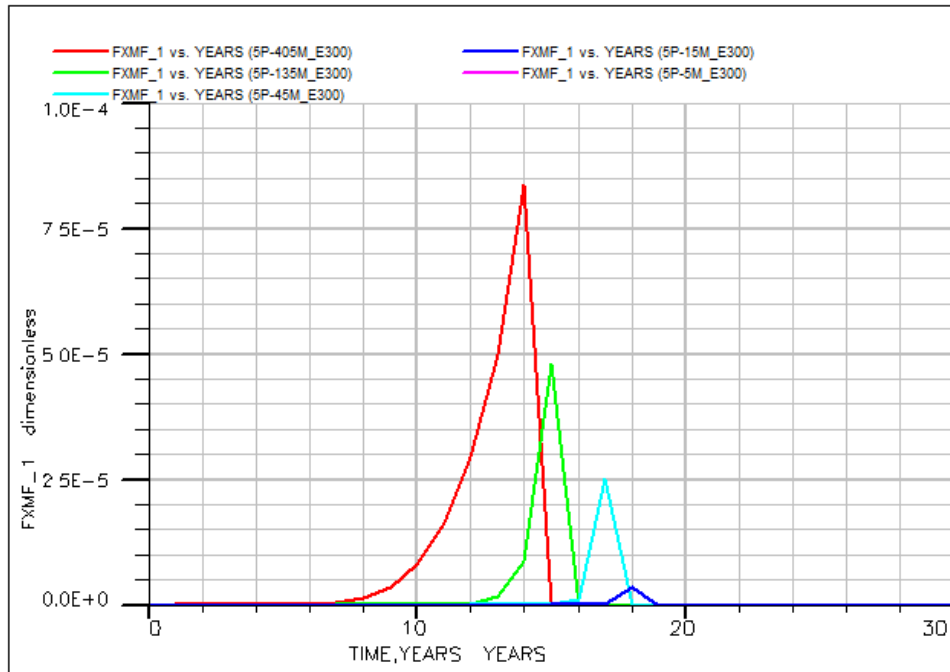


Figure 6-9 CO₂ mole fraction in produced water (FXMF₁) for models with different levels of grid resolution: **405m (red)**, **135m (green)**, **45m (light blue)**, **15m (blue)** and **5m (pink)**, showing the impact of grid resolution on the calculation of CO₂ migration, with numerical dispersion in coarser models leading to earlier breakthrough.

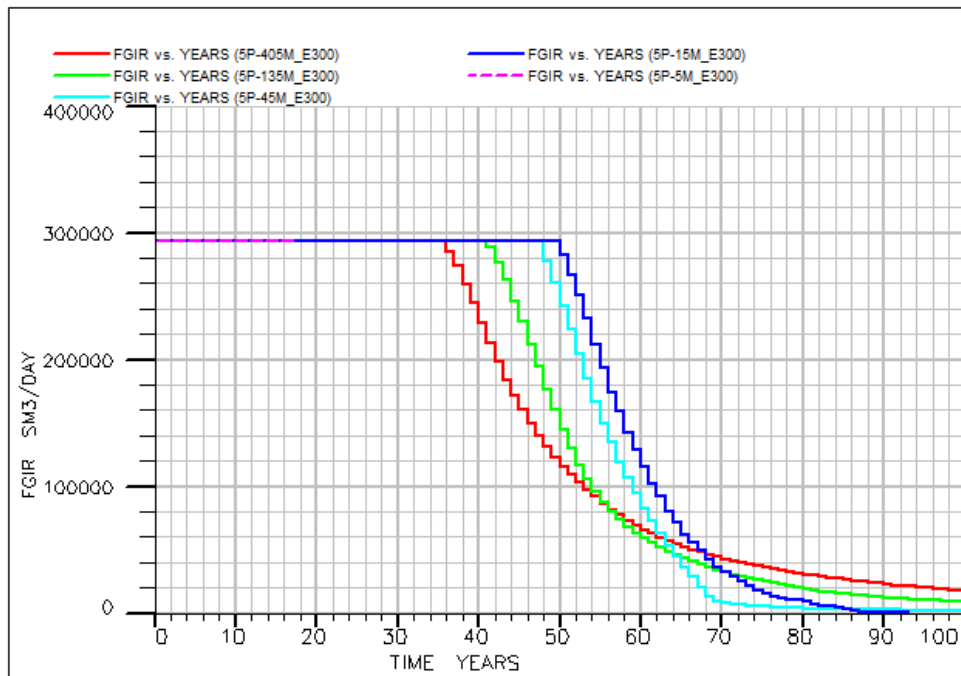


Figure 6-10 Field gas (CO₂) injection rate (FGIR) for models with different levels of grid resolution: **405m (red)**, **135m (green)**, **45m (light blue)**, **15m (blue)** and **5m (pink)**.

Figure 6-9 shows the time taken for CO₂ dissolved in the aqueous to break through, as measured by the CO₂ mole fraction in the produced brine. The criterion for well shut in was set to 1×10^{-4} . The figure shows that the coarser the model the earlier the well shut in event will be triggered. As a consequence, the well bottom hole pressure in the injection well will rise earlier in the coarser model, restricting the time period during which the target injection rate can be maintained, as shown in Figure 6-10. From this analysis, the aqueous CO₂ was displaced faster in the coarser model towards the producer than occurred in the finer models. This raises the question of which model is more accurate. It is generally accepted that coarser models lead to early breakthrough of injected fluid at the production wells, due to an effect known as numerical dispersion: the coarser the model the greater the numerical error. Refining a model should improve the accuracy: however, if further refinement makes little difference to the results, then the coarsest model that yields a similar result will generally be used, as this represents a model that is “good enough” but which does not entail undue computational effort. In this case, the 135m resolution models requiring 2-3 minutes to run a 16 year calculation seem accurate enough – certainly for screening type calculations.

The following section will include an analysis of the effect of grid resolution on the calculation of the impact of trapping mechanisms, including residual trapping and solubility trapping, on CO₂ storage. The impact on the migration of CO₂, especially in a tilted reservoir, will be considered.

6.1.4 Impact of Grid Resolution on Trapping

This part of the study begins by assessing vertical resolution, since in a gravity dominated reservoir CO₂ accumulates at the top of the reservoir, and is displaced faster if the top layer of grid cells is thinner, since less volume of CO₂ needs to enter a cell before it reaches a critical saturation and can continue to migrate to the next cell. The vertical grid resolution was studied based on the 135M model, with the grid resolution varying from 18 layers (12m each), through 54 layers (4m each) to 162 layers (1.333m each). The fraction of injected CO₂ in the mobile phase (FGCDM), in the immobile phase (FGCDI) and in the liquid phase, i.e. dissolved in water (FWCD), are calculated for the three different models, and are plotted in Figure 6-11 for the period of 1 year of injection, for 10 years of injection and for increments of 10 years thereafter up to 50 years.

Except for the result in year one, it is obvious that with an increase in time, more CO₂ is dissolved into the brine, and thus there is more immobile CO₂ because of residual trapping, and there is less mobile CO₂ in the model. The thinner the top layer is, the less the amount of immobile free phase CO₂, and the more the dissolved CO₂.

Figure 6-11 may only be used to compare the results for models of the same horizontal size, but with different degrees of vertical resolution, i.e. different aspect ratios. If comparing all of the results at a given time (say 16 years in this study) but from models with different resolutions, or cell volumes, we obtain a plot such as the one shown in Figure 6-12. With an increase in cell volume, the amount of immobile CO₂ is generally overestimated, as also is the amount of dissolved CO₂. The former could be overestimated by two orders of magnitude, while the later by 20-50%.

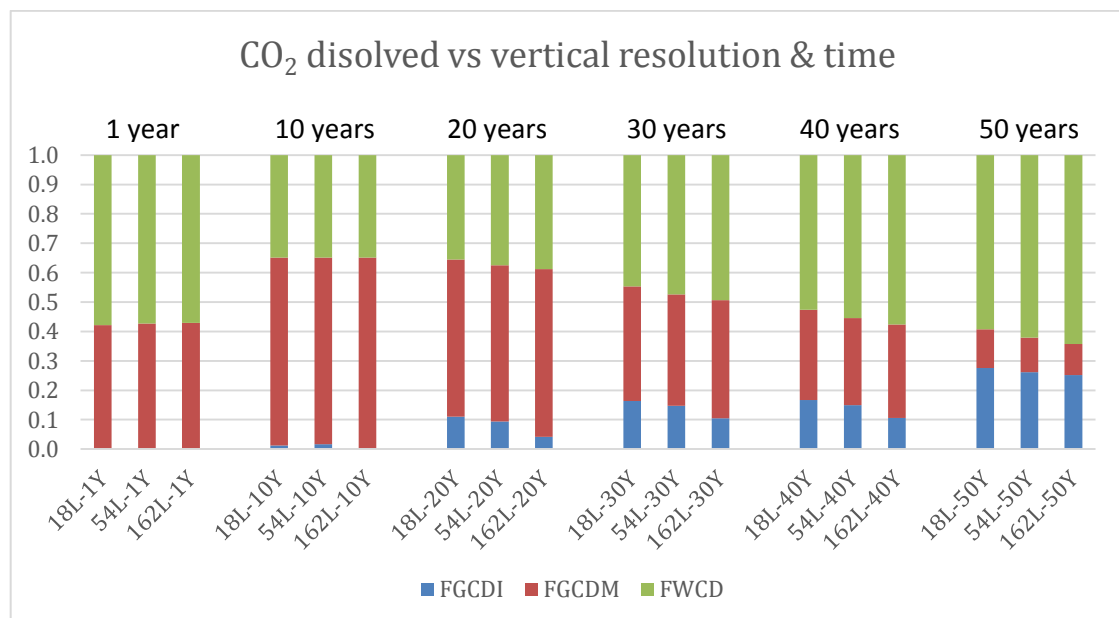


Figure 6-11 Fraction of injected CO₂ trapped by **residual trapping (FGCDI, blue)** and **solubility trapping (FWCD, green)**, and fraction as **free gas (FGCDM, red)** for different periods of injection. Results are from models with different vertical grid resolutions, as labelled. All the models in the diagram have the same size laterally (135m).

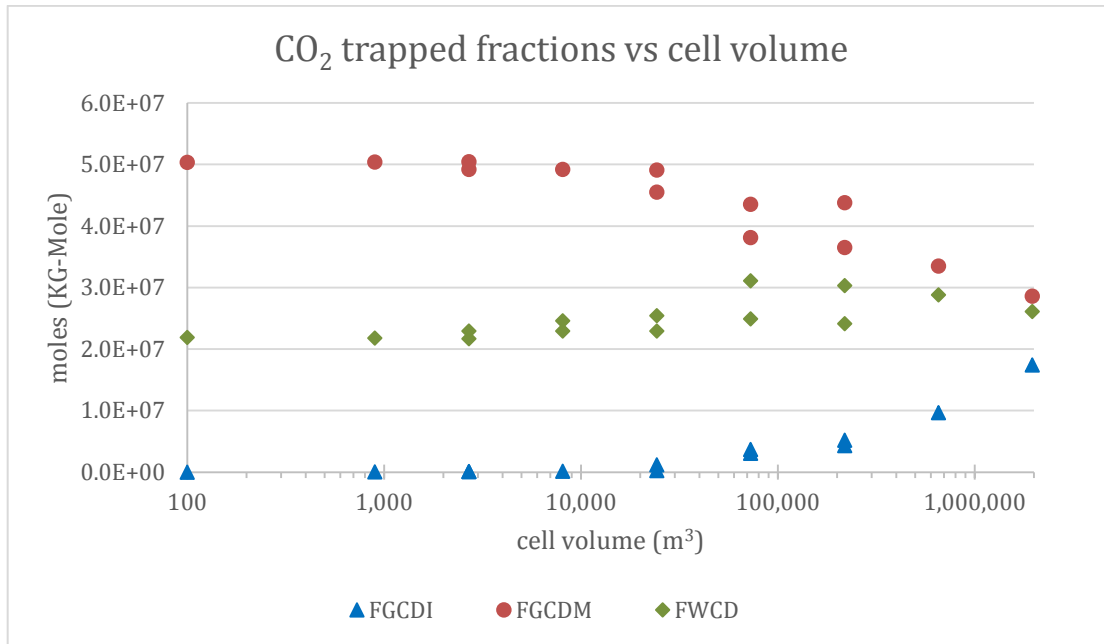


Figure 6-12 Impact of grid resolution on the calculated CO₂ trapping. With an increase in grid cell volume, the amount of **immobile CO₂ (FGCDI, blue)** and **dissolved CO₂ (FWCD, green)** are overestimated, but the **mobile CO₂ (FGCDM, red)** is underestimated.

6.1.5 CPU Saving

If the data in Figure 6-12 are separated out so that they are not plotted against cell volume, but against lateral cell size or vertical cell size, then we obtain Figures 6-13 and 6-14, respectively. From Figure 6-13 we may see that increased resolution in the vertical (z) direction does not improve the accuracy much. For example, changing the thickness of the layers from 18m to 0.444m only reduces the error by 22% (if we take it that the accurate value for the mobile CO₂ (FGCDM) is 5x10⁷ KG-mole, the error is 48% for the 405M-18 case and 27% for the 405M-486 case). However, the total number of cells increased by a factor of 27 times. If we increase the resolution in both the lateral (x and y) directions, say by using the model 135M-54, the accuracy can be improved by 13%. In Figure 6-14 it can also be seen that the most accurate result, say 5x10⁷ KG-mole, can be obtained from models with different vertical resolutions if the horizontal resolution is small enough (45M). Therefore, lateral resolution under this particular set of reservoir conditions is more important than vertical resolution.

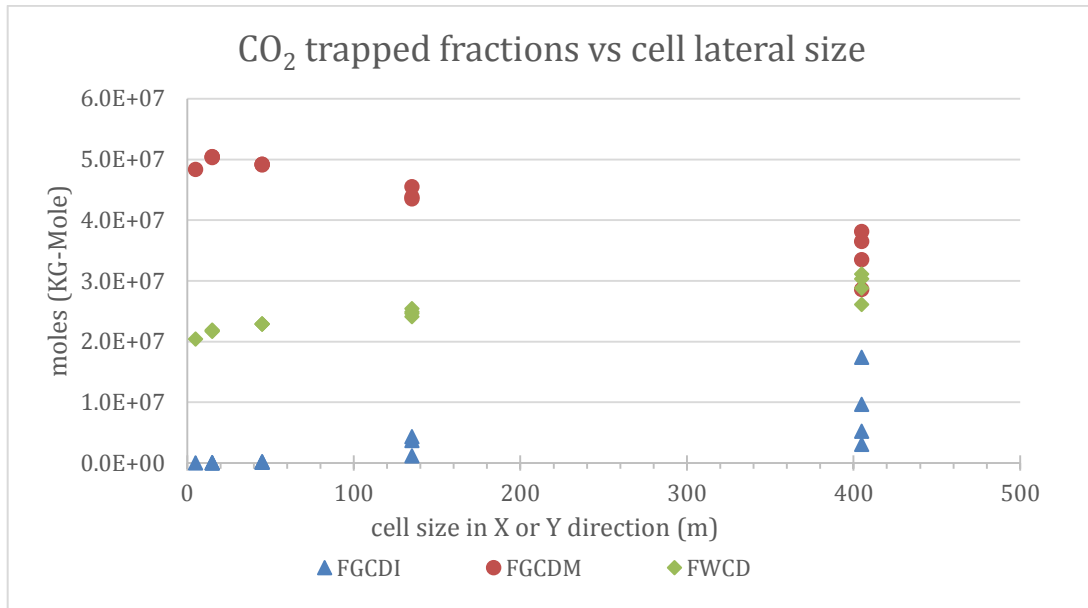


Figure 6-13 Impact of grid resolution on the calculated CO₂ trapping. With an increase in grid cell lateral size, the amount of **immobile CO₂ (FGCDI, blue)** and **dissolved CO₂ (FWCD, green)** increases, but the **mobile CO₂ (FGCDM, red)** decreases.

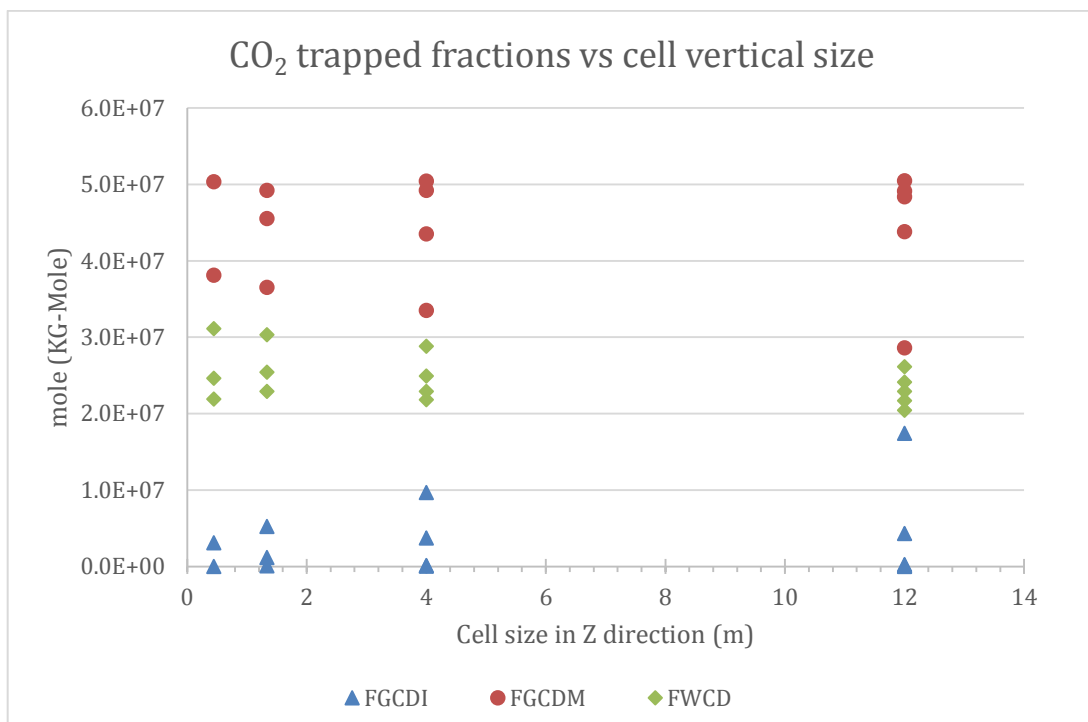


Figure 6-14 Impact of grid resolution on the calculated CO₂ trapping. With an increase in grid cell vertical size, the amount of **immobile CO₂ (FGCDI, blue)**, **dissolved CO₂ (FWCD, green)** and **mobile CO₂ (FGCDM, red)** vary, but not systematically.

6.2 Study of Sensitivity of CO₂ Migration to Grid Resolution in Tilted Homogenous Model

The previous study of grid resolution was performed using a flat synthetic model with dip angle equal to zero. The producer and the injector were located at opposite end of a diagonal crossing the model. In this final part of the study, the impact of dip angle on CO₂ migration is considered. The dip angle in the study was set to be 10 degree.

As shown in Figure 6-15, the producer and the injector in this study were now not set at either end of a diagonal, but along a straight line parallel to one of the axes. The numerical aquifer shown in red colour was connected to the two other boundaries, and enlarges the volume of the model by 7 times. The thickness of the model is 216m and the width and length of the model are each 1215m. Two grid resolutions were used; 135m laterally and 4m (54 layers) vertically, and 45m laterally and 1.33m (162 layers) vertically. The following figures show the mole fraction of CO₂ in the water phase (Figures 6-16 and 6-17) and the gas saturations (Figures 6-18 and 6-19) for cross sections between the two wells.

Two scenarios were considered in the study; one with the producer up-dip of the injector, as shown in Figure 6-16, and the other with the producer down-dip of the injector, as shown in Figure 6-17. Two injection rates were chosen for each of the scenarios; one being 0.2 Mt/y (Figures 6-16 to 6-18) and the other being 0.02 Mt/y (Figure 6-19). The higher rate may result in CO₂ breakthrough within 20 years as a consequence of viscous forces, whereas the lower rate will allow for more gravity segregation, and so will be more sensitive for tilted systems.

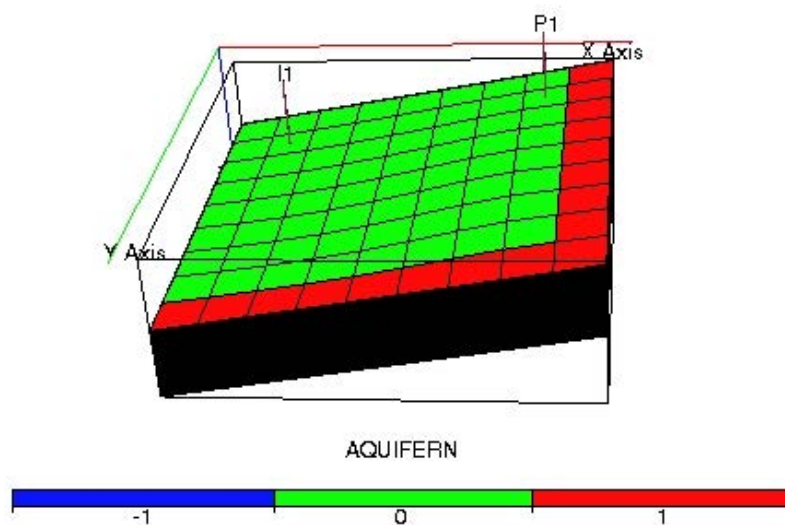


Figure 6-15 geometry of tilted model with numerical aquifer connected to the boundaries (shown in red). Producer P1 and injector I1 are aligned parallel to the edge of the model.

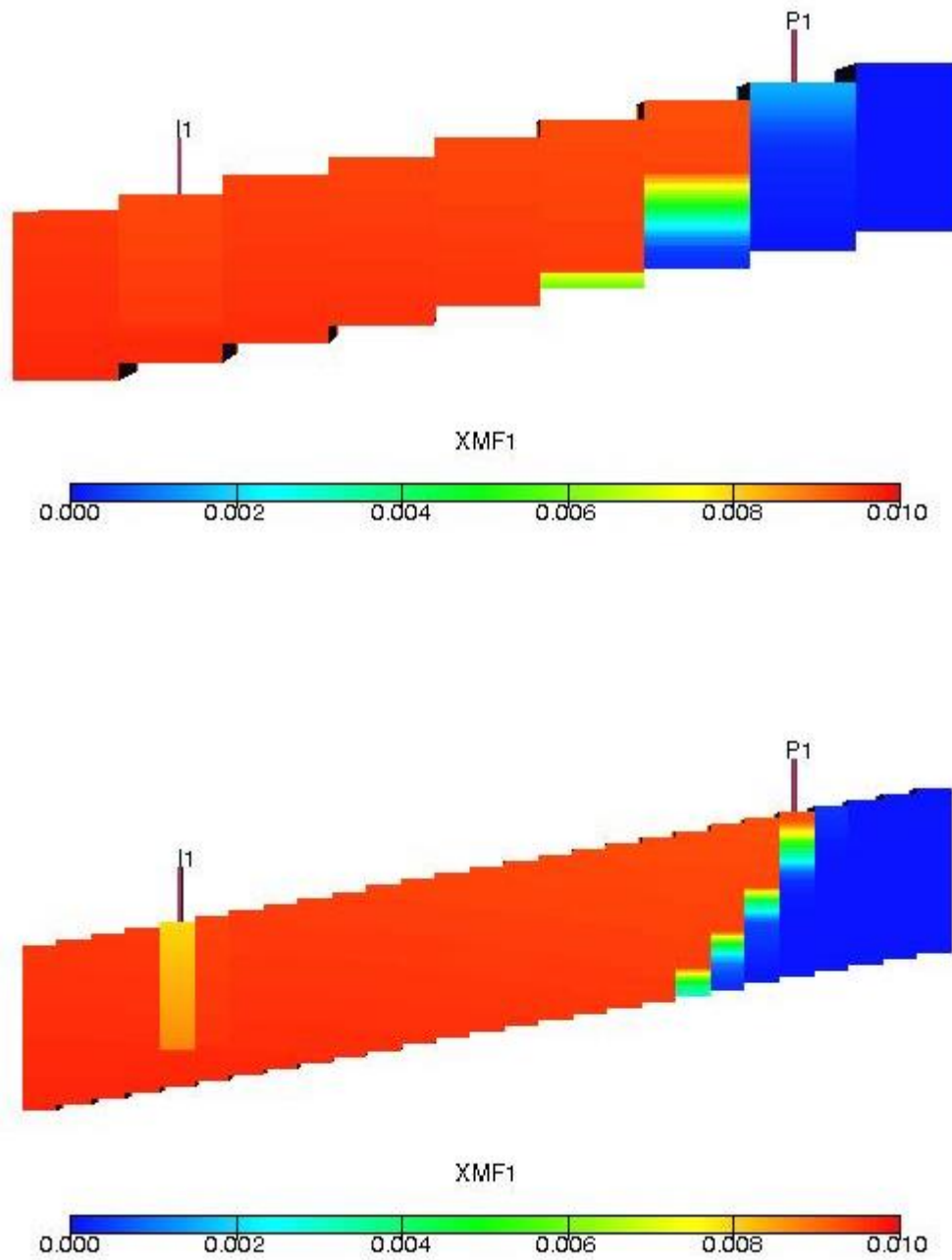


Figure 6-16 With a dip angle of 10 degrees and when the producer is **up-dip** of the injector, the distribution of CO₂ mole fraction (XMF1) shows the impact of grid resolution on CO₂ migration, since the breakthrough time is 2 years earlier in the coarser model (above) than in the finer model (below). The injection rate is 0.2 Mt/year.

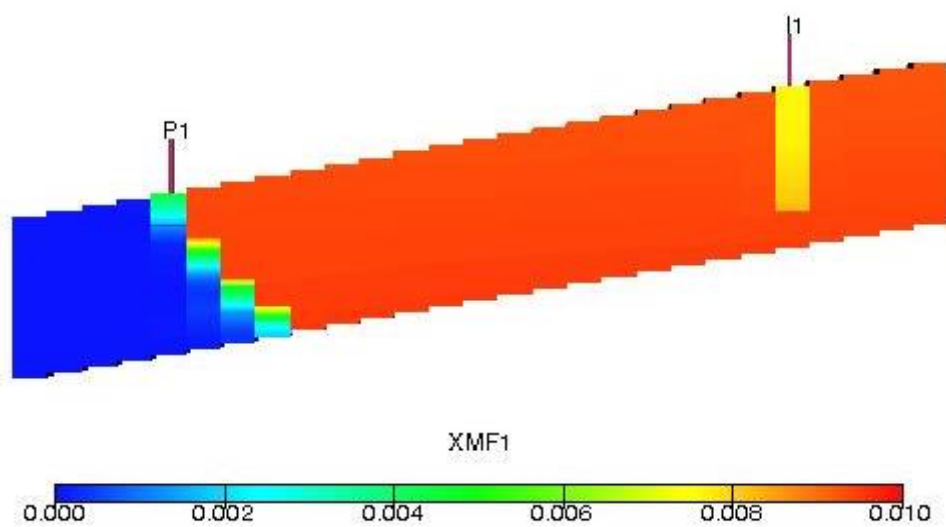
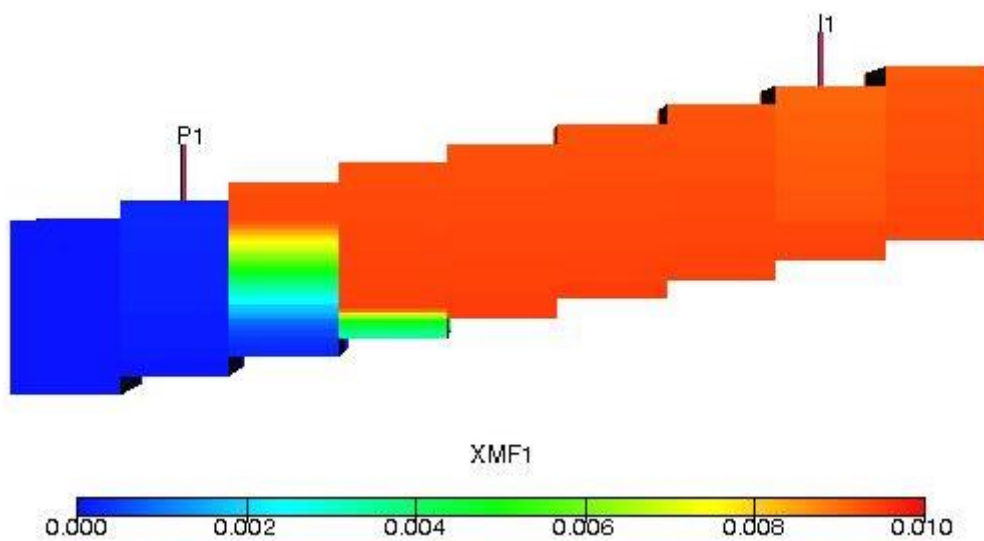


Figure 6-17 With a dip angle of 10 degrees and when the producer is **down-dip** of the injector, the distribution of CO₂ mole fraction (XMF1) shows the impact of grid resolution on CO₂ migration, since the breakthrough time is 3 years earlier in the coarser model (above) than in the finer model (below). The injection rate is 0.2 Mt/year. Note that sweep efficiency is slightly better when injecting up-dip (i.e the producer is down-dip), but not greatly.

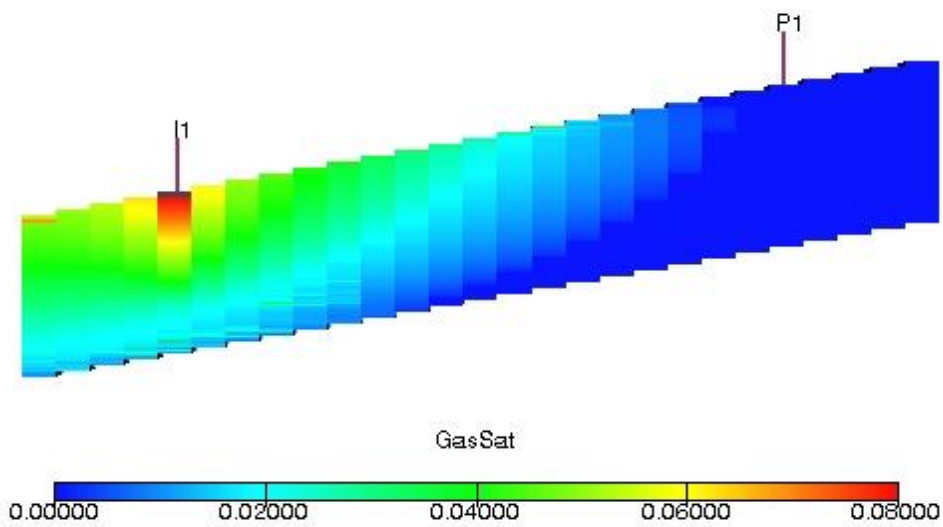
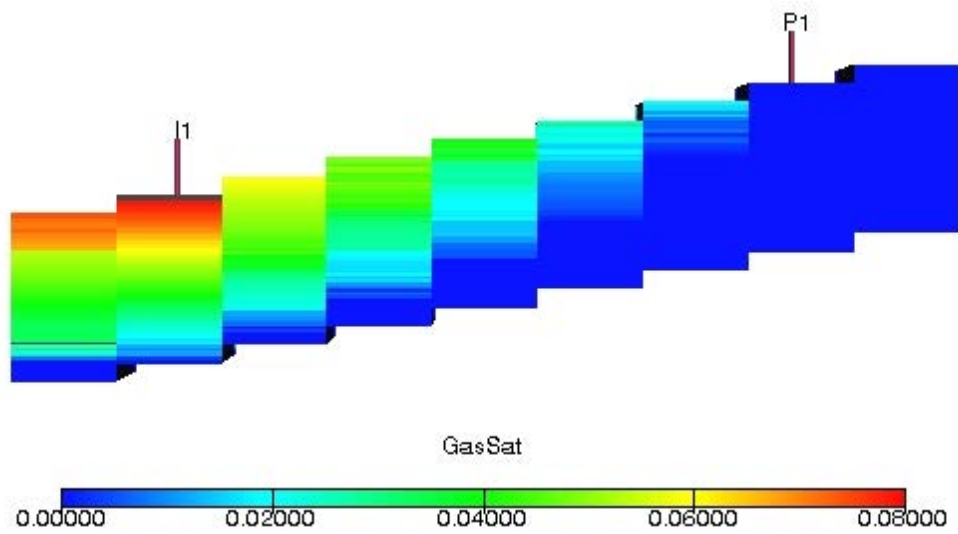


Figure 6-18 With a dip angle of 10 degrees and when the producer is **up-dip** of the injector, the distribution of CO₂ gas saturation (GasSat) shows the impact of grid resolution on CO₂ migration, since the breakthrough time is again 2 years earlier in the coarser model (above) than in the finer model (below). The injection rate is 0.2 Mt/year.

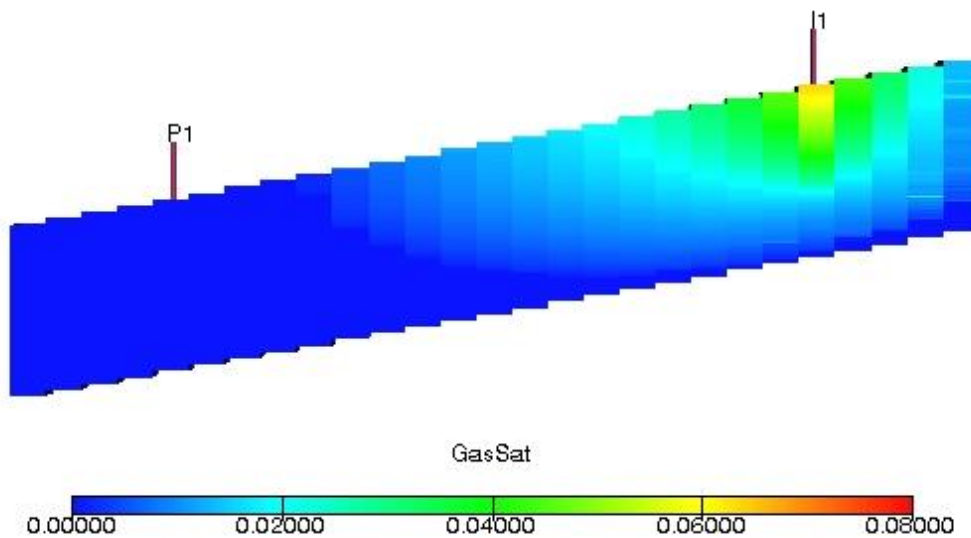
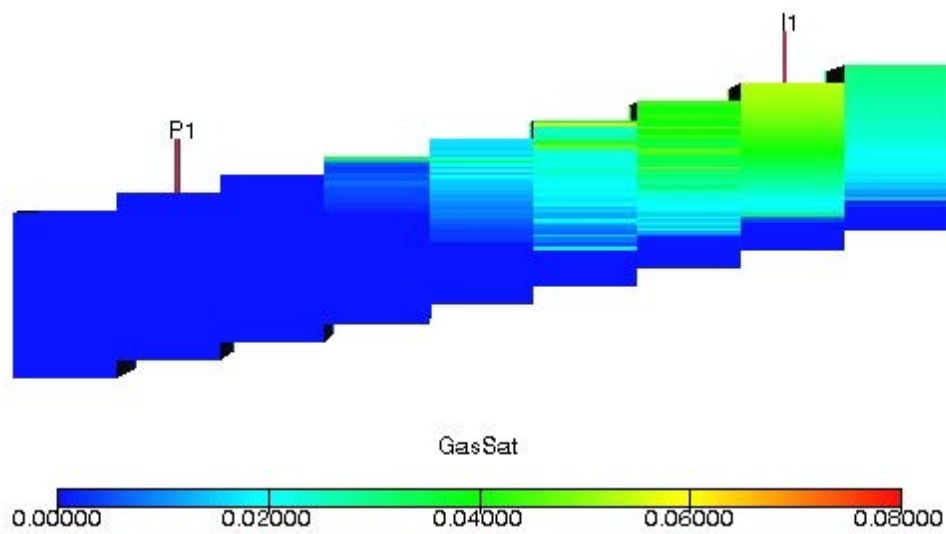


Figure 6-19 Again, with a dip angle of 10 degrees and when the producer is **down-dip** of the injector, the distribution of CO₂ gas saturation (GasSat) shows some impact of grid resolution on CO₂ migration, since the breakthrough time is 2 years earlier in the coarser model (above) than in the finer model (below). The injection rate is 0.02 Mt/year – 10 times lower than in the previous calculations.

7 Conclusions

This project addresses the potential to significantly increase CO₂ storage capacity by producing brine through dedicated production wells. This is a technique currently included in development plans for CO₂ storage sites. The production of water creates voidage to increase storage capacity and reduce the extent of pressure increase due to CO₂ injection. The following are the seven systems studied, in the order in which results are presented:

- 1) A **synthetic tilted structure**, selected specifically to demonstrate the potential increase in storage capacity that brine production may deliver. If the system initially is at a pressure near the maximum allowable pressure during CO₂ injection (such that only 0.55 Mt of CO₂ may be injected through a single well before the pressure limit is reached), meaning that this is not a viable store, then brine extraction via a single production well can increase the storage capacity (to 23.3 Mt), making the system a viable store. This system is used for proof of concept and to study the reservoir engineering conditions that are most favourable for the brine production concept, and economic calculations are not performed. However, it clearly identifies that brine production can make storage sites that are nearby to existing infrastructure, which might otherwise have been excluded from consideration, viable options by increasing their storage capacity.

Having demonstrated the concept of brine production using a synthetic system, the next four systems to be modelled are based on actual offshore or near shore aquifer structures found in the UK Continental Shelf, and they represent exemplars of the four principal types of system identified in CO₂Stored. In each of these four cases, results of the numerical simulations were used as inputs for the CBA tool, and the impacts on storage capacity and on the undiscounted lifetime cost of transport and storage (T&S) (calculated in £/tCO₂) were evaluated.

- 2) The **Forties 5 system** is sufficiently large that for lower CO₂ injection rates (order 2-5 Mt/y), brine production does not yield any increase in storage capacity, and therefore should not be considered. For an intermediate injection rate (10 Mt/y) the capacity of the system is such that initially there is no benefit from brine production. However, as pressure builds up over time, brine production becomes an increasingly useful method of increasing storage capacity. Above 15 Mt/y CO₂ injection rates, brine production may be considered from the outset, and may yield an increase in storage capacity of up to 13%. At very high injection rates, say 40 Mt/y, breakthrough of CO₂

at the production wells is so quick that any benefit of brine production is short lived. The economic calculations show that brine production yields no reduction in unit T&S costs: the conclusion is that the total system volume is sufficiently large that greater storage capacity can as readily be achieved by drilling another CO₂ injection well as by drilling a brine production well.

- 3) Study of the **Bunter Zone 4 system**, as was the case for the Forties system, shows that at lower CO₂ injection rates brine production yields no benefit. The nature of the Bunter aquifer, with higher permeabilities and dome structures, allows for higher injection rates being possible with no benefit from brine production – up to 15 Mt/y. The higher permeabilities and the large system volume mean that even at higher injection rates, the limit on CO₂ injection capacity is not a pressure constraint, but rather that the CO₂ will migrate out of the storage complex, say by reaching a spill point – and brine production does little to mitigate this risk. Thus the system shows no increase in storage capacity and no decrease in unit T&S costs as a consequence of brine production.
- 4) In the **Tay aquifer system**, however, there is potential for an increase in storage capacity of some 200%, and a resulting decrease in unit T&S costs from £7.9/tCO₂ to £7.2/tCO₂ as a consequence of brine production. What distinguishes this system is that while it is large, it is nonetheless bounded, and so, especially at higher injection rates, without brine production the pressure increase is such that injection has to be curtailed, whereas with brine production it may be maintained for longer.
- 5) In the **Firth of Forth system**, a near shore aquifer not included in CO₂Stored, maximum storage capacity may be increased from 100 Mt to 300 Mt by the use of brine production, and unit T&S costs may be reduced from £8.7/tCO₂ to £6.4/tCO₂. Since the aquifer is relatively close to potential CO₂ capture sites in Central Scotland, in the absence of brine production the CO₂ would have to be transported a much greater distance to reach the next closest storage sites in the Central North Sea.

In addition to the reduction in unit costs that brine production may be enable by extending injection in the same site rather than commencing injection in a new site, there is also a more difficult to quantify benefit of reduced risk associated with operating a site for which historical observed data has been collected compared to the development of a green field site. For example, a flow simulation model that has been history matched against historical injection (and production) data will provide a much more accurate forecast of performance than will a

model that has not been history matched, and therefore the continued management of an existing system will generally pose lower risk than the development of a new system. This principle also means that development of a system that is already associated with hydrocarbon production may result in a lower risk, since there will be much more data available for such a system. In addition the previous (and current) production of fluids for the sake of hydrocarbon recovery may be used to support the benefits derived from brine production. Thus two further systems are considered, one in which hydrocarbon production predates use of the site for CO₂ injection, while the other considers simultaneous production of oil and brine from a field that is in pressure communication with an aquifer into which CO₂ is injected. In neither case are economics calculated, since the CBA tool was not developed to consider hydrocarbon systems.

- 6) The CO₂ storage capacity of the depleted **Hamilton gas field** can be enhanced by brine production, provided this is consistent with maintaining the store pressure above that required for super-criticality of the injected CO₂. Since gas production was not supported by brine injection, the pressure at the start of CO₂ injection would be below that required for super-criticality. Thus, for the first 12 years there would be no benefit of brine production – CO₂ injection would simply re-pressurise the original gas reservoir. However, as the system pressure increases to CO₂ critical pressure, the compressibility of the CO₂ reduces significantly, and thereafter brine production can be used to increase storage capacity by limiting further pressure increases. The delay in starting brine production would lead to cost savings, and again the gathering of data before a decision on brine production was required.
- 7) In the case of **the North Sea oil field** studied, water injection can be partially replaced by CO₂ injection deep into the aquifer, and despite CO₂ breakthrough at the producers (and hence a need to recycle CO₂) a net amount of 54 Mt of CO₂ can be stored over a 20 year period, whilst increasing the oil recovery factor from 54% under pure water flooding in that same time period to over 59%, and reducing the requirement for water injection (with a modest reduction in water production also). The improvement in oil recovery may be attributed to microscopic (reduction in residual oil saturation in contacted zones) and macroscopic (better sweep efficiency) mechanisms. The prime interest in this study is, however, the potential to use CO₂ injection deep into the aquifer to at least partially replace water injection, here reduced water injection having a similar impact on storage potential to water production considered in the

other cases studied. Thus this scenario is not a conventional EOR scenario, which would be structured differently, but is a pressure management scenario that couples pressure management in the CO₂ project to pressure management in an oil recovery project by use of common wells.

In addition to the above, four specific circumstances were studied:

- (i) Where before a decision is made to inject CO₂ there is a desire to identify an increased storage capacity for an already attractive store, such as the Firth of Forth, to improve the value of the investment proposition. In the case of Firth of Forth, it was found that brine production could yield a T&S cost reduction of ~£5/tCO₂.
- (ii) Where after a period of CO₂ injection, say 10 years, new CO₂ emitters are identified, and so there is an opportunity to increase the injection rate. In this scenario, in the case of Firth of Forth it was found that brine production could yield a T&S cost reduction of ~£2/tCO₂.
- (iii) Where after a period of CO₂ injection, say 10 years again, an existing CO₂ emitter identifies that the period of CO₂ generation may be extended, and so there is an opportunity to prolong the period of injection. In this scenario, in the case of Firth of Forth it was found that brine production could yield a T&S cost reduction of ~£6/tCO₂.
- (iv) Where an injection well is drilled into what is anticipated to be a large high permeability store, such as the Bunter Store 4 system, but after drilling the well it is discovered that the rock around the injection well is compartmentalised, and so the volume of rock into which CO₂ may be injected is much smaller – say just the volume of Bunter Dome 36. In this scenario, in the case of Bunter 36 it was found that drilling brine production wells could yield a T&S cost reduction of ~£1/tCO₂ compared to drilling another CO₂ injection well elsewhere and abandoning the original well.

Assessments are also made of the impact of grid resolution on the accuracy of the fluid flow calculations, of the impact of high permeability “thief” zones, of potential risks and potential opportunities associated with brine production, and of whether or not there is opportunity to consider use of the type of data in CO₂Stored to develop analytical models that could at least in part provide the types of inputs for the CBA tool that were derived from the numerical

models. The rationale for this latter assessment is that numerical simulations require extensive input data, specialist commercial software, specialist operator knowledge and they are computationally intensive to carry out, whereas analytical calculations are more readily performed. While seven subsurface systems have been studied using the numerical simulations, only an analytical approach would enable the 400+ systems in CO₂Stored to be considered.

Grid resolution is an important constraint on the accuracy of numerical simulations of CO₂ injection and brine production. Increasing resolution (within current hardware limitations) always further improves accuracy, but at highest resolutions the changes are moderate. The key issue is the prediction of risk of CO₂ breakthrough at producers, and thus monitoring and contingency planning are required.

In conclusion, the work presented in this report identifies that brine production may be a very useful technique to upgrade confined stores from marginal to good or excellent prospects, to mitigate the risk of unexpected compartmentalisation of the storage complex, to reduce the risk of loss of integrity of a storage complex due to overpressure, and to extend the lifespan of an injection project.

8 Future Work

This work has identified that the risk of CO₂ breakthrough at brine production wells is dependent on inter well distances, the geometry of aquifer system, the density difference between brine and CO₂, and the distribution of permeabilities within the formation. CO₂ density and mobility are very sensitive to pressure and temperature near the CO₂ critical point. Thus a specific study of the impact of system temperature, pressure and permeability distribution (fining up vs. coarsening up permeabilities, say) on optimum inter well distances should be conducted.

Large volumes of permeable rock may be separated by relatively thin zones of impermeable rock. Thus, there may be potential storage volume in the vicinity of an identified aquifer. In some cases, lateral shale layers may be extensive but incomplete. Brine production from a lower sandstone interval may be very effective where an intervening but incomplete shale layer separates it from the upper interval into which CO₂ is injected, as the shale may act as a barrier to CO₂ migration to the production well, but the pressure depletion at the brine producer may nonetheless have a beneficial impact at the CO₂ injector. In such a scenario, the degree to which pressure transmission can take place across the barrier would be critical. Furthermore, there may be opportunities to deliberately engineer pressure communication between adjacent sandstone intervals, or between adjacent fault blocks, such that pressure propagation through the brine phase occurs, but the CO₂ remains in the vicinity of the injection well.

All injection calculations presented have been performed using numerical models. Analysis of the type of data contained in CO₂Stored identifies that it is possible to perform analytical calculations to predict the impact of brine production on storage capacities using only the data in CO₂Stored. The initial methodology to do that has been formulated, but requires further validation. These methods depend on identifying the volume of incremental CO₂ that can be injected before breakthrough occurs (the pressure constraint) or before the CO₂ advances beyond a spill point or other limit of the system (the migration constraint). These methods, which show promise, should be refined and tested against the numerical predictions, and if applicable, coupled with CO₂Stored.

9 References

- Armstrong, L.A., Ten Have, A. and Johnson, H.D. (1987) The geology of the Gannet Fields, central North Sea, UK sector. In: Petroleum Geology of North-West Europe (Ed. By J. Brooks and K. Glennie), 533-548, London.
- Computer Modelling Group Ltd (2016) CMOST User Guide. Calgary.
- Computer Modelling Group Ltd (2016) GEM User Guide. Calgary.
- Donley, J. (2007) Reservoir Architecture: The key to understanding reservoir performance in Gannet A. In Proc of Devex 2007, Aberdeen.
- ETI (2015) CO₂Stored database. <http://www.co2stored.co.uk/home/index> (Accessed May 2016).
- Fatt, I. (1958) Pore Volume Compressibilities of Sandstone Reservoir Rocks. *Journal of Petroleum Technology* **10**(3) (March).
- Ford, J.R. and Monaghan, A.A. (2009) Lithological Heterogeneity of the Mercia Mudstone and Sherwood Sandstone Groups in the Yorkshire-Lincolnshire Region, and Knox Pulpit Sandstone, Kinnesswood and Ballagan Formations in the Forth region : additional information for CASSEM Work Package One. British Geological Survey Report, CR/09/053
- Goater, A., Bijeljic, B. and Blunt, M. (2013) Dipping open aquifers – the effect of top – surface topography and heterogeneity on CO₂ storage efficiency, *IJGGC*, **17** 318-331
- Hall, H.N. (1953) Compressibility of Reservoir Rocks. *Trans. AIME*: 309.
- Holloway, S. and Vincent, C.J. (2006) Industrial carbon dioxide emissions and carbon dioxide storage potential in the UK, COAL R308 DTI/PUB URN 06/2027, British Geological Survey.
- Holloway, S. (1996) The underground disposal of carbon dioxide, JOU2 CT92-0031, British Geological Survey.
- Jennette, D.C., Garfield, T.R., Mohrig, D.C. and Cayley, G.T. (2000) The interaction of shelf accommodation, sediment supply and sea level in controlling the facies, architecture and sequence stacking patterns of the Tay and Forties/Sele Basin-Floor Fans, Central North Sea. In Proc. GCSSEPM Foundation 20th Annual Research Conference - deep-water reservoir of the world, (3-6 Dec. 2000).

Jin, M. and Mackay, E. (2009) Report to Scottish CCS Joint Study on Saline Aquifer Modelling, 22 January.

Jin, M., Pickup, G., Mackay, E., and Todd, A. (2010) Static and dynamic estimates of CO₂ storage capacity in two saline formations in the UK, SPE 131609.

Journel, A.G. and Huijbregts, C.J. (1997) Mining Geostatistics, seventh printing. San Diego, California: Academic Press Limited.

Monaghan, A.A., Ford, J., Milodowski, A. et al. (2012) New insights from 3D geological models at analogue CO₂ storage sites in Lincolnshire and eastern Scotland, UK. Proceedings of the Yorkshire Geological Society (May).

Monaghan, A.A., McInroy, D.B., Browne, M.A.E. and Napier, B.R. (2009) Kinnesswood and Ballagan Formations in the Forth Region - additional information for CASSEM work package one. Report CR/09/053, British Geological Survey, Edinburgh.

Monaghan, A.A., McInroy, D.B., Browne, M.A.E. and Napier, B.R. (2009) CASSEM work package one - Forth geological modelling. Report CR/08/151, British Geological Survey, Edinburgh.

Schlumberger (2014). ECLIPSE Reference Manual.

Smith, M., Campbell, D., Mackay, E., and Polson, D. (2012) CO₂ Aquifer storage site evaluation and monitoring, CASSEN Book, ISBN: 978-0-9751031-0-8, published by Scottish Carbon Capture and Storage (SCCS).

van der Meer, L.G.H. and Egberts, P.J.P. (2008) A general method for calculating subsurface CO₂ storage capacity. In Proc. 2008 Offshore technology conference, (5-8 May), OTC 19309.

Williams, J., Jin, M., Bentham, M., Pickup, G., Hannis, S., and Mackay, E., (2013) Modelling carbon dioxide storage within closed structures in the UK Bunter Sandstone Formation. *International Journal of Greenhouse Gas Control* **18** 38–50.